

TOPICS IN SUPERCONDUCTIVITY

TOPICS IN THE THEORY OF SUPERCONDUCTIVITY

By

CHARLES RICHARD LEAVENS, B.Sc.

A Thesis

Submitted to the School of Graduate Studies

in Partial Fulfilment of the Requirements

for the Degree

Doctor of Philosophy

McMaster University

August 1970

DOCTOR OF PHILOSOPHY (1970)
(Physics)

McMASTER UNIVERSITY
Hamilton, Ontario.

TITLE: Topics in the Theory of Superconductivity

AUTHOR: Charles Richard Leavens, B.Sc.
(McMaster University)

SUPERVISOR: Professor J. P. Carbotte

NUMBER OF PAGES: vi, 192

SCOPE AND CONTENTS:

Simple theoretical expressions for the zero temperature energy gap and the transition temperature of a weak coupling superconductor are derived and applied to an investigation of several phenomena.

The anisotropy of the energy gap in aluminium arising from the anisotropy in the phonon spectrum is calculated. The effect of this energy gap anisotropy on some thermodynamic properties of superconducting aluminium is investigated.

ACKNOWLEDGEMENTS

I wish to thank my research supervisor Dr. J. P. Carbotte for his generous and patient guidance and enthusiastic encouragement.

I wish to thank Dr. P. N. Trofimenkoff, Dr. P. Vashishta and my fellow students J. Copley, B. Hayman and P. Truant for many helpful discussions.

I wish to acknowledge the financial assistance of the National Research Council of Canada during the past three years.

Many thanks go to Miss Cathy Wivell for the accurate and speedy typing of this thesis.

TO MY PARENTS

TABLE OF CONTENTS

	<u>Page</u>	
CHAPTER I	INTRODUCTION	1
	1.1 Historical Introduction	1
	1.2 Scope of Thesis	5
CHAPTER II	NECESSARY BACKGROUND MATERIAL	9
	2.1 The One Parameter Model of BCS	9
	2.2 The Eliashberg Gap Equations	11
	2.3 The Morel-Anderson Equation and the McMillan Equation	16
	2.4 Anisotropy of the Superconducting Energy Gap	20
CHAPTER III	A CONTRIBUTION TO THE THEORY OF A WEAK COUPLING SUPERCONDUCTOR	27
	3.1 The Energy Gap of an Isotropic Weak Coupling Superconductor	27
	3.2 The Anisotropy of the Energy Gap in a Pure Single-Crystal Superconductor	60
	3.3 The Average Energy Gap in a Pure Single-Crystal Superconductor	66
	3.4 Effect of Pressure	70
	3.5 The Transition Temperature of an Isotropic Superconductor	91

	<u>Page</u>
3.6 The Transition Temperature of a Pure Single-Crystal Super- conductor	100
3.7 The Isotope Effect	102
CHAPTER IV THE ANISOTROPY OF THE ENERGY GAP IN SUPERCONDUCTING ALUMINIUM ARISING FROM THE ANISOTROPY OF THE PHONON DENSITY OF STATES	109
4.1 Calculation of Directional Electron- Phonon Mass-Enhancement Parameters	109
4.2 A Model Investigation of Bennett's One Iteration Procedure for Cal- culating Directional Energy Gaps	123
4.3 Calculation of the Anisotropic Energy Gap in Superconducting Aluminium	132
4.4 Some Effects of the Anisotropy of the Energy Gap in Aluminium	143
4.5 Temperature Dependence of the Energy Gap Anisotropy	154
CHAPTER V SUMMARY AND CONCLUSION	157
5.1 A Contribution to the Theory of a Weak Coupling Superconductor	157
5.2 Energy Gap Anisotropy in Aluminium	160
REFERENCES	163
APPENDIX ANISOTROPY OF THE ELECTRON-PHONON SCATTER- ING FUNCTION OF FERMI LIQUID THEORY	170

CHAPTER I

INTRODUCTION

1.1 HISTORICAL INTRODUCTION

The phenomenon of superconductivity was discovered in 1911 by Kamerlingh Onnes⁽¹⁾. The explanation of superconductivity was to remain 'the shame and despair of theoretical physics' for almost half a century⁽²⁾. The only successful theories developed during this time were phenomenological. The two fluid model developed by Gorter and Casimir⁽³⁾ met with considerable success in describing thermodynamic properties, but this was accomplished at the expense of an unphysical $x^{\frac{1}{2}}$ dependence of the total free energy of the electron fluid on the fraction x of the superfluid component. The phenomenological equations postulated by F. and H. London⁽⁴⁾ to replace Ohm's law in a superconductor were very successful in describing low frequency, long wavelength electromagnetic phenomena in superconductors. Important empirical modifications of these equations were made by Pippard⁽⁵⁾. The Landau-Ginzburg equations⁽⁶⁾, which were based on Landau's phenomenological theory of second order phase transitions, were very successful in treating situations in which the density of the superfluid could vary from point to point in the metal due to the presence of a

magnetic field. However, these equations were valid only near the transition temperature, T_c .

Great progress was made during the 1950's. Fröhlich⁽⁷⁾ proposed that the electron-phonon interaction was responsible for superconductivity. He showed that the electron-phonon interaction could lead to an effective electron-electron interaction which is attractive for electrons very near the Fermi surface. The experimental discovery of the isotope effect by Maxwell⁽⁸⁾ and Reynolds⁽⁹⁾ was striking confirmation of Fröhlich's proposal. Cooper⁽¹⁰⁾ investigated a model problem in which a pair of electrons with zero total momentum interacted with each other through an attractive two-body potential in the presence of an inert filled Fermi sea. He considered the special case in which the interaction was a constant ($-V$) when the electron energies were within an average phonon energy of the Fermi energy and zero otherwise. He found that a pair of electrons interacting through this potential were bound relative to the Fermi sea. This result suggested that in the presence of an attractive electron-electron interaction the Fermi sea would be unstable to the formation of electron pairs in zero total momentum states above the Fermi level. The stage was set for the theory of Bardeen, Cooper and Schrieffer⁽¹¹⁾, hereafter referred to as the BCS theory.

Bardeen, Cooper and Schrieffer were able to solve the complicated many body problem by isolating the correlations

that give rise to superconductivity. They assumed, in the spirit of the Landau theory of a Fermi liquid⁽¹²⁾, that the extremely complicated system of strongly interacting electrons and ions could be replaced by a system of quasiparticles (electrons in Bloch states of the normal metal and non-interacting phonons) with some residual interactions between them. The residual interaction between a pair of Bloch electrons has two components, the repulsive screened Coulomb interaction and the interaction mediated by the exchange of virtual phonons. This latter interaction is attractive when the quasiparticle energies are less than the energy of the phonon exchanged between them. BCS showed that when the residual interaction is attractive at the Fermi surface the formation of Cooper pairs becomes energetically favourable and a new ground state is formed which is characterized by correlated occupancy of time-reversed quasiparticle states⁽¹³⁾. BCS were able to show, using the simple model interaction mentioned above, that this new ground state has the essential features of the actual superconducting ground state. The BCS theory, as originally formulated, was a one parameter model, this parameter being the zero temperature energy gap or the transition temperature. With this parameter chosen phenomenologically the BCS theory agreed very well with experiment for a wide range of phenomena and a large number of materials^(14,15,16).

The BCS model is valid for weak coupling superconductors.

These are superconductors for which the Landau Fermi liquid theory is valid, which is the case if the quasiparticles used to form the BCS state are long lived. This condition is satisfied only if the thermal energy, $k_B T$, and the important quasiparticle excitation energies are much less than a typical phonon energy. If an electron has enough energy to emit real phonons its lifetime is very short and the Landau theory breaks down. This is the case for strong coupling superconductors which are characterized by large transition temperatures and low Debye temperatures.

Migdal⁽¹⁷⁾ showed using Green's function methods that for the electron-phonon interaction in a normal metal the corrections to lowest order self-consistent perturbation theory are of the order of the square root of the electronic to ionic mass ratio, $(m/M)^{1/2}$. Migdal's results for the normal metal were generalized to the superconducting case by modifying the usual Green's function techniques to take into account the anomalous processes corresponding to the formation and breakup of Cooper pairs^(18,19,20). This led to the Eliashberg gap equations, a set of two coupled non-linear integral equations which are believed to be very accurate, with errors not greater than a few percent⁽²¹⁾. These equations are not based on the Landau theory of a Fermi liquid and hence are valid even for strong coupling superconductors. Recently, McMillan and Rowell⁽²²⁾ established experimentally that the corrections to the Eliashberg equations

are no more than a few percent and used these equations to extract normal state properties of the electrons, phonons and their interactions from their tunneling data on strong coupling superconductors. This was done by numerically inverting the Eliashberg equations using an electronic computer.

It is truly remarkable that the theory of superconductivity which was virtually non-existent fifteen years ago has developed to the point where it can be used for an accurate investigation of normal state properties.

1.2 SCOPE OF THESIS

The work to be presented in this thesis consists of two quite distinct contributions to the theory of superconductivity. In Chapter III simple theoretical expressions for the zero temperature energy gap and the transition temperature of a weak coupling superconductor are derived and applied to an investigation of several phenomena. In Chapter IV the results of a detailed numerical investigation of the anisotropy of the energy gap in aluminium due to the anisotropy in the phonon density of states are presented. Chapter II serves a double purpose. The first is to present work previously done in the two areas investigated by the author; the second is to present results, such as the Eliashberg gap equations, which are essential to the work of Chapters III and IV.

Section 2.1 is a brief summary of the essential

results of the one parameter model of BCS. In section 2.2 the Eliashberg gap equations are written down and discussed. Particular emphasis is placed on the normal state information needed for these equations and the information about the superconducting state that one obtains by solving them. Section 2.3 is a discussion of two simple theoretical expressions for the transition temperature of a superconductor. The first is that of Morel and Anderson; the second is that of McMillan. In section 2.4 previous work relating to the anisotropy of the energy gap is reviewed in considerable detail.

In section 3.1 the Eliashberg gap equations for an isotropic superconductor are reduced to a much simpler set of integral equations which are appropriate for a weak coupling superconductor. In the weak coupling limit an approximate analytical solution of these equations is derived. In the remainder of this section an attempt is made to justify this solution for weak and medium coupling superconductors. In section 3.2 the simplified integral equations of section 3.1 are generalized so as to be suitable for an anisotropic pure single-crystal superconductor. In section 3.3 an expression is derived for the average energy gap in a pure single-crystal superconductor in terms of certain gross features of the anisotropy. In section 3.4 the pressure dependence of the BCS parameter $N(0)V$, of the isotropic energy gap, and of the anisotropy of the energy gap in a pure

single crystal is investigated. Section 3.5 contains the derivation of a simple expression for the transition temperature of a weak coupling isotropic superconductor. A correction to the BCS value for the ratio of twice the energy gap to the transition temperature is obtained and the pressure dependence of this ratio investigated. In section 3.6 an expression for the transition temperature in a pure single-crystal superconductor is derived. A new expression for the isotope effect is obtained in section 3.7 and the pressure dependence of the isotope effect exponent is investigated.

In section 4.1 a detailed description is given of the method of calculating the function, $\alpha^2 F(\nu, \theta, \phi)$, which is central to most of this thesis. This function contains the normal state information about the electron-phonon interaction and the phonon density of states that is essential to the Eliashberg gap equations. The results of the author's calculations of this function for aluminium are presented. Results for the anisotropy of the mass enhancement factor are also presented for the same element. In section 4.2 a simple model is used to investigate the convergence of an iteration procedure to determine the directional energy gaps $\Delta_0(\theta, \phi)$. Directional energy gaps calculated by one iteration of the Eliashberg equations are compared in section 4.3 with those calculated by one iteration of the integral equations of section 3.1. These simplified integral equations

are used to perform a second iteration. In section 4.4 an anisotropy distribution function for the energy gap in Al is calculated and the mean squared anisotropy determined. These are used to investigate the effect of anisotropy on some thermodynamic properties of superconducting Al. The temperature dependence of the anisotropy of the energy gap in Al is studied in section 4.5.

In Chapter V the results of Chapters III and IV are summarized and conclusions presented.

An appendix contains the results of a detailed study for Na, K and Rb of the anisotropy of the Legendre polynomial moments of the electron-phonon scattering function. These moments are important in the Landau-Silin theory of a charged normal Fermi liquid.

CHAPTER II

NECESSARY BACKGROUND MATERIAL

2.1 THE ONE PARAMETER MODEL OF BCS

In this very brief section we present only those results of the BCS theory that are needed in Chapters III and IV.

In the BCS theory the excitations of a superconducting system are long lived quasiparticles which have the temperature dependent dispersion relation

$$E_{\underline{k}} = (\epsilon_{\underline{k}}^2 + \Delta^2(\underline{k}, T))^{1/2} \quad (2.1)$$

$\epsilon_{\underline{k}}$ is the single-particle energy (measured relative to the Fermi level) of an electron in the Bloch state (of the normal metal) of wavevector \underline{k} and $\Delta(\underline{k}, T)$ is the temperature dependent energy gap which vanishes as the transition temperature is approached from below. The BCS integral equation for $\Delta(\underline{k}, T)$ is

$$\Delta(\underline{k}, T) = \sum_{\underline{k}'} V_{\underline{k}\underline{k}'} \frac{\Delta(\underline{k}', T)}{2E_{\underline{k}'}} \tanh(E_{\underline{k}'}/2k_B T) \quad (2.2)$$

where $V_{\underline{k}\underline{k}'}$ is the electron-electron interaction matrix element and k_B is the Boltzmann constant.

In order to calculate superconducting properties

BCS introduced the model interaction

$$V_{\underline{k}\underline{k}'} = -V \quad , \quad |\epsilon_{\underline{k}}|, |\epsilon_{\underline{k}'}| < \omega_D \quad (\hbar=1) \quad , \\ = 0 \quad \text{otherwise} \quad , \quad (2.3)$$

where ω_D is the Debye frequency. It follows from (2.2) that the model energy gap $\Delta(\underline{k}, T)$ is equal to a constant $\Delta(T)$ if $|\epsilon_{\underline{k}}| < \omega_D$ and is zero otherwise. In the weak coupling limit ($\Delta(0) \ll \omega_D$) two important results can be derived analytically. They are

$$\Delta(0) = 2\omega_D e^{-1/N(0)V} \quad (2.4)$$

and

$$k_B T_c = 1.134 \omega_D e^{-1/N(0)V} \quad , \quad (2.5)$$

where $N(0)$ is the single spin electron density of states at the Fermi level. The simple model of BCS is a one parameter model, the single parameter being $N(0)V$ or equivalently $\Delta(0)$ or T_c , and leads to a law of corresponding states for different metals.

BCS suggested that $-V$ should be the average of $V_{\underline{k}\underline{k}'}$ for scattering at the Fermi surface:

$$-V = \iint \frac{d\Omega_{\underline{k}}}{4\pi} \frac{d\Omega_{\underline{k}'}}{4\pi} V_{\underline{k}\underline{k}'} \quad , \quad (|\underline{k}| = |\underline{k}'| = k_F) \quad (2.6)$$

where

$$V_{\underline{k}\underline{k}'} = V_{\underline{k}\underline{k}'}^{\text{ph}} + V_{\underline{k}\underline{k}'}^{\text{c}} \quad . \quad (2.7)$$

$V_{\underline{k}\underline{k}'}^{\text{ph}}$ is the matrix element for the phonon mediated electron-electron interaction and $V_{\underline{k}\underline{k}'}^{\text{C}}$ is the matrix element for the repulsive screened Coulomb interaction between the electrons. However, there is no a priori reason for cutting the Coulomb interaction off at ω_D . Bogoliubov et. al. (23) considered a more realistic model interaction in which the phonon mediated interaction was still cut-off at ω_D but the screened Coulomb interaction was cut-off at E_F (because the characteristic length for the Coulomb repulsion between electrons in a metal is k_F^{-1}). They found in this way that the BCS parameter should be given by

$$N(0)V = N(0)V_{\text{ph}} - N(0)U_{\text{C}} \quad (2.8)$$

where

$$N(0)U_{\text{C}} = \frac{N(0)V_{\text{C}}}{1 + N(0)V_{\text{C}} \log(E_F/\omega_D)} \quad (2.9)$$

V_{ph} and V_{C} are the Fermi surface averages of $-V_{\underline{k}\underline{k}'}^{\text{ph}}$ and $V_{\underline{k}\underline{k}'}^{\text{C}}$ respectively.

One of the results to be presented in this thesis is a new expression for the BCS parameter $N(0)V$. This expression was derived from the Eliashberg gap equations which are the subject of the next section.

2.2 THE ELIASHBERG GAP EQUATIONS

Within the very sophisticated and very accurate 'strong

coupling' theory of superconductivity^(18,19,20) a superconductor is completely characterized by a frequency and wavevector dependent generalization, $\Delta(\omega, \underline{k})$, of the BCS energy gap and a renormalization function $Z_s(\omega, \underline{k})$. The central result of the strong coupling theory is a set of non-linear integral equations, the Eliashberg gap equations, which relate $\Delta(\omega, \underline{k})$ and $Z_s(\omega, \underline{k})$ to certain properties of the metal in its normal state. Since there are many derivations of the Eliashberg equations in the literature^(20,21,24) we simply write them down. Their one dimensional form, which is appropriate for an isotropic superconductor, is

$$\Delta(\omega) Z_s(\omega) = \int_0^{\omega_c} d\omega' \operatorname{Re} \left\{ \frac{\Delta(\omega')}{\sqrt{\omega'^2 - \Delta^2(\omega')}} \right\} [K_+(\omega, \omega') - N(0) U_c],$$

$$[1 - Z_s(\omega)] \omega = \int_0^{\omega_c} d\omega' \operatorname{Re} \left\{ \frac{\omega'}{\sqrt{\omega'^2 - \Delta^2(\omega')}} \right\} K_-(\omega, \omega') \quad , (2.10)$$

where

$$K_{\pm}(\omega, \omega') = \int_0^{\infty} dv \alpha^2(v) F(v) \left[\frac{1}{\omega' + \omega + v + i0^+} \mp \frac{1}{\omega' - \omega + v - i0^+} \right]. (2.11)$$

The essential normal state information is contained in the function

$$\alpha^2(v) F(v) = N(0) \iint \frac{d\Omega_{\underline{k}}}{4\pi} \frac{d\Omega_{\underline{k}'}}{4\pi} \sum_{\lambda} |g_{\underline{k}\underline{k}',\lambda}|^2 \delta(v - \omega_{\underline{k}-\underline{k}',\lambda}) \quad (2.12)$$

and the number⁽²³⁾

$$\mu^* \equiv N(0)U_c = \frac{N(0)V_c}{1+N(0)V_c \log(E_F/\omega_c)} \quad (2.13)$$

In (2.12), which is written for the special case of a spherical Fermi surface, $d\Omega_k \equiv \sin \theta d\theta d\phi$ is an element of area on the Fermi surface at the point $\underline{k} \equiv (k_F, \theta, \phi)$, $g_{\underline{k}\underline{k}'}^*$ is the electron-phonon coupling constant, and $\omega_{\underline{k}-\underline{k}'}^\lambda$ is the phonon frequency corresponding to the wavevector $(\underline{k}-\underline{k}')$ and polarization index λ . $\alpha^2(\nu)F(\nu)$ is an average of the square of the electron-phonon coupling constant for all those processes in which an electron scatters from any point \underline{k} on the Fermi surface to all points \underline{k}' on the Fermi surface that can be reached by the virtual emission of a single phonon of frequency ν . In (2.13) V_c is the average of the screened Coulomb interaction for scattering at the Fermi surface. The upper phonon cut-off ω_c is usually taken to be five to ten times the Debye frequency ω_D . Equation (2.13) takes Coulomb excitations in the region $\omega_c < \omega < E_F$ ($\omega_c \ll E_F$) into account. It is quite reasonable that the Coulomb interaction can be taken into account by a single number. When the normal metal becomes superconducting important modifications

* θ, ϕ are the usual polar angles and are measured relative to the [100], [010] and [001] directions which are taken as the k_x, k_y and k_z directions, respectively.

of the electronic structure occur only in a small shell in momentum space about the Fermi level. The thickness of this shell is of the order of 10 meV and is very small compared with the scale, E_F , on which the Coulomb effects vary significantly.

It should be noted that we have written down the Eliashberg equations only for the zero temperature case. The finite temperature equations are considerably more complicated and are not needed for an understanding of the original work to be presented in this thesis.

In order to calculate $\alpha^2(\nu)F(\nu)$ one needs detailed information about the lattice vibrations in the form of the phonon frequencies $\omega_{\underline{q}\lambda}$ and polarization vectors $\underline{\epsilon}(\underline{q},\lambda)$ everywhere within the first Brillouin zone. It is worth mentioning at this point that for the very low temperatures of interest in superconductivity the harmonic theory of lattice vibrations is valid to a very good approximation. Although the phonon frequencies can be calculated within pseudopotential theory it is more usual to take them from experiment. The technique of inelastic neutron scattering⁽²⁶⁾ is capable of measuring phonon dispersion curves with considerable accuracy. Although these measurements are usually made only in high symmetry directions information can be obtained for off symmetry directions by means of a Born-von Kármán force constant fit to the measurements made in the symmetry directions.

We also need the electron-phonon coupling constant.

In the one orthogonalized-plane-wave (OPW) approximation and for \underline{k} and \underline{k}' both on the Fermi surface it is given by⁽²⁵⁾

$$g_{\underline{k}\underline{k}'\lambda} = -i \frac{\underline{q} \cdot \underline{\epsilon}(\underline{q}, \lambda)}{\sqrt{2MN\omega(\underline{q}, \lambda)}} W(\underline{q}) \quad (2.14)$$

where $\underline{q} \equiv \underline{k} - \underline{k}'$, M is the ionic mass, N is the number of ions per unit volume and $W(\underline{q})$ is the pseudopotential form factor for scattering at the Fermi surface.

With the above information the Eliashberg equations can be solved by numerical iteration. Since first principle calculations of the Coulomb parameter μ^* are unreliable at present it is usual to treat it as an adjustable parameter which is varied during the iteration procedure so that the gap edge

$$\Delta_0 \equiv \text{Re}\{\Delta(\Delta_0)\} \quad (2.15)$$

is equal to the experimental value at the end of each complete iteration. Convergence is obtained when μ^* and $\Delta(\omega)$ are the same for two consecutive iterations. This converged value of μ^* is used in all subsequent calculations.

McMillan and Rowell⁽²²⁾ used the Eliashberg gap equations to extract the function $\alpha^2(\nu)F(\nu)$ and the Coulomb parameter μ^* from their superconducting tunneling data. According to tunneling theory⁽²⁰⁾ the ratio of the differential conductance in the superconducting state to that in the normal state at an applied voltage $eV = \omega$ is

$$\frac{(dI/dV)_s}{(dI/dV)_n} = \rho(\omega) \equiv \operatorname{Re}\left\{\frac{\omega}{\sqrt{\omega^2 - \Delta^2}(\omega)}\right\} \quad (2.16)$$

where $\rho(\omega)$ is the normalized single-particle tunneling density of states $N_s(\omega)/N(0)$. The function $\alpha^2(\nu)F(\nu)$ and the Coulomb parameter μ^* were adjusted until the density of states $\rho(\omega)$ emerging from the Eliashberg equations was equal to the experimental density of states for $\omega < \omega_D$. The calculated density of states was then compared with the experimental density of states in the region $\omega > \omega_D$. In this way McMillan and Rowell not only determined the normal state data needed in the theory of superconductivity for several strong coupling superconductors but also showed experimentally that the corrections to the present theory of superconductivity are not greater than a few percent. This justified the theoretical claim⁽¹⁸⁾ that the corrections to the Eliashberg gap equations were of the order of the square root of the electronic to ionic mass ratio, i.e. $(m/M)^{1/2}$.

2.3 THE MOREL-ANDERSON EQUATION AND THE MCMILLAN EQUATION

In this section we discuss very briefly two well known theoretical expressions for the transition temperature of a superconductor. Both of these expressions are similar in form to the simple BCS expression, equation (2.5), so that they can be used to identify the BCS parameter $N(0)V$ with certain normal state parameters.

Using both the deformation potential theorem⁽²⁷⁾ and

the Gorkov⁽²⁸⁾ formulation of superconductivity Morel and Anderson⁽²⁹⁾ argued that umklapp processes are no more effective than normal processes in superconductivity and that in fact only the local electron-phonon interaction, mediated by the high frequency phonons, is important in superconductivity. They further argued that the effective phonon spectrum is well approximated by an Einstein model because the high frequency phonons are sharply peaked about a few definite frequencies. Using a single Einstein peak for the effective phonon spectrum they obtained an approximate solution for the transition temperature within the strong coupling formalism which correctly takes into account the retarded nature of the electron-phonon interaction. They included in their calculation an instantaneous Coulomb repulsion between the electrons and showed that the Bogoliubov expression for μ^* , equation (2.9), is a consequence of the different frequency dependences of the electron-phonon and Coulomb interactions. That is, they showed that the weakening of the Coulomb interaction relative to the retarded electron-phonon interaction is a result of its instantaneous nature. Their result for the transition temperature is

$$k_B T_C = 1.14 \omega_D e^{-1/(\lambda - \mu^*)} \quad (2.17)$$

where λ is the electron-phonon mass-enhancement parameter which is given by

$$\lambda = 2 \int \frac{d\nu}{\nu} \alpha^2(\nu) F(\nu) \quad (2.18)$$

It is assumed in (2.17) that the Einstein peak is at ω_D .
Morel and Anderson made the identification

$$N(0)V = \lambda - \mu^* \quad (2.19)$$

We now describe in some detail the derivation of the McMillan equation. The Eliashberg equations at the transition temperature are

$$\begin{aligned} \Delta(\omega)Z(\omega) &= \int_0^\infty \frac{d\omega'}{\omega'} \operatorname{Re}\{\Delta(\omega')\} \int_0^{\omega_0} d\nu \alpha^2(\nu)F(\nu) \{ [N(\nu)+f(-\omega')] \\ &\times \left[\frac{1}{\omega'+\nu+\omega} + \frac{1}{\omega'+\nu-\omega} \right] - [N(\nu)+f(\omega')] \left[\frac{1}{-\omega'+\nu+\omega} \right. \\ &\left. + \frac{1}{-\omega'+\nu-\omega} \right] \} - N(0)V_c \int_0^{E_B} \frac{d\omega'}{\omega'} \operatorname{Re}\{\Delta(\omega')\} [1-2f(\omega')], \\ [1-Z(\omega)]\omega &= \int_0^\infty d\omega' \int_0^{\omega_0} d\nu \alpha^2(\nu)F(\nu) \{ [N(\nu)+f(-\omega')] \\ &\times \left[\frac{1}{\omega'+\nu+\omega} - \frac{1}{\omega'+\nu-\omega} \right] + [N(\nu)+f(\omega')] \\ &\times \left[\frac{1}{-\omega'+\nu+\omega} - \frac{1}{-\omega'+\nu-\omega} \right] \} \end{aligned} \quad (2.20)$$

where ω_0 is the maximum phonon frequency, E_B is the electronic band width and $N(\omega)$ and $f(\omega)$ are the Bose and Fermi functions $[\exp(\omega/k_B T_c) + 1]^{-1}$ respectively.

McMillan assumed a trial solution of the form

$$\begin{aligned}\Delta(\omega) &= \Delta_0, & 0 < \omega < \omega_0 \\ &= \Delta_\infty, & \omega > \omega_0\end{aligned}\quad .(2.21)$$

He substituted this trial solution into the right hand side of (2.20) and required that

$$\Delta(0) = \Delta_0,$$

and
$$\Delta(\infty) = \Delta_\infty \quad .(2.22)$$

He neglected thermal phonons and in the integrals over ω' neglected ω' with respect to ν (ν with respect to ω') in the phonon propagators $[\pm\omega'+\nu]^{-1}$ when the range of integration was $0 < \omega' < \omega_0$ ($\omega_0 < \omega'$). In this way he obtained the approximate theoretical expression

$$k_B T_c = \omega_0 e^{-\frac{1+\lambda}{\lambda-\mu^* - (\langle\omega\rangle/\omega_0)\lambda\mu^*}} \quad , (2.23)$$

where $\langle\omega\rangle$ is defined by

$$\langle\omega\rangle = 2 \int_0^{\omega_0} d\nu \alpha^2(\nu) F(\nu) / \lambda \quad .(2.24)$$

The next step in McMillan's procedure was to solve the Eliashberg equation numerically and to fit the solution to the theoretical formula, equation (2.23). For this work

$F(\nu)$ was chosen to be the experimental phonon density of states of Nb and $\alpha^2(\nu)$ was taken to be

$$\begin{aligned}\alpha^2(\nu) &= \alpha^2 & \nu > 100^\circ\text{K} \\ &= 0 & \nu < 100^\circ\text{K}\end{aligned}\quad .(2.25)$$

T_c and μ^* were fixed and the Eliashberg equations were iterated. α^2 was adjusted at the end of each iteration so that $\Delta(0)$ remained fixed. When convergence was reached the solution was fitted to equation (2.23). This was repeated for several values of T_c and μ^* . A good fit to the various sets of data was obtained with the formula

$$k_B T_c = \frac{\theta_D}{1.45} e^{-\frac{1.04(1+\lambda)}{\lambda - \mu^*(1+0.62\lambda)}}\quad .(2.26)$$

This is the well known McMillan formula. It has been found to work quite well for some superconductors but fails badly for others, for example Hg and amorphous Ga.

2.4 ANISOTROPY OF THE SUPERCONDUCTING ENERGY GAP

The superconducting energy gap associated with an electronic state of momentum \underline{k} depends on the orientation of \underline{k} with respect to the crystallographic axes. This energy gap anisotropy arises from a number of sources, the more important of which are: anisotropy in the phonon spectrum, distortions of the Fermi surface from sphericity, and anisotropy in the single spin electron density of states at

the Fermi surface. In a pure single-crystal superconductor the electrons are able to take maximum advantage of the anisotropy in the effective electron-electron interaction in forming pairs. In a 'dirty' superconductor⁽¹³⁾, that is a superconductor containing appreciable amounts of physical or chemical impurities, an electron is rapidly scattered about the Fermi surface. The effect of this smearing of electronic states over the Fermi surface is that the electrons are no longer able to take full advantage of the anisotropy in forming pairs. Hence the effect of impurities is to weaken superconductivity. Another effect of the smearing of the electronic states over the Fermi surface is that the experimentally observed energy gap for a 'dirty' superconductor is essentially isotropic.

Markowitz and Kadanoff⁽³¹⁾ were able to account theoretically for the experimentally observed effect of impurities upon the critical temperature^(32,33,34). They considered the simplest possible model (which exhibited anisotropy) for the pairing potential. This was the factorable potential

$$V_{\underline{k}\underline{k}'} = (1+a(\Omega)) V(1+a(\Omega')) \quad (2.27)$$

where Ω and Ω' are the angular coordinates of \underline{k} and \underline{k}' . Using this model interaction they showed (within the strong coupling formalism) that the transition temperature of a

pure single-crystal is given by

$$k_B T_c = 1.14 \omega_D e^{-\frac{1}{(1+\langle a^2 \rangle) N(0) V}} \quad (2.28)$$

where

$$\langle a^2 \rangle \equiv \int \frac{d\Omega}{4\pi} a^2(\Omega) \quad (2.29)$$

while that of an isotropic or 'dirty' superconductor is given by the usual BCS result

$$k_B T_c = 1.14 \omega_D e^{-\frac{1}{N(0) V}}$$

Clem⁽³⁵⁾ used the factorable interaction matrix element of Markowitz and Kadanoff to investigate (within the weak coupling formalism of BCS) the effects of energy gap anisotropy upon the thermodynamic properties of pure single-crystal superconductors. He showed that within this model the directional energy gap is

$$\Delta(\Omega) = \langle \Delta(\Omega) \rangle (1+a(\Omega)) \quad (2.30)$$

where the average energy gap is given by

$$\langle \Delta(\Omega) \rangle \equiv \int \frac{d\Omega}{4\pi} \Delta(\Omega) = \left(1 + \left(\frac{1}{N(0) V} - \frac{3}{2}\right) \langle a^2 \rangle\right) 2\omega_D e^{-\frac{1}{N(0) V}}, \quad (2.31)$$

to lowest order in the anisotropy. He introduced an anisotropy distribution function $P(a)$ by defining $P(a)da$ to be the fraction of the Fermi surface for which the anisotropy

function $a(\Omega)$ has a value between a and $a+da$. Knowledge of this function and of the average energy gap is all that is needed to calculate some thermodynamic properties such as the low temperature specific heat and nuclear spin-lattice relaxation rate. Clem calculated both of these properties for various values of the parameter $\langle a^2 \rangle$ using a rectangular model for the distribution function $P(a)$. His model is

$$P(a) = \frac{1}{(2\sqrt{3}\langle a^2 \rangle)^{-1}}, \quad a_{\min} < a < a_{\max},$$

$$= 0 \quad \text{otherwise}$$

where a_{\min} and a_{\max} are the minimum and maximum values of $a(\Omega)$ encountered anywhere on the Fermi surface. Experimental results⁽³⁶⁾ for the variation of the low temperature specific heat with impurity concentration are in qualitative agreement with Clem's theory.

Bennett's first-order calculation of the directional energy gap in lead⁽³⁷⁾ was the first realistic calculation of gap anisotropy. He assumed that the anisotropy in the phonon density of states was the dominant source of gap anisotropy and neglected all other sources (the effect of energy-band structure was included as a perturbation after the major calculation involving just the anisotropic phonon density of states was performed). Bennett reduced the three dimensional strong coupling integral equations for the directional energy gap $\Delta(\omega, \theta, \phi)$ to one dimensional integrals

by assuming that in a first-order calculation whenever $\Delta(\omega, \theta', \phi')$ appeared in an integrand it could be replaced by the isotropic gap, $\Delta(\omega)$, for dirty lead. With this assumption the energy gap anisotropy was directly related to the anisotropy $[K_{\pm}(\omega, \omega', \theta, \phi) - K_{\pm}(\omega, \omega')]$ in the phonon kernels. The anisotropic phonon kernels are given by

$$K_{\pm}(\omega, \omega', \theta, \phi) = \int_0^{\infty} d\nu \alpha^2 F(\nu, \theta, \phi) \left[\frac{1}{\omega' + \omega + \nu + i0^+} \pm \frac{1}{\omega' - \omega + \nu - i0^+} \right] \quad (2.32)$$

where

$$\alpha^2 F(\nu, \theta, \phi) = N(0) \int \frac{d\Omega_{\mathbf{k}'}}{4\pi} \sum_{\lambda} |g_{\mathbf{k}\mathbf{k}', \lambda}|^2 \delta(\nu - \omega_{\mathbf{k} - \mathbf{k}', \lambda})^* \quad (2.33)$$

The above features of Bennett's calculation were followed in our calculation of the energy gap anisotropy in aluminium. We now continue with the discussion of Bennett's work emphasizing the improvements that we have incorporated in our work. The electron-phonon coupling involves the phonon frequencies and eigenvectors and hence is highly anisotropic. Bennett ignored this source of anisotropy and considered only the anisotropy in the directional phonon frequency distribution $F(\nu, \theta, \phi)$. He took $\alpha^2(\nu, \theta, \phi)$ to be a constant

* For convenience we have written $\alpha^2(\nu, \theta, \phi)F(\nu, \theta, \phi)$ as $\alpha^2 F(\nu, \theta, \phi)$. We do not imply that $\alpha^2(\nu, \theta, \phi)$ is independent of frequency and direction as it is in Bennett's work.

independent of frequency and direction. Furthermore he assumed that the electron-phonon coupling was the same for all polarizations. These simplifications were not made in our work. Bennett expanded the phonon frequencies in a series of Kubic harmonics. The series was truncated after the first three terms and the three expansion coefficients (for each value of the wavevector \underline{q} and each polarization index λ) were obtained by fitting to the experimental dispersion curves measured in the three principal symmetry directions by means of inelastic neutron scattering. $F(\nu, \theta, \phi)$ was calculated and then expanded in the first three Kubic harmonics. As a consequence the calculation of the directional energy gap reduced to the determination of the coefficients of an expansion of $\Delta(\omega, \theta, \phi)$ in terms of the first three Kubic harmonics. It is perfectly legitimate to expand the energy gap in terms of Kubic harmonics but it is not at all obvious that it is a good approximation to truncate the expansion after the first three terms. In our work we did not employ Kubic harmonics. Instead we calculated the phonon frequencies and eigenvectors for non-symmetry directions using a Born-von Kármán force constant fit to the dispersion curves measured in the high symmetry directions. The directional energy gaps were calculated at a large number of points on the irreducible $(\frac{1}{48})$ th of the Fermi surface. It was not possible to obtain even a good qualitative fit to these gaps using the lowest three Kubic harmonics. The above are significant improvements in Bennett's method of calculating

the energy gap anisotropy and are the justification for the large amount of computer time used in our calculations.

CHAPTER III

A CONTRIBUTION TO THE THEORY OF A WEAK COUPLING SUPERCONDUCTOR

3.1 THE ENERGY GAP OF AN ISOTROPIC WEAK COUPLING SUPERCONDUCTOR

In this section we derive a very simple expression for the energy gap at the gap edge, $\text{Re}\{\Delta(\Delta_0)\} = \Delta_0$, of an isotropic or 'dirty' weak coupling superconductor at zero temperature, by introducing certain simplifying approximations into the Eliashberg gap equations.

At low temperatures an electronic state has a long lifetime if its excitation energy is much less than a typical phonon energy (of order ω_D). For a weak coupling superconductor the gap parameter, Δ_0 , is much less than a typical phonon energy so that the energy gap, $\Delta(\Delta_0)$, and the renormalization function at the gap edge, $Z_S(\Delta_0)$, are real to a very good approximation. Hence the Eliashberg gap equations for the energy gap at the gap edge reduce to

$$\Delta_0 Z_S(\Delta_0) = \int_0^{\omega_c} d\omega' \text{Re}\left\{\frac{\Delta(\omega')}{\sqrt{\omega'^2 - \Delta^2(\omega')}}\right\} [K_+^R(\Delta_0, \omega') - N(0)U_c] \quad , (3.1)$$

$$[1 - Z_S(\Delta_0)]\Delta_0 = \int_0^{\infty} d\omega' \text{Re}\left\{\frac{\omega'}{\sqrt{\omega'^2 - \Delta^2(\omega')}}\right\} K_-^R(\Delta_0, \omega') \quad , (3.2)$$

where the real parts of the kernels are given by

$$K_{\pm}^R(\Delta_0, \omega') = P \int_0^{\infty} dv \alpha^2(v) F(v) \left[\frac{1}{\omega' + \Delta_0 + v} \pm \frac{1}{\omega' - \Delta_0 + v} \right], \quad (3.3)$$

and

$$\alpha^2(v) F(v) = N(0) \int \int \frac{d\Omega_{\mathbf{k}}}{4\pi} \frac{d\Omega_{\mathbf{k}'}}{4\pi} \sum_{\lambda} |g_{\mathbf{k}\mathbf{k}',\lambda}|^2 \delta(v - \omega_{\mathbf{k}-\mathbf{k}',\lambda}) \quad (3.4)$$

The Coulomb pseudopotential parameter is given by (24,29)

$$\mu^* \equiv N(0) U_c = \frac{N(0) V_c}{1 + N(0) V_c \log(E_F / \omega_c)} \quad (3.5)$$

where V_c is the average of the screened Coulomb potential for scattering at the Fermi surface.

We assume that in calculating Δ_0 for a weak coupling superconductor we can ignore damping and detailed retardation effects. That is, we assume that $\Delta(\omega')$ is real and we include only its gross frequency dependence. We assume that $\Delta(\omega')$ has the form

$$\begin{aligned} \Delta(\omega') &= \Delta_0, \quad \Delta_0 \leq \omega' \leq \omega_c, \\ &= \Delta_c, \quad \omega' > \omega_c, \end{aligned} \quad (3.6)$$

where Δ_c is given by (38)

$$\Delta_c = -\mu^* \log\left(\frac{2\omega_c}{\Delta_0}\right) \Delta_0 \quad (3.7)$$

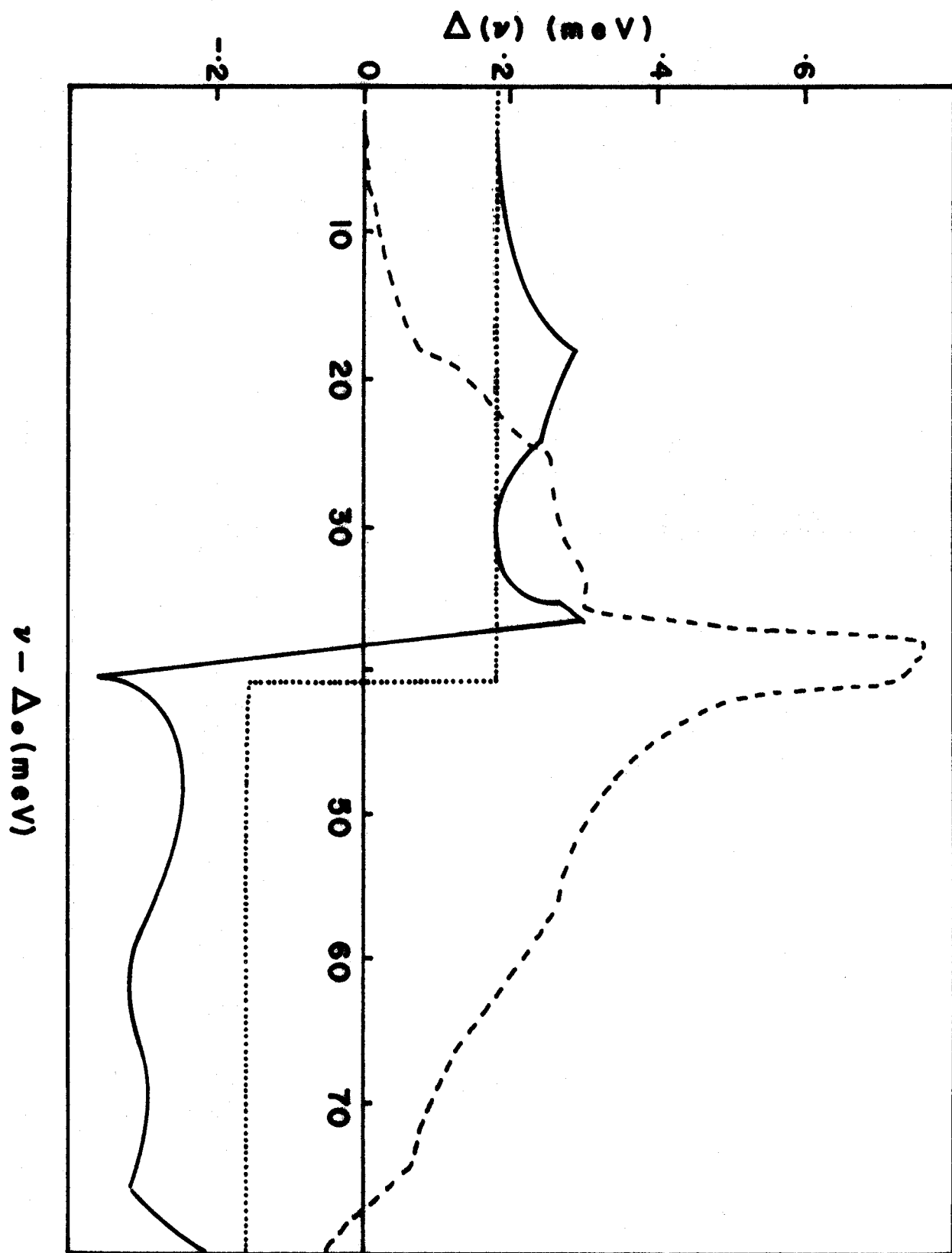
and where ω_c is the highest phonon frequency, i.e. the high frequency cut-off of the function $\alpha^2(\nu)F(\nu)$. We know from detailed solutions of the Eliashberg gap equations for a weak coupling superconductor⁽²⁵⁾ that, for small ω' , the imaginary part of $\Delta(\omega')$ is very small and the real part depends only slightly on ω' . Because of this, approximation (3.6) is a reasonable one for the purpose of calculating Δ_0 . Small values of ω' are weighted heavily in the integrand of (3.1). Equation (3.2) depends on $\Delta(\omega')$ only through the quasiparticle density of states⁽²⁰⁾

$$\rho(\omega') \equiv \text{Re}\left\{\frac{\omega'}{\sqrt{\omega'^2 - \Delta^2(\omega')}}\right\}$$

Hence for a weak coupling superconductor (3.2) is very insensitive to $\Delta(\omega')$ in the region, $\omega' \gg \Delta_0$, where $\Delta(\omega')$ deviates significantly from our model solution, equation (3.6). This is reflected in the fact that, at the present time, the tunneling experiments are not sufficiently accurate to yield the function $\alpha^2(\nu)F(\nu)$ for a weak coupling superconductor, such as aluminium, by inversion of the Eliashberg gap equations^(21,22).

Figure (3.1) shows the real and imaginary parts of the energy gap in aluminium as calculated in reference 25. Also shown is our model solution (3.6). Although our model energy gap looks considerably different from the actual energy gap for $\omega' \gg \Delta_0$ it must be remembered that the Eliashberg

FIGURE 3.1 The real (solid line) and imaginary (dashed line) parts of the energy gap, $\Delta(\nu) = \Delta_1(\nu) + i\Delta_2(\nu)$, for aluminium as calculated in reference (25). Also shown, the model energy gap (3.6) used extensively in this work (dotted line). $\nu - \Delta_0$ is the energy measured relative to the gap edge. For the model energy gap the gap edge, Δ_0 , is .180 meV, the high frequency cut-off, ω_c , is 41.4 meV and the Coulomb pseudopotential parameter, μ^* , is .14.



equations are not very sensitive to the detailed behaviour of $\Delta(\omega')$ in this region, especially to that of the imaginary part.

Using the assumed form for $\Delta(\omega')$ we obtain

$$\begin{aligned}
 -\mu^* \int_0^{\omega_c} d\omega' \operatorname{Re} \left\{ \frac{\Delta(\omega')}{\sqrt{\omega'^2 - \Delta^2(\omega')}} \right\} &= -\mu^* \int_{\Delta_0}^{\omega_c} d\omega' \frac{\Delta_0}{\sqrt{\omega'^2 - \Delta_0^2}} \\
 &= -\mu^* \log \left(\frac{2\omega_c}{\Delta_0} \right) \Delta_0, \quad (\Delta_0 \ll \omega_c) \quad ; (3.8)
 \end{aligned}$$

$$\begin{aligned}
 \int_0^{\infty} d\omega' \operatorname{Re} \left\{ \frac{\omega'}{\sqrt{\omega'^2 - \Delta^2(\omega')}} \right\} K_-^R(\Delta_0, \omega') &= -2 \left[\int_{\Delta_0}^{\omega_c} d\omega' \frac{\omega'}{\sqrt{\omega'^2 - \Delta_0^2}} \right. \\
 \times P \int_0^{\omega_c} d\nu \frac{\alpha^2(\nu) F(\nu)}{(\omega'+\nu)^2 - \Delta_0^2} &+ \left. \int_{\omega_c}^{\infty} d\omega' \int_0^{\omega_c} d\nu \frac{\alpha^2(\nu) F(\nu)}{(\omega'+\nu)^2} \right] \Delta_0 \quad . (3.9)
 \end{aligned}$$

The second term in the above expression has been simplified by using the fact that $\omega' \gg \Delta_0, |\Delta_c|$ in the range of integration $\omega_c < \omega' < \infty$.

$$\begin{aligned}
 \int_0^{\omega_c} d\omega' \operatorname{Re} \left\{ \frac{\Delta(\omega')}{\sqrt{\omega'^2 - \Delta^2(\omega')}} \right\} K_+^R(\Delta_0, \omega') &= 2 \int_{\Delta_0}^{\omega_c} \frac{d\omega'}{\sqrt{\omega'^2 - \Delta_0^2}} \\
 \times P \int_0^{\omega_c} d\nu \alpha^2(\nu) F(\nu) \frac{(\omega'+\nu)\Delta_0}{(\omega'+\nu)^2 - \Delta_0^2} & \\
 &= 2N(0) \iint \frac{d\Omega_{\mathbf{k}}}{4\pi} \frac{d\Omega_{\mathbf{k}'}}{4\pi} \int_0^{\omega_c} \frac{d\varepsilon'}{\varepsilon'} \sum_{\lambda} |g_{\mathbf{k}\mathbf{k}'\lambda}|^2 \frac{(\varepsilon'+\omega_{\mathbf{k}-\mathbf{k}'\lambda})\Delta_0}{(\varepsilon'+\omega_{\mathbf{k}-\mathbf{k}'\lambda})^2 - \Delta_0^2} \quad . (3.10)
 \end{aligned}$$

In (3.10) $\epsilon' \equiv \sqrt{\omega'^2 - \Delta_0^2}$ is the free particle kinetic energy measured relative to the Fermi energy and $E' \equiv \sqrt{\epsilon'^2 + \Delta_0^2}$ is the quasiparticle energy. We have introduced the definition of $\alpha^2(\nu)F(\nu)$, equation (3.4), into equation (3.10) and transformed to the kinetic energy variable ϵ' in order to make explicit an approximation that might go unnoticed otherwise.

Let us consider the integral over ϵ' in equation (3.10) for fixed directions of \underline{k} and \underline{k}' . If we take into account the fact that the variation of $\omega_{\underline{k}-\underline{k}',\lambda}$ and $g_{\underline{k}\underline{k}',\lambda}$ with $\epsilon' \equiv k'^2/2m$ is negligible in the very thin shell $-\omega_c < \epsilon' < \omega_c$ ($\omega_c \ll E_F$) for the momentum transfers, $\underline{q} \equiv \underline{k}-\underline{k}'$, of importance in superconductivity, we can do the integral over ϵ' analytically. Small momentum transfers are unimportant in superconductivity for two reasons: 1) the square of the electron-phonon coupling constant goes to zero as q for small q ,

i.e.
$$|g_{\underline{q}\lambda}|^2 \propto |\underline{q} \cdot \underline{\epsilon}_\lambda(\underline{q})|^2 / \omega_{\underline{q}\lambda}$$

where $\omega_{\underline{q}\lambda} \propto q$ for small q ; 2) the phonon density of states goes to zero as ω^2 for small ω and hence the number of available normal modes of the system of ions that can be excited with an electron momentum transfer \underline{q} is very severely restricted for small q . We define k'_{\min} and k'_{\max} by

$$E_F - \omega_c = \frac{k'_{\min}{}^2}{2m}, \quad E_F + \omega_c = \frac{k'_{\max}{}^2}{2m}.$$

In doing the integral over ε' , k' varies over the range $k'_{\min} < k' < k'_{\max}$. Since $(k'_{\max} - k'_{\min}) \ll k_F = O(k_D)$, $\omega_{\underline{k}-\underline{k}'\lambda}$ and $g_{\underline{k}\underline{k}'\lambda}$, for the momentum transfers of interest, do not vary significantly over the range of k' encountered in the ε' integral and can be evaluated at $|\underline{k}'| = k_F$ and treated as constants when doing the integral.

It is usual, for convenience in numerical calculations, to take advantage of the fact that the phonon density of states is very small at low ω by cutting the density of states off at some small value of ω . We use a cut-off, $\omega^* = 2\Delta_0$, which for a weak coupling superconductor, is much smaller than the most important phonon frequencies (this is certainly not the case for a strong coupling superconductor). We note that Morel and Anderson⁽²⁹⁾, in their derivation of a simple expression for T_c , carried the importance of the high frequency phonons to an extreme in assuming that the effective phonon density of states could be approximated by an Einstein model with a delta function at the longitudinal phonon peak. Our low frequency cut-off at ω^* greatly simplifies the calculation without leaving out any important phonons. Of course, the results are not sensitive to the exact cut-off as long as it is sufficiently small.

The ω' integrals can be reduced to standard forms after a few transformations. Each ω' integral has two analytical solutions, one appropriate for $\nu < 2\Delta_0$ and the other for $\nu > 2\Delta_0$. Since the region $\nu < 2\Delta_0$ is unimportant

for a weak coupling superconductor we cut the phonon spectrum, and hence $\alpha^2 F$, off at a frequency $\omega^* = 2\Delta_0$. Hence we need only the solutions for $\nu > 2\Delta_0$. These are

$$2 \int_{\Delta_0}^{\omega_c} \frac{d\omega'}{\sqrt{\omega'^2 - \Delta_0^2}} \frac{\omega' + \nu}{(\omega' + \nu)^2 - \Delta_0^2} = K(\nu, \omega_c, \Delta_0) ,$$

$$K(\nu, \omega_c, \Delta_0) \equiv \sum_{i=1}^2 \frac{1}{\sqrt{p_i^2 - \Delta_0^2}} \log \left\{ \frac{\omega_c + p_i - \sqrt{\omega_c^2 - \Delta_0^2} + \sqrt{p_i^2 - \Delta_0^2}}{\omega_c + p_i - \sqrt{\omega_c^2 - \Delta_0^2} - \sqrt{p_i^2 - \Delta_0^2}} \right. \\ \left. \times \frac{\Delta_0 + p_i - \sqrt{p_i^2 - \Delta_0^2}}{\Delta_0 + p_i + \sqrt{p_i^2 - \Delta_0^2}} \right\} \quad (3.11)$$

and

$$2 \int_{\Delta_0}^{\omega_c} \frac{d\omega'}{\sqrt{\omega'^2 - \Delta_0^2}} \frac{\omega'}{(\omega' + \nu)^2 - \Delta_0^2} = L(\nu, \omega_c, \Delta_0) ,$$

$$L(\nu, \omega_c, \Delta_0) \equiv \frac{1}{\Delta_0} \sum_{i=1}^2 (-1)^{i+1} \frac{p_i}{\sqrt{p_i^2 - \Delta_0^2}} \log \left\{ \frac{\omega_c + p_i - \sqrt{\omega_c^2 - \Delta_0^2} + \sqrt{p_i^2 - \Delta_0^2}}{\omega_c + p_i - \sqrt{\omega_c^2 - \Delta_0^2} - \sqrt{p_i^2 - \Delta_0^2}} \right. \\ \left. \times \frac{\Delta_0 + p_i - \sqrt{p_i^2 - \Delta_0^2}}{\Delta_0 + p_i + \sqrt{p_i^2 - \Delta_0^2}} \right\} \quad (3.12)$$

In (3.11) and (3.12) $p_1 \equiv \nu + \Delta_0$; $p_2 \equiv \nu - \Delta_0$.

Combining equations (3.1), (3.2), (3.8), (3.9), (3.10)

(3.11) and (3.12) we obtain a greatly simplified approximate set of Eliashberg gap equations for the gap at the gap edge in a weak coupling superconductor. These are

$$\Delta_0 Z_S(\Delta_0) = \left\{ \int_0^{\omega_C} dv \alpha^2(v) F(v) K(v, \omega_C, \Delta_0) - \mu^* \log\left(\frac{2\omega_C}{\Delta_0}\right) \right\} \Delta_0 \quad , (3.13)$$

$$Z_S(\Delta_0) = 1 + \int_0^{\omega_C} dv \alpha^2(v) F(v) \left[L(v, \omega_C, \Delta_0) + \frac{2}{v + \omega_C} \right] \quad . (3.14)$$

This set of equations can be iterated to convergence in a very short time on an electronic computer. It takes one or two seconds to obtain convergence to .01% (starting from a reasonable trial solution) on the CDC 6400.

We now derive an approximate analytical solution to (3.13) and (3.14) which is valid if the most important phonon frequencies are much larger than Δ_0 for the metal under consideration.

For a weak coupling superconductor, $Z_S(\omega)$ is a slowly varying function of ω for small ω . Since Δ_0 is very small for a weak coupling superconductor, we can, to a good approximation, replace $Z_S(\Delta_0)$ by $Z_n(0)$, the zero frequency normal state renormalization function. $Z_n(0)$ is given by the well known expression⁽²¹⁾

$$Z_n(0) = 1 + \lambda \quad , (3.15)$$

where

$$\lambda \equiv 2 \int \frac{dv}{v} \alpha^2(v) F(v) \quad .(3.16)$$

(3.15) and (3.16) are obtained by setting $\Delta(\omega') = 0$ in equation (3.2). Table (3.1) contains $Z_n(0)$ calculated using equations (3.15) and (3.16) and $Z_s(\Delta_0)$ calculated using (3.13) and (3.14) for a weak coupling superconductor (Al) and three medium coupling superconductors (Tl, In, Sn). The details of the calculation will be given later. It is seen that replacing $Z_s(\Delta_0)$ by $Z_n(\Delta_0)$ is indeed a good approximation for the superconductors of interest here.

TABLE 3.1

COMPARISON OF THE SUPERCONDUCTING AND NORMAL STATE
RENORMALIZATION PARAMETERS

ELEMENT	$Z_n(0)$	$Z_s(\Delta_0)$	$\frac{Z_n(0)}{Z_s(\Delta_0)}$
Al	1.463	1.462	1.001
Tl	1.774	1.761	1.007
In	1.822	1.805	1.009
Sn	1.787	1.777	1.006

Equation (3.13) is not so easily disposed of. We first obtain a much simpler expression for $K(v, \omega_c, \Delta_0)$, which

is a very good approximation for all important values of ν (i.e. $\nu \gg \Delta_0$). We expand the right hand side of (3.11) in terms of the small quantity (Δ_0/ν) to obtain, after a good deal of algebra,

$$K(\nu, \omega_c, \Delta_0) = \frac{2}{\nu} \log\left(\frac{2\nu}{\Delta_0(1+\nu/\omega_c)}\right) + O\left(\left(\frac{\Delta_0}{\nu}\right)^2\right) .$$

Our approximate expression for $K(\nu, \omega_c, \Delta_0)$ is then

$$\tilde{K}(\nu, \omega_c, \Delta_0) \equiv \frac{2}{\nu} \log\left(\frac{2\nu}{\Delta_0(1+\nu/\omega_c)}\right) \quad .(3.17)$$

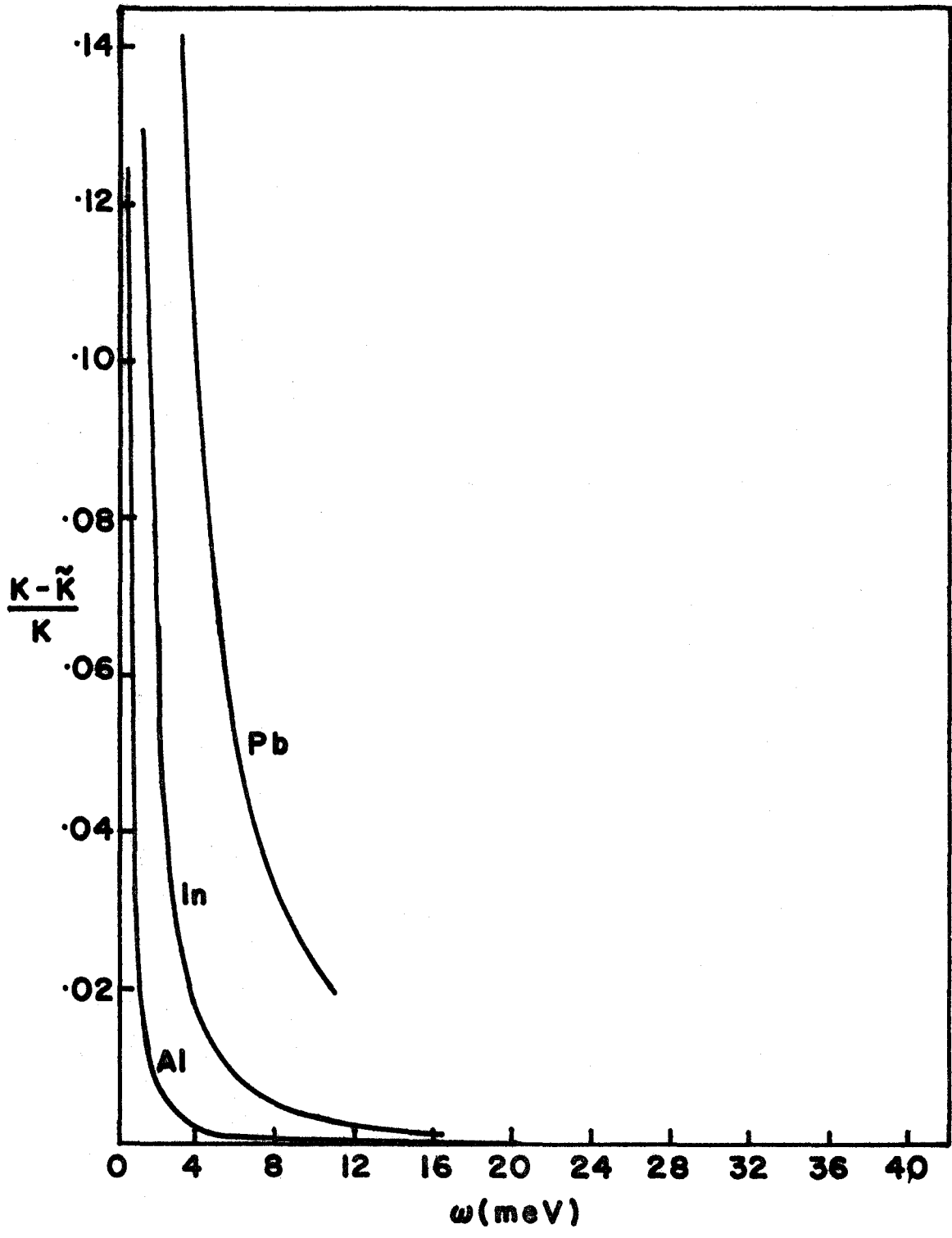
Figure 3.2 is a plot of the relative error, $(K-\tilde{K})/\tilde{K}$, versus phonon frequency ν , for $\omega^* < \nu < \omega_c$, for a weak coupling (Al), medium coupling (In), and a strong coupling superconductor (Pb). It is clear from the graph that \tilde{K} is a very good approximation to K for a weak coupling superconductor, a fairly good approximation for a medium coupling superconductor, but a poor one for a strong coupling superconductor.

If we substitute (3.17) into (3.13) we obtain

$$\Delta_0 = \frac{1}{1+\lambda} \left\{ 2 \int_0^{\omega_c} \frac{d\nu}{\nu} \alpha^2(\nu) F(\nu) \log\left(\frac{\nu/\omega_c}{1+\nu/\omega_c}\right) + \left[2 \int_0^{\omega_c} \frac{d\nu}{\nu} \alpha^2(\nu) F(\nu) - \mu^* \right] \right. \\ \left. \times \log\left(\frac{2\omega_c}{\Delta_0}\right) \right\} \Delta_0 \quad .(3.18)$$

We recall that the renormalization parameter, λ , is given

FIGURE 3.2 The relative error $(K-\tilde{K})/K$ versus phonon frequency ω . The low frequency cut-offs are .36 meV, 1.08 meV and 2.77 meV for Al, In and Pb respectively. The high frequency cut-offs are 41.4 meV, 16.2 meV and 11.0 meV for Al, In and Pb respectively.



by

$$\lambda \equiv 2 \int_0^{\omega_c} \frac{d\nu}{\nu} \alpha^2(\nu) F(\nu)$$

and define a new parameter, $\bar{\lambda}$, by the equation

$$\bar{\lambda} \equiv 2 \int_0^{\omega_c} \frac{d\nu}{\nu} \alpha^2(\nu) F(\nu) \log\left(\frac{\nu/\omega_c}{1+\nu/\omega_c}\right) \quad .(3.19)$$

We assume that Δ_0 is non zero so that it can be cancelled from both sides of (3.18). Substituting (3.16) and (3.19) into the resulting equation and solving for Δ_0 we obtain the very simple result

$$\Delta_0 = 2\omega_c e^{-\frac{1+\lambda-\bar{\lambda}}{\lambda-\mu^*}} \quad .(3.20)$$

This equation is the basis for much of the work to follow.

The usual BCS result for the energy gap in a weak coupling superconductor⁽¹¹⁾ is

$$\Delta_0 = 2\omega_D e^{-\frac{1}{N(0)V}} \quad , (3.21)$$

where V is the average effective electron-electron interaction for scattering at the Fermi surface. Our result is formally identical with this result and suggests that, to the extent that ω_c and ω_D are the same, the BCS parameter, $N(0)V$, should be given by

$$N(0)V = \frac{\lambda-\mu^*}{1+\lambda-\bar{\lambda}} \quad .(3.22)$$

Since $\bar{\lambda}$ is comparable in magnitude to λ but of opposite sign there is no cancellation between λ and $\bar{\lambda}$ in the denominator of (3.22) so that our expression for $N(0)V$ is quite different from the Morel-Anderson result⁽²⁹⁾

$$[N(0)V]^{MA} = \lambda - \mu^* \quad .(3.23)$$

If we renormalize the Morel-Anderson result by introducing the renormalization parameter $Z_n(0) \equiv 1 + \lambda$ into their analysis we obtain

$$[N(0)V]_Z^{MA} = \frac{\lambda - \mu^*}{1 + \lambda} \quad .(3.24)$$

This equation falls out of our analysis if we make one further approximation. Essentially the same approximation was made by McMillan⁽³⁰⁾ in the derivation of his equation for T_c for a strong coupling superconductor. Consider the integral

$$\int_{\Delta_0}^{\omega_c} \frac{d\omega'}{\sqrt{\omega'^2 - \Delta_0^2}} \frac{(\omega' + \nu)}{(\omega' + \nu)^2 - \Delta_0^2}$$

which we have evaluated analytically. One can argue that since small values of ω' are weighted heavily in the integrand and since the important phonon frequencies, ν , are large we can neglect ω' and Δ_0 in comparison with ν to obtain

$$\int_{\Delta_0}^{\omega_c} \frac{d\omega'}{\sqrt{\omega'^2 - \Delta_0^2}} \frac{(\omega' + \nu)}{(\omega' + \nu)^2 - \Delta_0^2} \approx \frac{1}{\nu} \int_{\Delta_0}^{\omega_c} \frac{d\omega'}{\sqrt{\omega'^2 - \Delta_0^2}} \approx \frac{1}{\nu} \log\left(\frac{2\omega_c}{\Delta_0}\right) .$$

With this rather crude approximation* we readily obtain the Morel-Anderson result, equation (3.24).

Table (3.2) is a comparison of the values of $N(0)V$ given by the three equations (3.22), (3.23) and (3.24) for Al, Tl, In, Sn, Zn and Pb. (We have included results for Pb even though the approximations that we have made are not justified for a strong coupling superconductor.) A discussion of our choice of the parameters λ , $\bar{\lambda}$ and μ^* , used in calculating $N(0)V$, will be given later. We just note at this point that the value of μ^* occurring in (3.23) and (3.24) is not exactly the same as the value occurring in (3.22). The ratio of the two values of μ^* is given by equation (3.5) to be

$$\frac{1+N(0)V_c \log(E_F/\omega_c)}{1+N(0)V_c \log(E_F/\omega_D)}$$

Since ω_c is roughly the same as ω_D the difference between the two values of μ^* is negligible, at least for a qualitative comparison of the different expressions for $N(0)V$, and is ignored. Table 3.2 also contains the experimental values of $N(0)V$. $[N(0)V]_{\text{Exp}}^{\text{MA}}$ is taken from reference (15) and is obtained by fitting the BCS equation

$$k_B T_c = 1.134 \omega_D e^{-\frac{1}{N(0)V}}$$

* It is a good approximation only if $\log(2\omega_c/\Delta_0)\lambda \gg -\bar{\lambda}$ which would be realized only for an extremely weak coupling superconductor.

to the experimental transition temperature. $[N(0)V]_{\text{Exp}}$ is obtained by fitting the equation

$$\Delta_0 = 2\omega_c e^{-\frac{1}{N(0)V}}$$

to the experimental energy gap Δ_0^{Exp} . The difference between $[N(0)V]_{\text{Exp}}$ and $[N(0)V]_{\text{Exp}}^{\text{MA}}$ for a given metal reflects the difference between ω_c and ω_D , and the deviation from the BCS ratio, $2\Delta_0/k_B T_c = 3.53$.

Table 3.2 contains two values of $N(0)V$ for those metals for which we have calculated λ and $\bar{\lambda}$ from $\alpha^2(\nu)F(\nu)$. The first entry is calculated with $\alpha^2(\nu)F(\nu)$ cut-off at $\omega^* = 2\Delta_0^{\text{Exp}}$ and the second entry is calculated with no low frequency cut-off (excepting any cut-off inherent in the experimental data). It is evident from the table that the value of $N(0)V$ is very insensitive to the exact choice of the low frequency cut-off (provided, of course, that it is not unreasonably large).

It is also evident from the table that our expression for $N(0)V$ is much better than the Morel-Anderson expressions (3.23) and (3.24) (even, it appears, for strong coupling superconductors for which our expression is not to be taken seriously).

In this thesis we do not use equation (3.20) to calculate superconducting energy gaps from first principles. Instead we attempt to establish the validity of equation (3.20)

TABLE 3.2
 A COMPARISON OF THEORETICAL AND EXPERIMENTAL VALUES
 OF $N(0)V$

ELEMENT	$N(0)V$	$[N(0)V]_{Exp}$	$[N(0)V]^{MA}$	$[N(0)V]_{Z}^{MA}$	$[N(0)V]_{Exp}^{MA}$
Al	.163 .163	.163	.32	.22	.175
Tl	.244 .244	.246	.67	.38	.27
In	.241 .241	.244	.72	.39	.29
Sn	.236 .236	.240	.64	.36	.25
Zn	.17	.17	.31	.22	.18
Pb	.322 .324	.362	1.4	.55	.39

for weak and medium coupling superconductors. This is very difficult to do by a direct comparison with experimental energy gaps, because unless one is very certain of the parameters ω_c , λ , $\bar{\lambda}$ and μ^* (especially the latter three), one does not know whether poor agreement with experiment is due to a failure of the equation or to a poor choice of the parameters entering it. This problem is especially critical for weak coupling superconductors because of the extreme sensitivity of Δ_0 to $N(0)V$ when $N(0)V$ is small. Fortunately we can circumvent this problem by realizing that equation (3.20) is an approximate solution of the Eliashberg gap equations for the special case $\Delta(\omega) = \Delta(\Delta_0)$. What we really want to establish is that (3.20) is a good solution for a weak coupling and a fairly good solution for a medium coupling superconductor. Since it is generally believed that the corrections to the Eliashberg gap equations are of the order of the square root of the electronic to ionic mass ratio, $(m/M)^{1/2}$ (18,22), i.e. a few percent, we compare our results for Δ_0 indirectly with experiment by comparing them directly with the Eliashberg values of Δ_0 . Of course, this comparison is meaningful only if exactly the same normal state data is used in both calculations. This is very easily and accurately accomplished for the parameters ω_c , λ and $\bar{\lambda}$ which are obtained from the function $\alpha^2(\nu)F(\nu)$ used as input data in the gap equations. If we denote by μ_E^* and ω_c^E the parameters used in the Eliashberg equations then the

obvious choices for μ^* and μ_E^* are, (using equation (3.5)),

$$\mu^* = \frac{N(0)V_C}{1+N(0)V_C \log(E_F/\omega_C)} \quad , (3.25)$$

$$\mu_E^* = \frac{N(0)V_C}{1+N(0)V_C \log(E_F/\omega_C^{E})} \quad , (3.26)$$

where $N(0)V_C$ is given by some approximate calculation, such as an RPA calculation. With the above prescription one could very clearly delineate the range and extent of validity of equation (3.20) by solving the Eliashberg gap equations for a series of values of μ_E^* and a series of $\alpha^2(\nu)F(\nu)$'s ranging from weak coupling-like to strong coupling-like, and of different shapes, and comparing the solutions for Δ_0 with the solutions given by (3.20). The μ^* 's and α^2F 's used in this comparison could be arbitrary, not corresponding to any particular real metal, as long as they were reasonable. Unfortunately this detailed comparison is very time consuming and completely out of the question at McMaster with the present rather severe restrictions on computer usage. So we are limited to those metals for which solutions have already been generated at McMaster by P. N. Trofimenkoff⁽³⁹⁾, the present author, and, much more extensively, P. Vashishta⁽⁴⁰⁾. When we exclude the strong coupling metals we are limited to weak coupling Al and medium coupling Tl, In, and Sn. Unfortunately, the obvious scheme, mentioned above, for calculating μ^* and μ_E^* has to be abandoned because μ_E^* was

treated as an adjustable parameter in solving the Eliashberg equations. As the zero temperature gap equations are iterated μ_E^* is adjusted so that at the end of each complete iteration the gap at the gap edge, Δ_0 , is equal to the experimental value, Δ_0^{Exp} . Self consistency is obtained when $\Delta(\omega')$ and μ_E^* have both converged. We denote this converged value of μ_E^* by $\mu_E^*(\text{Exp})$. Let us denote by $\mu_E^*(\text{TF})$ the value of μ_E^* given by equation (3.26) when $N(0)V_C$ is calculated using the Thomas-Fermi approximation⁽⁴¹⁾ for the screened Coulomb interaction. The corresponding value of μ^* is denoted by μ_{TF}^* . A reasonable procedure is to apply the same correction factor, $(\mu_E^*(\text{Exp})/\mu_E^*(\text{TF}))$, to both Thomas-Fermi values of μ^* . We do this and obtain

$$\mu^* = \left(\frac{\mu_E^*(\text{Exp})}{\mu_E^*(\text{TF})} \right) \mu_{\text{TF}}^* = \frac{1 + [N(0)V]_{\text{TF}} \log(E_F/\omega_C^E)}{1 + [N(0)V]_{\text{TF}} \log(E_F/\omega_C)} \mu_E^*(\text{Exp}). \quad (3.27)$$

Fortunately, of the metals considered, only the results for Al are very sensitive to μ^* .

Table 3.3 contains $\mu_E^*(\text{EXP})$, μ_{TF}^* and μ^* . The values of $\mu_E^*(\text{EXP})$ are taken from reference (40). Also included for comparison purposes are the values of μ^* used by Cohen in reference (42). He scaled the RPA values of $N(0)V_C$ by a constant factor to obtain a μ^* for Zn in agreement with the experimental isotope effect exponent β ⁽⁴³⁾.

We note that there is good agreement between our values of μ^* and those of Cohen except in the case of Sn.

TABLE 3.3
 THE COULOMB PSEUDOPOTENTIAL PARAMETER μ^*

ELEMENT	μ_E^* (EXP) ^a	μ_{TF}^*	μ^*	μ_{COHEN}^* ^b
Al	.166	.101	.140	.14
Tl	.126	.095	.107	.11
In	.138	.097	.117	.12
Sn	.171	.096	.145	.12
Zn	--	--	--	.12

a. Reference 40

b. Reference 42

The Thomas-Fermi values, μ_{TF}^* , are consistently lower than μ^* and μ_{COHEN}^* , and differ little from .10 for the metals considered.

Table 3.4 contains the parameters ω_c , λ , $-\bar{\lambda}$ and μ^* that are needed to obtain Δ_0 from equation (3.20). λ , $\bar{\lambda}$ and ω_c were obtained from the experimental $\alpha^2(\nu)F(\nu)$'s for Tl⁽⁴⁴⁾, In⁽⁴⁴⁾ and Sn⁽²²⁾. For Al $\alpha^2(\nu)F(\nu)$ was calculated as discussed elsewhere in this thesis. Zn is included in the table because of the availability of an accurate empirical value of λ ⁽⁴⁵⁾. ω_c was taken from the calculated phonon frequency distribution of Young and Koppel⁽⁴⁶⁾. μ^* was taken from Cohen's paper⁽⁴²⁾ and $-\bar{\lambda}$ was set equal to λ (a reasonable estimate on the basis of the other entries in the table). Δ_0^{EXP} for Zn was determined by applying the BCS ratio $2\Delta_0(0)/k_B T_c = 3.53$ to the value of T_c for Zn tabulated in reference (42).

Table 3.4 contains three values of Δ_0 . The first is the value given by equation (3.20), the second is obtained by solving the simplified integral equations (3.13) and (3.14), and the third, denoted by Δ_0^{EXP} , is the 'solution' obtained by iterating the Eliashberg gap equations⁽⁴⁰⁾. The values of Δ_0^{EXP} for Al, Tl, In and Sn are taken from references (47), (44), (44) and (22) respectively. Where there are two entries for a given metal, the first corresponds to cutting $\alpha^2(\nu)F(\nu)$ off at a value $\omega^* = 2\Delta_0^{EXP}$ and the second corresponds to no cut-off. These double entries are included to demonstrate

TABLE 3.4

COMPARISON OF CALCULATED AND EXPERIMENTAL ENERGY GAPS

ELEMENT	λ	$-\bar{\lambda}$	ω_c (mev)	μ^*	Δ_0^{Calc} (mev)		Δ_0^{EXP} (mev)
					(1)	(2)	
Al	.463	.517	41.4	.140	.179	.180	.181 ^a
	.465	.525			.180	--	
Tl	.774	.9595	10.7	.107	.354	.374	.369 ^b
	.781	.982			.355	--	
In	.822	1.098	16.2	.117	.512	.549	.540 ^c
	.835	1.142			.5145	--	
Sn	.787	.932	18.5	.145	.535	.556	.575 ^d
	.787	.932			.535	--	
Zn	.43	.43	26.3	.12	.130	--	.133 ^e

- a. Reference 47
 b. Reference 44
 c. Reference 44
 d. Reference 22
 e. Reference 42

the insensitivity of the energy gap to the cut-off.

The agreement with Δ_0^{EXP} obtained using the simplified integral equations is excellent; that obtained using equation (3.20) is about as good as one could hope to obtain using a simple analytical expression (excluding, of course phenomenological expressions). The worst agreement is for Sn. Equation (3.20) gives a result that is too low by 7%, equations (3.13) and (3.14) give a result that is too low by 3%. Cohen's value of μ^* for Sn would give results somewhat too high. Equation (3.20) gives essentially the same result as the simple integral equations, for Al. For the medium coupling superconductors the approximations made in going from (3.13) and (3.14) to (3.20), i.e. replacing K by K and $Z_s(\Delta_0)$ by $Z_n(0)$ lead to errors of roughly 4 to 7%. It must be kept in mind that solving the Eliashberg gap equations is a very difficult numerical problem and that because of the various singularities that must be 'integrated through' when doing the principal value integrals and the rather coarse integration meshes that must be used to save computer time it is very difficult to estimate the accuracy of the Eliashberg solutions. Hence the discrepancies between the three values of Δ_0 , although largely due to the simplifying approximations that we have made, are to some extent due to our choice of μ^* and to numerical inaccuracy in the solution of the gap equations.

It seems safe to conclude from the results presented

in Table 3.4 that given reliable normal state data, for example $\alpha^2(\nu)F(\nu)$ and μ^* , equation (3.20) could be used with confidence to calculate the superconducting energy gap of a weak coupling superconductor and perhaps even that of a medium coupling superconductor.

There are some very interesting experimental results for a In-Tl alloy series⁽⁴⁴⁾. The energy gap Δ_0 varies anything but smoothly from the value .540 meV for pure indium to .369 meV for pure thallium as the thallium concentration increases. The tunneling data have been inverted to obtain an experimental $\alpha^2(\nu)F(\nu)$ and μ_E^* (EXP) for each alloy⁽⁴⁴⁾. Hence we can readily calculate λ , $-\bar{\lambda}$ and ω_c . Unfortunately the experimental values of the Coulomb pseudo-potential parameter, μ_E^* (EXP), do not vary smoothly in going from pure indium to pure thallium and the variation from the average value is quite large. Furthermore there is a strong correlation between μ_E^* (EXP) and Δ_0^{EXP} ; when Δ_0^{EXP} is large, μ_E^* (EXP) is small, and visa versa. The energy gap of a medium coupling superconductor is fairly sensitive to μ^* and to obtain good quantitative agreement with the experimental results one would need reliable values of μ^* (which would certainly vary with alloy composition in roughly the same manner as μ_E^* (EXP)). Rather than become involved in the difficult task of trying to obtain reliable values of μ^* to use in equation (3.20) we use the same value of μ^* for all alloy compositions. For this average value of μ^*

we use

$$\frac{\mu_{\text{EXP}}^* (\text{In}) + \mu_{\text{EXP}}^* (\text{Tl})}{2}$$

where $\mu_{\text{EXP}}^* (\text{In})$ and $\mu_{\text{EXP}}^* (\text{Tl})$ are obtained by fitting equation (3.20) to the gaps, Δ_0^{EXP} , for the pure metals.

$\mu_{\text{EXP}}^* (\text{In}) = .108$, and $\mu_{\text{EXP}}^* (\text{Tl}) = .100$, so that we take $\mu^* = .104$. Of course, using an average value of μ^* , we cannot hope for good quantitative agreement with the experimental results. Table 3.5 contains λ , $-\bar{\lambda}$, ω_c , $\mu_E^* (\text{EXP})$, Δ_0^{EXP} and Δ_0^{CALC} for the alloy series. Figure 3.3 is a comparison of the calculated energy gaps with the experimental results. The qualitative agreement is excellent. It is evident from the tabulated values of $\mu_E^* (\text{EXP})$ and Δ_0^{EXP} that reliable values of μ^* could only improve the overall quantitative agreement, which is already fairly good.

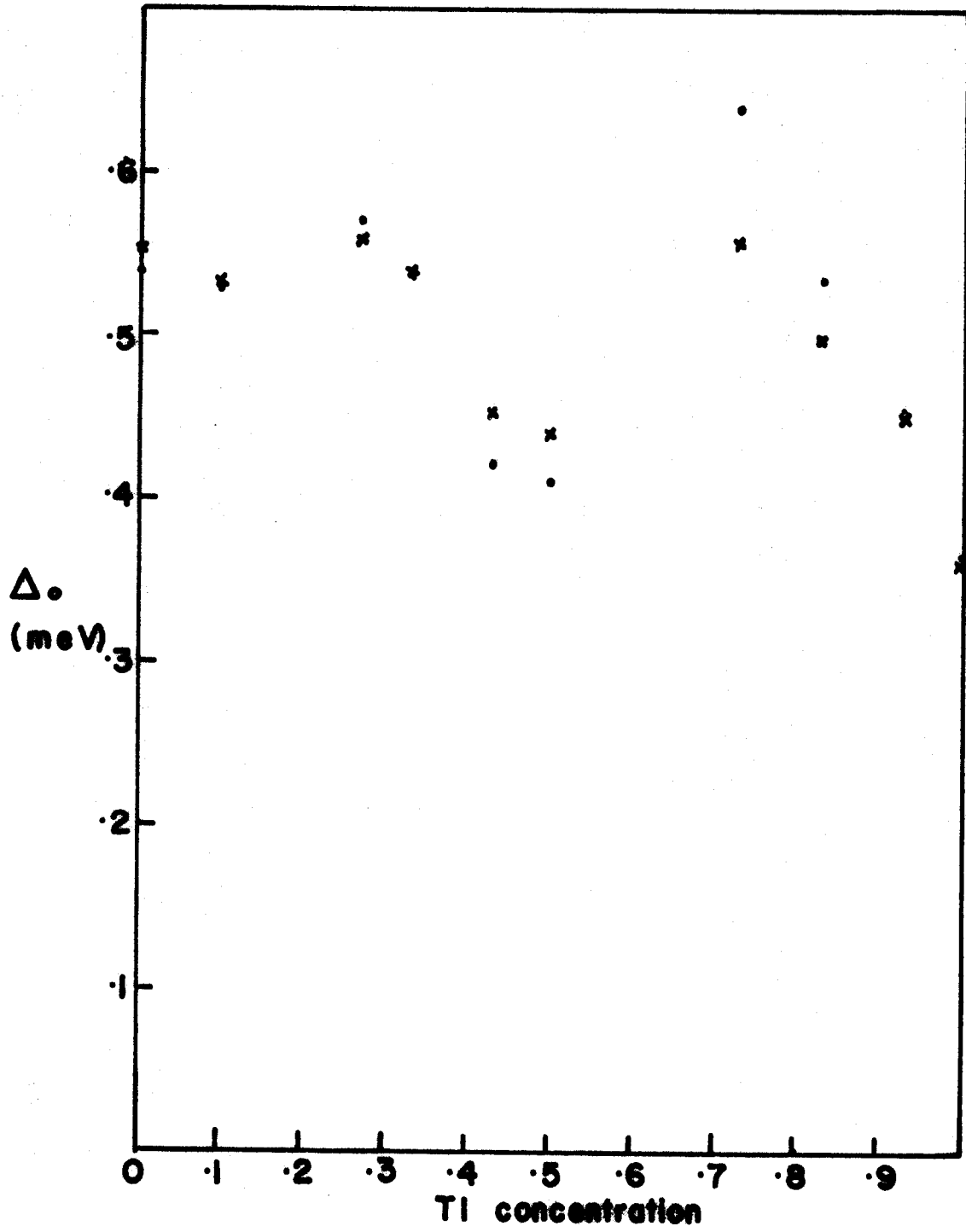
It is worth noting that, although its theoretical basis is rather weak for strong coupling superconductors, equation (3.20) does not give unreasonable results even for this class of superconductors. Table 3.6 contains ω_c , λ and $-\bar{\lambda}$ for the strong coupling superconductors amorphous Ga, Pb, amorphous Bi, and Hg. These parameters are calculated using the experimental $\alpha^2 F$'s obtained from tunneling data. $\alpha^2 F$ and Δ_0^{EXP} for amorphous gallium, lead, amorphous bismuth and mercury are taken from references (48), (22), (48), and (49) respectively. Also tabulated are the experimental energy

TABLE 3.5
 COMPARISON OF EXPERIMENTAL AND CALCULATED ENERGY GAPS FOR
 A Tl-In ALLOY SERIES

CONCENTRATION		λ	$-\bar{\lambda}$	ω_c (mev)	μ_E^* (EXP) ^a	Δ_0^{EXP} ^a (mev)	Δ_0^{CALC} (mev)
In	Tl						
1.0	0.0	.834	1.14	16.2	.125	.540	.552
.9	.1	.850	1.20	15.9	.122	.530	.533
.73	.27	.933	.135	14.7	.126	.570	.559
.67	.33	.899	1.31	15.3	.127	.536	.539
.57	.43	.847	1.24	14.5	.134	.421	.453
.50	.50	.835	1.24	14.9	.133	.411	.4405
.27	.73	1.09	1.74	13.5	.112	.640	.557
.17	.83	.980	1.50	13.3	.119	.535	.498
.07	.93	.889	1.22	11.9	.132	.453	.451
0.0	1.0	.780	.983	10.7	.127	.369	.360

a. Reference 44

FIGURE 3.3 Experimental (•) and calculated (x) energy
gaps for a Tl-In alloy series versus Tl con-
centration.



gaps, Δ_0^{EXP} , and the energy gaps calculated using equation (3.20) with $\mu^* = 0$ (a reasonable approximation for a strong coupling superconductor). The agreement is good enough to indicate that equation (3.20) could be used (in much the same way that McMillan used his approximate equation for T_c) as the basis for a semiphenomenological expression for the energy gap of a strong coupling superconductor. Equation (3.20) with $\mu^* = 0$,

$$\Delta_0 = 2\omega_c e^{-\frac{1+\lambda-\bar{\lambda}}{\lambda}}, \quad (3.28)$$

is to be contrasted with the simplified McMillan formula for the transition temperature of a strong coupling superconductor (30)

$$T_c \approx \theta_D e^{-\frac{1+\lambda}{\lambda}}. \quad (3.29)$$

As pointed out earlier, McMillan's equation does not contain a parameter corresponding to $\bar{\lambda}$ because of his rather crude approximation to an integral. From the excellent qualitative agreement that we have obtained for strong coupling superconductors it is evident that we could fit the measured energy gap with the expression

$$\Delta_0 = 2\omega_c e^{-\frac{1+\lambda-\alpha\bar{\lambda}}{\lambda-\mu^*}} \quad (3.30)$$

and that the fitted value of the adjustable parameter α would not differ very much from 1 for any superconductor. The

TABLE 3.6

COMPARISON OF CALCULATED AND EXPERIMENTAL ENERGY GAPS
FOR STRONG COUPLING SUPERCONDUCTORS. ($\mu^*=0$)

ELEMENT	λ	$-\bar{\lambda}$	ω_c (mev)	Δ_0^{EXP} (mev)	Δ_0^{CALC} (mev)
amorphous					
Ga	1.70	3.20	26.7	1.66 ^a	1.67
Pb	1.51	1.80	11.05	1.385 ^b	1.28
amorphous					
Bi	1.78	3.18	13.95	1.21 ^c	.97
Hg	1.45	2.66	14.45	.83 ^d	.85

a. Reference 48

b. Reference 22

c. Reference 48

d. Reference 49

fitted α would certainly never be small enough, for a strong coupling superconductor, to render $-\alpha\bar{\lambda}$ negligible in comparison to $1+\lambda$ because $-\bar{\lambda}$ is considerably larger than λ for these superconductors. Table 3.7 contains the empirical values of α for amorphous Ga, Pb, amorphous Bi, and Hg. The exact value of μ^* is not important for these metals, because λ is so large, and we arbitrarily set it equal to .12.

This is a reasonable choice since Cohen's values for Ga, Pb and Hg are .11, .12 and .13 respectively⁽⁴²⁾. It is to be noted that α is indeed close to 1 for all these metals.

It seems clear from the above considerations that the theoretical McMillan equation⁽³⁰⁾,

$$T_c = \omega_c e^{-\frac{1+\lambda}{\lambda-\mu^* - (\frac{\langle\omega\rangle}{\omega_c})\lambda\mu^*}} \quad , (3.31)$$

is lacking an essential ingredient, the finite temperature analogue of $\bar{\lambda}$, and that the semiphenomenological expression based on (3.31),

$$T_c = \frac{\theta_D}{1.45} e^{-\frac{1.04(1+\lambda)}{\lambda-\mu^*(1+0.62\lambda)}} \quad , (3.32)$$

could be improved by the incorporation of the finite temperature analogue of $\alpha\bar{\lambda}$.

In any case, $\bar{\lambda}$ is a very necessary ingredient of our expression for Δ_0 , even for a qualitative estimate of the energy gap of a strong coupling superconductor. An

TABLE 3.7

EMPIRICAL VALUES OF α . ($\mu^* = .12$)

ELEMENT	α
Ga	.873
Pb	.750
Bi	.760
Hg	.855

interesting example is a comparison of Pb and Hg using equation (3.28). ω_c is equal to 11 and 14 meV for Pb and Hg respectively and $(1+\lambda)/\lambda$ is equal to 1.66 and 1.69 for the two respective metals. If $\bar{\lambda}$ did not occur in (3.28) the fact that the values of $(1+\lambda)/\lambda$ are almost the same for the two metals would lead us to the qualitative conclusion that $\Delta_0(\text{Hg}) > \Delta_0(\text{Pb})$ (because $\omega_c(\text{Hg}) > \omega_c(\text{Pb})$). This conclusion is completely wrong; $\Delta_0(\text{Pb})$ is very considerably larger than $\Delta_0(\text{Hg})$. It is only when we include $\bar{\lambda}$ in equation (3.28) and the fact that $-\bar{\lambda}$ is considerably larger for Hg than for Pb, 2.66 as compared to 1.80, that we arrive at the correct qualitative result.

Let us return to our semiempirical expression (3.30) for a moment. If the empirical values of α for two strong coupling superconductors happened to be very nearly the same and if $\alpha^2(\nu)F(\nu)$ were available for a two component alloy of the two elements it would be a good test of (3.30) to calculate Δ_0 for the alloy using a (weighted) average value of α .

It seems quite clear from the evidence presented in this section that equation (3.20) is a very good approximate solution of the Eliashberg equations for the energy gap at the gap edge of a weak coupling superconductor. Although not quite so good a solution for medium coupling superconductors, it can be used with confidence for a qualitative study of many phenomena in these superconductors, for example,

the effect of alloying on the energy gap. The weak coupling integral equations (3.13) and (3.14) can be solved very quickly on an electronic computer and should give essentially the same results as the Eliashberg equations when calculating the energy gap parameter, Δ_0 , of weak or medium coupling superconductors. Any small loss in accuracy is more than compensated for by the huge saving in computer time.

In the next few sections we use the formalism developed in this section to study several interesting effects.

3.2 THE ANISOTROPY OF THE ENERGY GAP IN A PURE SINGLE-CRYSTAL WEAK COUPLING SUPERCONDUCTOR

Bennett⁽³⁷⁾ used an approximate procedure to calculate the energy gap $\Delta_0(\theta, \phi)$ at the point $\underline{k} \equiv (k_F, \theta, \phi)$ on the Fermi surface of a strong coupling superconductor (Pb). Bennett's procedure is now described very briefly; it was described in more detail in Chapter II. The Eliashberg gap equations containing in the kernels $K_{\pm}(\omega, \omega')$ the function α^2F appropriate to the isotropic or 'dirty' metal,

$$\alpha^2F(\nu) = N(0) \iint \frac{d\Omega_{\underline{k}}}{4\pi} \frac{d\Omega_{\underline{k}'}}{4\pi} \sum_{\lambda} |g_{\underline{k}\underline{k}'\lambda}|^2 \delta(\nu - \omega_{\underline{k}-\underline{k}'\lambda}) ,$$

are iterated until convergence is reached. The isotropic α^2F is then replaced by the directional α^2F ,

$$\alpha^2F(\nu, \theta, \phi) = N(0) \int \frac{d\Omega_{\underline{k}'}}{4\pi} \sum_{\lambda} |g_{\underline{k}\underline{k}'\lambda}|^2 \delta(\nu - \omega_{\underline{k}-\underline{k}'\lambda}) , \quad (3.33)$$

(all other quantities occurring on the right hand side of the Eliashberg equations are fixed once and for all at their converged 'isotropic' values) and one more iteration is performed to yield approximate values for $\Delta(\omega, \theta, \phi)$ and $Z_S(\omega, \theta, \phi)$. It is important to note that it is quite out of the question, at the present time, to iterate the Eliashberg equations, in their strong coupling form, a second time. The computer time and memory required would be enormous.

We now apply the principle of Bennett's procedure to the simplified weak coupling integral equations, (3.13) and (3.14), to obtain an approximate expression for the energy gap at the gap edge in a pure single-crystal superconductor. We obtain

$$\Delta_0^{(1)}(\theta, \phi) = \frac{1}{Z_S^{(1)}(\theta, \phi)_0} \left\{ \int_0^{\omega_c} dv \alpha^2 F(v, \theta, \phi) K(v, \omega_c, \Delta_0) - \mu^* \right. \\ \left. \times \log\left(\frac{2\omega_c}{\Delta_0}\right) \right\} \Delta_0 \quad (3.34)$$

where

$$Z_S^{(1)}(\theta, \phi)_0 = 1 + \int_0^{\omega_c} dv \alpha^2 F(v, \theta, \phi) \left[L(v, \omega_c, \Delta_0) + \frac{2}{v + \omega_c} \right] \quad (3.35)$$

In the above equations Δ_0 is the solution obtained by iterating the integral equations, (3.13) and (3.14), to convergence (using the isotropic function $\alpha^2 F(v)$, of course). Our success in the previous section in calculating the isotropic energy gap Δ_0 , using equations (3.13) and (3.14),

indicates that for weak and medium coupling superconductors one can save a huge amount of computer time (at the expense of a very small loss in accuracy) by using equations (3.34) and (3.35), rather than the Eliashberg equations, to study the anisotropy of the energy gap $\Delta_0(\theta, \phi)$. We can make one further simplification by replacing $Z_s^{(1)}(\theta, \phi)_0$ by $Z_n(\theta, \phi)_0$, which is given by

$$Z_n(\theta, \phi)_0 = 1 + 2 \int \frac{dv}{v} \alpha^2 F(v, \theta, \phi) \quad .(3.36)$$

As shown in the previous section this is a very good approximation.

Equations (3.34) and (3.36) have been tested for Al and found to work very well. This was accomplished by calculating $\Delta_0(\theta, \phi)$ for several values of (θ, ϕ) using both the Eliashberg equations and the much simpler equations (3.34) and (3.36). The Eliashberg equations, containing the isotropic $\alpha^2 F(v)$, were iterated to convergence to obtain the solutions $\Delta(\omega)$ and $Z(\omega)$ appropriate to the isotropic case. Bennett's procedure was then used to generate $\Delta_0^{(1)}(\theta, \phi)$ for about 30 different directions. The value of μ^* to be used in (3.34) was determined, using equations (3.13) and (3.14), by requiring that the weak coupling value of Δ_0 be the same as the Eliashberg value $\text{Re}\{\Delta(\Delta_0)\}$. With this value of μ^* equations (3.34) and (3.36) were used to calculate $\Delta_0^{(1)}(\theta, \phi)$. The agreement between the two sets of directional energy

gaps was excellent, the discrepancies being considerably less than 1%. These discrepancies are very small compared to the anisotropy in $\Delta_0^{(1)}(\theta, \phi)$. Table 3.8 contains $\Delta_0^{(1)}(\theta, \phi)$ for several directions (θ, ϕ) as calculated using the two different sets of equations.

Actually we can simplify things even further for a weak coupling superconductor by replacing $K(v, \omega_c, \Delta_0)$ in (3.34) by $\tilde{K}(v, \omega_c, \Delta_0)$. As shown in the previous section this is a very good approximation for Al. We obtain

$$\Delta_0^{(1)}(\theta, \phi) = \frac{1}{1 + \lambda(\theta, \phi)} \{ \bar{\lambda}(\theta, \phi) + [\lambda(\theta, \phi) - \mu^*] \log\left(\frac{2\omega_c}{\Delta_0}\right) \} \Delta_0 \quad (3.37)$$

where

$$\lambda(\theta, \phi) = 2 \int_0^{\omega_c} \frac{dv}{v} \alpha^2 F(v, \theta, \phi) \quad (3.38)$$

and

$$\bar{\lambda}(\theta, \phi) = 2 \int_0^{\omega_c} \frac{dv}{v} \alpha^2 F(v, \theta, \phi) \log\left(\frac{v/\omega_c}{1+v/\omega_c}\right) \quad (3.39)$$

The value of Δ_0 to be used in (3.37) is the value given by equation (3.20). (3.37) is generalized, in a later section to investigate the pressure dependence of the anisotropy of the energy gap in Al.

Since the weak coupling integral equations are so much simpler than the Eliashberg equations it does not take an unreasonable amount of computer time to go beyond the one

TABLE 3.8

A COMPARISON OF TWO DIFFERENT CALCULATIONS OF THE
DIRECTIONAL ENERGY GAPS IN ALUMINIUM

θ	ϕ	$\Delta_0^{(1)}(\theta, \phi)$ (1)	$\Delta_0^{(1)}(\theta, \phi)$ (2)
0.	0.	.1847	.1856
15.	0.	.1934	.1943
22.5	0.	.2077	.2087
30.	0.	.2035	.2043
37.5	0.	.1806	.1813
45.	0.	.1768	.1774
54.75	45.	.1474	.1471

(1) $\Delta_0^{(1)}(\theta, \phi)$ as calculated using the Eliashberg gap equations.

(2) $\Delta_0^{(1)}(\theta, \phi)$ as calculated using equations (3.34) and (3.36).

iteration result of Bennett. We first rewrite equations (3.34) and (3.35) in their exact form

$$\Delta_0(\underline{k}) = \frac{N(0)}{Z_s(\underline{k})_0} \left\{ \int \frac{d\Omega_{\underline{k}'}}{4\pi} \sum_{\lambda} |g_{\underline{k}\underline{k}'\lambda}|^2 K(\omega_{\underline{k}-\underline{k}'\lambda}, \omega_c, \Delta_0(\underline{k}')) \Delta_0(\underline{k}') \right. \\ \left. - U_c \int \frac{d\Omega_{\underline{k}'}}{4\pi} \log\left(\frac{2\omega_c}{\Delta_0(\underline{k}')} \right) \Delta_0(\underline{k}') \right\} \quad , (3.40)$$

$$Z_s(\underline{k})_0 = 1 + N(0) \int \frac{d\Omega_{\underline{k}'}}{4\pi} \sum_{\lambda} |g_{\underline{k}\underline{k}'\lambda}|^2 [L(\omega_{\underline{k}-\underline{k}'\lambda}, \omega_c, \Delta_0(\underline{k}')) \\ + \frac{2}{\omega_{\underline{k}-\underline{k}'\lambda} + \omega_c}] \Delta_0(\underline{k}') \quad , (3.41)$$

where $\underline{k} \equiv (k_F, \theta, \phi)$. K and L are given by equations (3.11) and (3.12) with one minor modification. p_1 and p_2 are now given by

$$p_1 \equiv \omega_{\underline{k}-\underline{k}'\lambda} + \Delta_0(\underline{k}) ; p_2 \equiv \omega_{\underline{k}-\underline{k}'\lambda} - \Delta_0(\underline{k}) \quad . (3.42)$$

Equations (3.34) and (3.35) follow at once from (3.40) and (3.41) if we replace $\Delta_0(\underline{k}')$ and $\Delta_0(\underline{k})$ on the right hand side by the isotropic solution Δ_0 and make use of the definition of $\alpha^2 F(\nu, \theta, \phi)$.

A second iteration can be performed by inserting the first iteration result* for the directional energy gap,

* One needs a scheme for interpolating from the finite set of one iteration results for $\Delta_0(\underline{k}')$ to obtain $\Delta_0^{(1)}(\underline{k}')$ for any point (k_F, θ, ϕ) . This will be discussed in detail in Chapter IV.

$\Delta_0^{(1)}(\underline{k}')$, into the right hand sides of (3.40) and (3.41) and performing the surface integrals over $\Omega_{\underline{k}'}$. These integrals are very easily calculated by changing the weight factor in the $\alpha^2 F(\nu, \theta, \phi)$ computer programme, which will be discussed in detail in Chapter IV, from $|g_{\underline{k}\underline{k}', \lambda}|^2$ to

$$|g_{\underline{k}\underline{k}', \lambda}|^2 K(\omega_{\underline{k}-\underline{k}', \lambda}, \omega_c, \Delta_0^{(1)}(\underline{k}')) \Delta_0^{(1)}(\underline{k}'),$$

and $|g_{\underline{k}\underline{k}', \lambda}|^2 [L(\omega_{\underline{k}-\underline{k}', \lambda}, \omega_c, \Delta_0^{(1)}(\underline{k}')) + \frac{2}{\omega_{\underline{k}-\underline{k}', \lambda} + \omega_c}] \Delta_0^{(1)}(\underline{k}')$,

respectively. The results for $\Delta_0^{(2)}(\underline{k})$ will be discussed in detail later. We only remark here that the results of the second iteration are little changed from the first iteration results.

The main purpose of this section has been to present equations that will be used in some of the following sections, particularly in Chapter IV.

3.3 THE AVERAGE ENERGY GAP IN A PURE SINGLE-CRYSTAL WEAK COUPLING SUPERCONDUCTOR

When impurities are added to a pure single-crystal superconductor the transition temperature decreases (32,33,34). This is experimental evidence that the average energy gap in a pure single-crystal is larger than the isotropic energy gap in the corresponding 'dirty' superconductor. We use equation (3.40) to derive an approximate expression for the

average energy gap

$$\langle \Delta_0(\underline{k}) \rangle \equiv \int \frac{d\Omega_{\underline{k}}}{4\pi} \Delta_0(\underline{k})$$

in a pure single-crystal weak coupling superconductor. This expression can be used in conjunction with the directional energy gaps calculated by the one iteration procedure discussed above to estimate $\langle \Delta_0(\underline{k}) \rangle$.

We replace $K(\omega_{\underline{k}-\underline{k}'\lambda}, \omega_c, \Delta_0(\underline{k}'))$ in equation (3.40) by the approximate form $K(\omega_{\underline{k}-\underline{k}'\lambda}, \omega_c, \Delta_0(\underline{k}'))$ to obtain

$$\begin{aligned} \Delta_0(\underline{k}) z_s(\underline{k})_0 = N(0) \left\{ \int \frac{d\Omega_{\underline{k}'}}{4\pi} 2 \sum_{\lambda} \frac{|g_{\underline{k}\underline{k}'\lambda}|^2}{\omega_{\underline{k}-\underline{k}'\lambda}} \left[\log \left(\frac{\omega_{\underline{k}-\underline{k}'\lambda}/\omega_c}{1+\omega_{\underline{k}-\underline{k}'\lambda}/\omega_c} \right) \right. \right. \\ \left. \left. + \log \left(\frac{2\omega_c}{\Delta_0(\underline{k}')} \right) \right] \Delta_0(\underline{k}') - U_c \int \frac{d\Omega_{\underline{k}'}}{4\pi} \log \left(\frac{2\omega_c}{\Delta_0(\underline{k}')} \right) \Delta_0(\underline{k}') \right\}. \end{aligned}$$

We average both sides of this equation over all directions of \underline{k} to obtain

$$\begin{aligned} \int \frac{d\Omega_{\underline{k}}}{4\pi} \Delta_0(\underline{k}) z_s(\underline{k})_0 = \int \frac{d\Omega_{\underline{k}'}}{4\pi} \bar{\lambda}(\underline{k}') \Delta_0(\underline{k}') + \int \frac{d\Omega_{\underline{k}'}}{4\pi} \lambda(\underline{k}') \\ \times \log \left(\frac{2\omega_c}{\Delta_0(\underline{k}')} \right) \Delta_0(\underline{k}') - \mu^* \int \frac{d\Omega_{\underline{k}'}}{4\pi} \\ \times \log \left(\frac{2\omega_c}{\Delta_0(\underline{k}')} \right) \Delta_0(\underline{k}') \quad , (3.41) \end{aligned}$$

where

$$\lambda(\underline{k}') \equiv 2N(0) \int \frac{d\Omega_{\underline{k}}}{4\pi} \sum_{\lambda} \frac{|g_{\underline{k}\underline{k}'\lambda}|^2}{\omega_{\underline{k}-\underline{k}'\lambda}} = 2 \int_0^{\omega_c} \frac{d\nu}{\nu} \alpha^2 F(\nu, \underline{k}') \quad (3.42)$$

and

$$\begin{aligned} \bar{\lambda}(\underline{k}') &\equiv 2N(0) \int \frac{d\Omega_{\underline{k}}}{4\pi} \frac{\Sigma}{\lambda} \frac{|g_{\underline{k}-\underline{k}'\lambda}|^2}{\omega_{\underline{k}-\underline{k}'\lambda}} \log\left(\frac{\omega_{\underline{k}-\underline{k}'\lambda}/\omega_c}{1+\omega_{\underline{k}-\underline{k}'\lambda}/\omega_c}\right) \\ &= 2 \int_0^{\omega_c} \frac{dv}{v} \alpha^2 F(v, \underline{k}') \log\left(\frac{v/\omega_c}{1+v/\omega_c}\right) \end{aligned} \quad (3.43)$$

We define the anisotropy parameters $a_{\underline{k}}$, $b_{\underline{k}}$ and $\bar{b}_{\underline{k}}$ by the expressions

$$\Delta_0(\underline{k}) = \langle \Delta_0(\underline{k}) \rangle (1+a_{\underline{k}}) ,$$

$$\lambda(\underline{k}) = \langle \lambda(\underline{k}) \rangle (1+b_{\underline{k}}) ,$$

and

$$\bar{\lambda}(\underline{k}) = \langle \bar{\lambda}(\underline{k}) \rangle (1+\bar{b}_{\underline{k}}) , \quad (3.44)$$

where

$$\langle f(\underline{k}) \rangle \equiv \int \frac{d\Omega_{\underline{k}}}{4\pi} f(\underline{k})$$

for any function $f(\underline{k})$.

Since $|a_{\underline{k}}|, |b_{\underline{k}}|, |\bar{b}_{\underline{k}}| \ll 1$

we can expand both sides of (3.41) in terms of these small quantities and retain only the lower order terms on the right hand side. We ignore the very small difference between Z_s and Z_n and obtain

$$\int \frac{d\Omega_{\underline{k}}}{4\pi} \Delta_0(\underline{k}) Z_s(\underline{k})_0 = \langle \Delta_0 \rangle (1+\langle \lambda \rangle (1+\langle ab \rangle)) ,$$

$$\int \frac{d\Omega_{\underline{k}'}}{4\pi} \bar{\lambda}(\underline{k}') \Delta_0(\underline{k}') = \langle \bar{\lambda} \rangle \langle \Delta_0 \rangle (1 + \langle \bar{a} \bar{b} \rangle) \quad ,$$

$$\int \frac{d\Omega_{\underline{k}'}}{4\pi} \lambda(\underline{k}') \log\left(\frac{2\omega_c}{\Delta_0(\underline{k}')} \right) \Delta_0(\underline{k}') \approx \langle \lambda \rangle \langle \Delta_0 \rangle \{ (1 + \langle \bar{a} \bar{b} \rangle) \log\left(\frac{2\omega_c}{\langle \Delta_0 \rangle}\right) - \frac{1}{2} \langle a^2 \rangle - \langle \bar{a} \bar{b} \rangle \} \quad ,$$

$$\int \frac{d\Omega_{\underline{k}'}}{4\pi} \log\left(\frac{2\omega_c}{\Delta_0(\underline{k}')} \right) \Delta_0(\underline{k}') \approx \langle \Delta_0 \rangle \left\{ \log\left(\frac{2\omega_c}{\langle \Delta_0 \rangle}\right) - \frac{\langle a^2 \rangle}{2} \right\} \quad .$$

Substituting these expressions into (3.41) and solving for $\langle \Delta_0 \rangle$ we obtain

$$\langle \Delta_0(\underline{k}) \rangle = 2\omega_c e^{-\frac{1 + (1 + \frac{1}{2} \langle a^2 \rangle + 2 \langle \bar{a} \bar{b} \rangle) \lambda - (1 + \langle \bar{a} \bar{b} \rangle) \bar{\lambda} - \frac{1}{2} \langle a^2 \rangle \mu^*}{(1 + \langle \bar{a} \bar{b} \rangle) \lambda - \mu^*}} \quad . (3.45)$$

This equation is to be contrasted with the expression for the isotropic energy gap in a 'dirty' superconductor

$$\Delta_0 = 2\omega_c e^{-\frac{1 + \lambda - \bar{\lambda}}{\lambda - \mu^*}} \quad . (3.20)$$

Equation (3.45) is not very useful as it stands because we do not know the values of the quantities $\langle a^2 \rangle$, $\langle \bar{a} \bar{b} \rangle$ and $\langle \bar{a} \bar{b} \rangle$ (because we do not know $\Delta_0(\underline{k})$). Knowledge of $\Delta_0(\underline{k})$ requires iterating the integral equations (3.40) and (3.41) until convergence is reached, which is a very formidable task even after all the simplifications that we have made. The

assumption that we make, which is a very reasonable one, is that, even though the anisotropy function $a_{\underline{k}}$ may change somewhat between the first and last iterations, the gross average properties of this function, such as $\langle a^2 \rangle$, $\langle ab \rangle$ and $\langle a\bar{b} \rangle$, do not change appreciably. Hence to estimate $\langle \Delta_0(\underline{k}) \rangle$ we use the one iteration results for $\Delta_0(\underline{k})$ to calculate $\langle a^2 \rangle$, $\langle ab \rangle$ and $\langle a\bar{b} \rangle$. Our results for Al are reported in detail elsewhere in this thesis. We just note at the present time that (3.45) gives the correct qualitative result that $\langle \Delta_0(\underline{k}) \rangle$ is a few percent larger than Δ_0 . One cannot obtain this result in a straightforward way from the one iteration results for $\Delta_0(\underline{k})$. That is, if one averages the one iteration results for $\Delta_0(\underline{k})$ over all angles it is found that $\langle \Delta_0^{(1)}(\underline{k}) \rangle < \Delta_0$. By applying an analysis similar to the above one to equation (3.37) one can easily show that

$$\langle \Delta_0^{(1)}(\underline{k}) \rangle = \frac{\Delta_0}{1 + \frac{\lambda \langle ab \rangle^{(1)}}{1+\lambda}} \quad .(3.46)$$

This is slightly less than Δ_0 because there is a very strong correlation between $\lambda(\underline{k})$ and $\Delta_0^{(1)}(\underline{k})$ so that $\langle ab \rangle^{(1)}$ is positive.

3.4 EFFECT OF PRESSURE ON A WEAK COUPLING SUPERCONDUCTOR

In this section we use equation (3.20) and equations (3.13) and (3.14) to investigate the dependence of the isotropic energy gap on the fractional volume change, v , for Al, Tl, In and Sn. We then iterate the weak coupling

integral equations once to obtain an approximate expression for the dependence of the directional energy gaps on v . This expression is then applied to aluminium.

The fractional volume change is defined by

$$v \equiv - \frac{\Delta\Omega}{\Omega_s} > 0 \quad (3.47)$$

where Ω is the volume of the metal when it is subjected to a hydrostatic pressure P ; Ω_s is the standard or zero pressure volume; $\Delta\Omega \equiv \Omega - \Omega_s$.

(i) Pressure Dependence of the Energy Gap for an Isotropic Weak Coupling Superconductor

The zero temperature isotropic energy gap for a superconductor which has undergone a fractional volume change, v , is given by equation (3.20) when the v dependence of the various quantities involved is introduced.

$$\Delta_0(v) = 2\omega_c(v) e^{-\frac{1+\lambda(v)-\bar{\lambda}(v)}{\lambda(v)-\mu^*(v)}} \quad (3.48)$$

We define $\gamma_{\underline{q}\lambda}(v)$ by the expression

$$\omega_{\underline{q}\lambda}(v) \equiv \gamma_{\underline{q}\lambda}(v) \omega_{\underline{q}\lambda}(0) \quad (3.49)$$

We assume that the variation of $\gamma_{\underline{q}\lambda}(v)$ with momentum transfer, \underline{q} , and polarization index, λ , is not important, and replace the exact relation (3.49) by the approximate relation

$$\omega_{\underline{q}\lambda}(v) = \gamma(v) \omega_{\underline{q}\lambda}(0) \quad (3.50)$$

To calculate the phonon frequency shifts we use the Grüneisen relation⁽⁵⁰⁾,

$$\gamma_G(\underline{q}, \lambda) = \frac{\partial \ln \omega_{\underline{q}\lambda}}{\partial \ln \Omega} \quad , (3.51)$$

where $\gamma_G(\underline{q}, \lambda)$ is the Grüneisen parameter for the mode (\underline{q}, λ) . In terms of an average Gruneisen parameter, γ_G , the scale factor, $\gamma(v)$, is given by

$$\gamma(v) = (1-v)^{-\gamma_G} \quad . (3.52)$$

In the Thomas-Fermi approximation $N(0)U_c$ varies more slowly than $\frac{1}{k_F}$ with volume change⁽³⁹⁾. This variation is very slow for small volume changes and will be neglected. That is, we assume $\mu^*(v) = \mu^*(0)$ in what follows.

$\lambda(v)$ and $\bar{\lambda}(v)$ can be calculated by a simple modification of the α^2F computer programme which involves scaling all phonon frequencies by the factor $\gamma(v)$ and scaling all lengths by the factor $(\Omega/\Omega_0)^{1/3}$. The only non-trivial change in $\lambda(v)$ and $\bar{\lambda}(v)$, which cannot be immediately written down, is the effect of rescreening the pseudopotential form factor, $W(q/2k_F)$, to take into account the changed conduction electron density. Since the effect of rescreening the pseudopotential is small relative to the effect of scaling the phonon frequencies and since this direct method of calculating $\lambda(v)$ and $\bar{\lambda}(v)$ is quite time consuming, especially if one wants to consider a large number of values of v , we use the rescaling procedure of Carbotte and

Trofimenkoff^(51,39), instead. These authors showed by a detailed numerical investigation of $[\alpha^2(\nu)F(\nu)]_\nu$ for Al that to a good approximation

$$[\alpha^2(\nu)F(\nu)]_\nu = \frac{B(\nu)}{\gamma^2(\nu)} [\alpha^2(\nu/\gamma(\nu))F(\nu/\gamma(\nu))]_0 \quad (3.53)$$

where

$$B(\nu) \equiv \left[\int_0^1 dt t^3 |W(t)|^2 \right]_\nu / \left[\int_0^1 dt t^3 |W(t)|^2 \right]_0 \quad (3.54)$$

They used the above scaling law to investigate the pressure dependence of the energy gap by solving the Eliashberg gap equations at zero and finite pressure. This is an extremely time consuming undertaking and they were able to consider only one, or at most two, finite values of ν for each of the metals investigated. Our very simple result, equation (3.48), is only an approximate solution of the Eliashberg gap equations (for a weak coupling superconductor) but does not suffer from the numerical uncertainties involved in the complicated principal value integrals of the gap equations or in the necessarily coarse mesh of points used to represent the function $\alpha^2(\nu)F(\nu)$.

From equation (3.53) it readily follows that

$$\lambda(\nu) = \frac{B(\nu)}{\gamma^2(\nu)} \lambda(0) \quad (3.55)$$

It is not quite so easy to show that

$$\bar{\lambda}(v) = \frac{B(v)}{\gamma^2(v)} \bar{\lambda}(0) \quad (3.56)$$

The proof is as follows: Generalizing the definition of $\bar{\lambda}$, equation (3.19), to finite v and using the scaling law,

(3.53), we obtain

$$\begin{aligned} \bar{\lambda}(v) &\equiv 2 \int_0^{\omega_c(v)} \frac{dv}{v} [\alpha^2(v)F(v)]_v \log\left(\frac{v/\omega_c(v)}{1+v/\omega_c(v)}\right) \quad (3.57) \\ &= \frac{B(v)}{\gamma^2} \cdot 2 \int_0^{\gamma\omega_c(0)} \frac{dv}{v} [\alpha^2(v/\gamma)F(v/\gamma)]_0 \log\left(\frac{v/\gamma\omega_c(0)}{1+v/\gamma\omega_c(0)}\right) \quad (\gamma \equiv \gamma(v)) \\ &= \frac{B(v)}{\gamma^2} \cdot 2 \int_0^{\omega_c(0)} \frac{dv'}{v'} [\alpha^2(v')F(v')]_0 \log\left(\frac{v'/\omega_c(0)}{1+v'/\omega_c(0)}\right) \quad (v' \equiv v/\gamma) \\ &= \frac{B(v)}{\gamma^2(v)} \bar{\lambda}(0) \end{aligned}$$

Substituting (3.50), (3.55) and (3.56) into (3.48) we obtain

$$\Delta_0(v) = 2\gamma(v) \omega_c(0) e^{-\frac{1+\eta(v)[\lambda(0)-\bar{\lambda}(0)]}{\eta(v)\lambda(0)-\mu^*}} \quad (3.58)$$

where

$$\eta(v) \equiv \frac{B(v)}{\gamma^2(v)} \quad (3.59)$$

We note that, within our model, the v dependence of the BCS parameter $N(0)V$ is given by

$$[N(0)V]_v = \frac{\eta(v)\lambda(0) - \mu^*}{1 + \eta(v)[\lambda(0) - \bar{\lambda}(0)]} \quad (3.60)$$

Figure 3.4 is a plot of $[N(0)V]_v$ versus v for Al, Sn, Tl and In. The determination of $\eta(v)$ for the various metals will be discussed later. We note that the decrease of $[N(0)V]_v$ with increasing v is linear to a good approximation.

The simplified integral equations (3.13) and (3.14) are readily generalized to finite v . Using the scaling law (3.53) we obtain

$$\Delta_0(v) Z_S^V(\Delta_0(v)) = \left\{ \frac{B(v)}{\gamma(v)} \int_0^{\omega_c(0)} dv [\alpha^2(v)F(v)]_0 K(\gamma(v)v, \gamma(v)\omega_c(0)), \right.$$

$$\left. \Delta_0(v) - \mu^* \log\left(\frac{2\gamma(v)\omega_c(0)}{\Delta_0(v)}\right) \right\} \Delta_0(v) \quad ; (3.61)$$

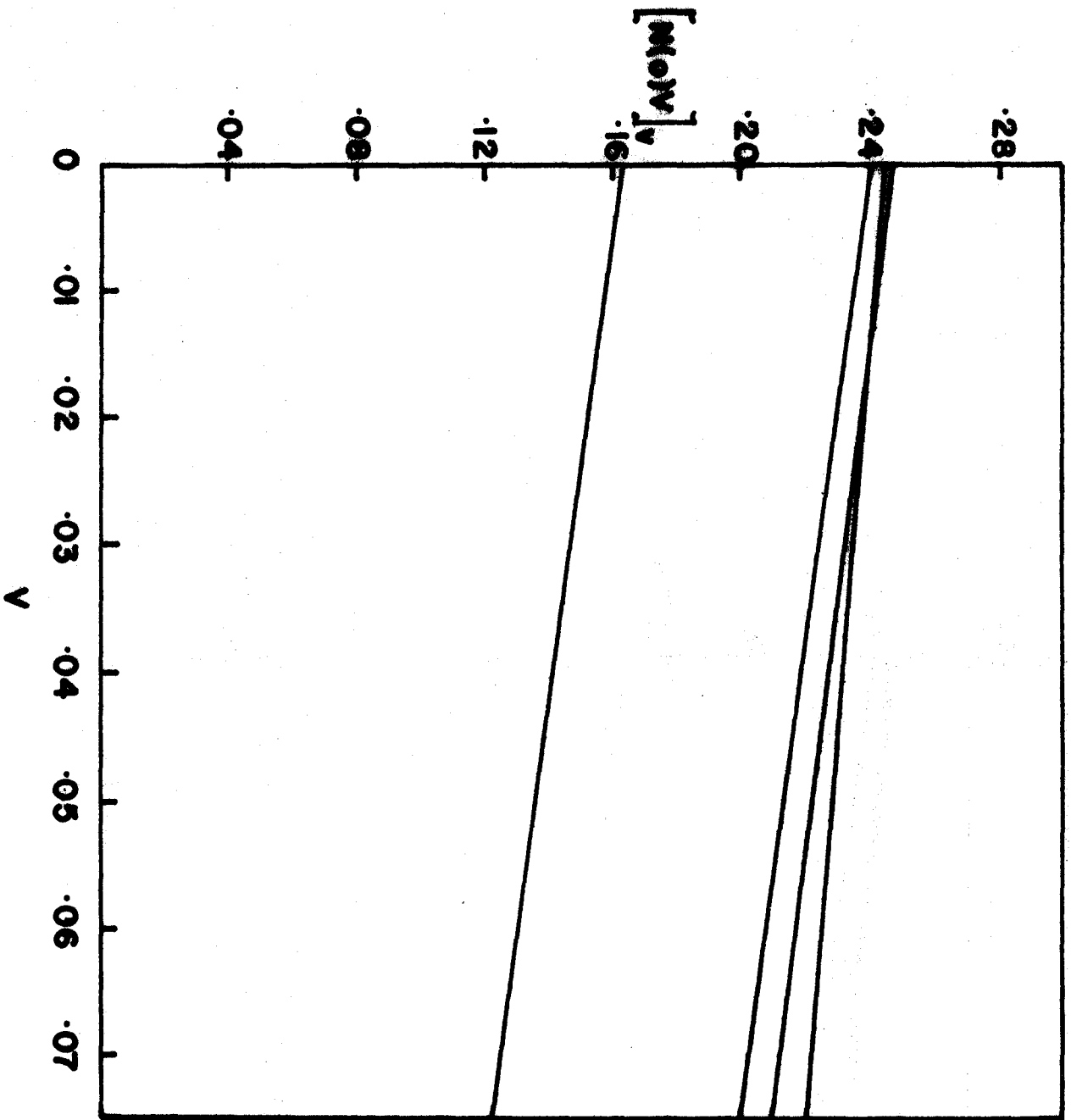
$$Z_S^V(\Delta_0(v)) = 1 + \frac{B(v)}{\gamma(v)} \int_0^{\omega_c(0)} dv [\alpha^2(v)F(v)]_0 [L(\gamma(v)v, \gamma(v)\omega_c(0)),$$

$$\left. \Delta_0(v) + \frac{1}{\gamma(v)} \cdot \frac{2}{v + \omega_c(0)} \right] \quad (3.62)$$

These equations have been put in a form that is convenient for numerical calculations.

We use equation (3.58) and the integral equations

FIGURE 3.4 The dependence of the BCS parameter $[N(0)V]_v$
on the fractional volume change $v \equiv -\Delta\Omega/\Omega_s$.



(3.61) and (3.62) to calculate the ratio $\Delta_0(v)/\Delta_0(0)$ for Al, Sn, Tl and In. We use the Grüneisen parameters γ_G used by Carbotte, Trofimenkoff and Vashishta^(39,52) in their investigation of the pressure dependence of superconductivity. We obtain $B(v)$ for arbitrary v by interpolating between the values of $B(v)$ tabulated by them for $v = .025$ and $v = .050$ and calculated using equation (3.54). Table 3.9 contains γ_G , $B(.025)$ and $B(.050)$ for the metals considered here. Since we want to compare the results of the simple equation (3.58) with those of the more correct equations (3.61) and (3.62) we use the values of λ and $-\bar{\lambda}$ obtained by cutting $\alpha^2(v)F(v)$ off at a value $\omega^* = 2\Delta_0^{\text{EXP}}(0)$. The results are not very sensitive to this cut-off (as shown previously) and this choice of cut-off avoids numerical difficulties associated with the factors $(p_i^2 - \Delta_0^2)^{-\frac{1}{2}}$ occurring in both $K(v, \omega_c, \Delta_0)$ and $L(v, \omega_c, \Delta_0)$. The only tricky point is the choice of μ^* to be used for each metal. $\Delta_0(v)$ as given by (3.58) is very sensitive to the factor $\eta(v)\lambda(0) - \mu^*$ occurring in the exponential and hence quite sensitive to μ^* . The only unambiguous procedure is to use that value of μ^* which gives the correct zero pressure energy gap. We denote these values of μ^* , obtained from (3.58) and equations (3.61) and (3.62), by $\mu_{\text{EXP}}^*(1)$ and $\mu_{\text{EXP}}^*(2)$ respectively. This procedure is the correct one from another point of view. We compare our results for $\Delta_0(v)$ with those obtained by solving the Eliashberg gap equations. In this latter calculation, done by

TABLE 3.9
 PARAMETERS USED IN INVESTIGATING THE PRESSURE
 DEPENDENCE OF THE ENERGY GAP

ELEMENT	γ_G	B(.025)	B(.050)	$\mu_{EXP}^*(1)$	$\mu_{EXP}^*(2)$
Al	2.22	1.0263	1.0563	.1335	.1336
Tl	2.25	1.0250	1.0500	.1006	.1090
In	1.80 2.50	1.0273	1.0604	.1087	.1196
Sn	2.25	1.0200	1.0445	.1339	.1402

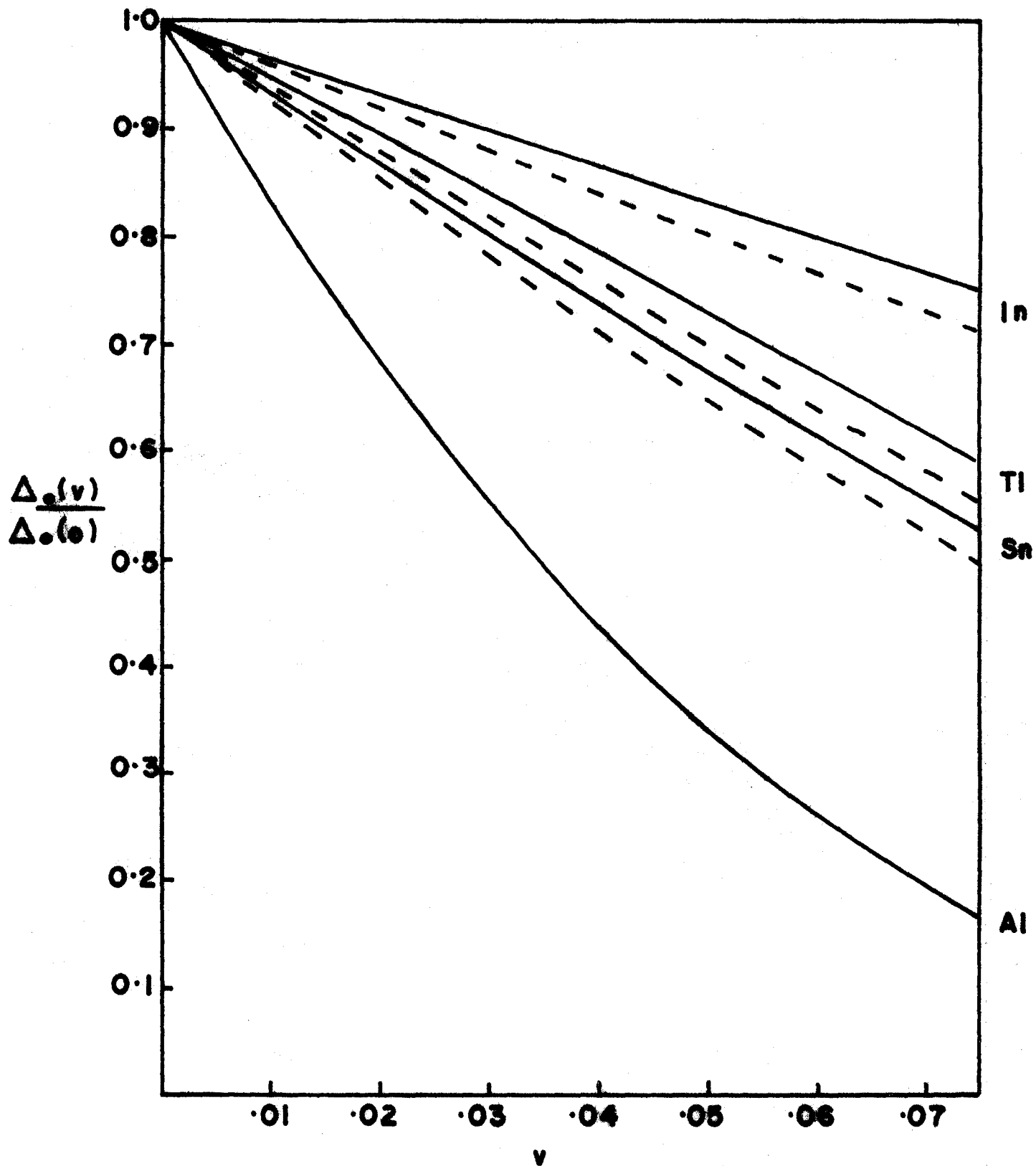
P. Vashishta⁽⁵²⁾, the Coulomb pseudopotential parameter is adjusted to give the correct zero pressure energy gap, $\Delta_0(0)$. We should do the same if our comparison is to be meaningful. It should be remarked that our procedure is a most stringent test of the relevant equations. We could easily pick values of μ^* that would give very good agreement with Vashishta's values of $\Delta_0(v)/\Delta_0(0)$ and at the same time a fairly good value of $\Delta_0(0)$. For example, in the work of Carbotte and Trofimenkoff reasonable qualitative agreement with their results for $T_c(v)/T_c(0)$, obtained by solving the Eliashberg gap equations, was obtained using the Morel-Anderson equation,

$$T_c = 1.13 \theta_D e^{-\frac{1}{\lambda - \mu^*}}$$

with the same value of μ^* used in both calculations. This agreement loses its significance when it is realized that the Morel-Anderson results for $T_c(0)$ are very bad. Table 3.9 contains the values of $\mu_{\text{EXP}}^*(1)$ and $\mu_{\text{EXP}}^*(2)$ that are used to calculate $\Delta_0(v)/\Delta_0(0)$. $\mu_{\text{EXP}}^*(1)$ was used above in the calculation of $[N(0)V]_v$ and is used below in the calculation of the pressure dependence of the isotope effect.

Figure 3.5 is a graph of $\Delta_0(v)/\Delta_0(0)$ versus v . The solid curves are the results obtained using equation (3.58) and the broken curves are those obtained using equations (3.61) and (3.62). There is very good qualitative agreement between the two sets of curves for the medium coupling

FIGURE 3.5 The dependence of the energy gap on the fractional volume change $v \equiv - \Delta\Omega/\Omega_s$, as calculated using equation (3.58) (solid lines) and as calculated by solving the coupled set of equations (3.61) and (3.62) (broken lines).



elements and excellent quantitative agreement for weak coupling Al.

Table 3.10 contains three values of the ratio $\Delta_0(v)/\Delta_0(0)$ for $v = .025$ and $v = .050$. They were calculated using equation (3.58), equations (3.61) and (3.62), and the Eliashberg gap equations⁽⁵²⁾, respectively. The Eliashberg solutions are those of P. Vashishta and were calculated by scaling the phonon frequencies according to

$$\gamma(v) = 1 + \gamma_G v \quad .$$

This same scaling was used in calculating our values for $\Delta_0(v)/\Delta_0(0)$ in table 3.10. (The calculations for figure 3.5 were done for values of $\gamma(v)$ given by (3.52).)

We note that there is very good quantitative agreement between the values of $\Delta_0(v)$ obtained by solving the Eliashberg gap equations and those obtained by solving the greatly simplified integral equations (3.61) and (3.62). The discrepancies are probably less than the numerical uncertainties in the Eliashberg results. The Eliashberg equations were solved for a fixed number of points (45) in the $\alpha^2(v)F(v)$ spectrum. For a fractional volume change v , $\omega_c(v) = \gamma(v)\omega_c(0)$. Hence to be consistent one should increase the number of points used to represent the function $\alpha^2(v)F(v)$ by the factor $\gamma(v)/\gamma(0)$. The values for $\Delta_0(v)$ calculated using equation (3.58) are in fairly good quantitative agreement with the other values.

TABLE 3.10
 A COMPARISON OF THREE DIFFERENT CALCULATIONS
 OF THE RATIO $\Delta_0(v)/\Delta_0(0)$

$$v = .025$$

ELEMENT	γ_G	(1)	(2)	(3)
Tl	2.25	.875	.86	.85
In	1.80	.92	.90	.895
	2.50	.865	.84	.83
Sn	2.25	.84	.825	.81

$$v = .050$$

ELEMENT	γ_G	(1)	(2)	(3)
Tl	2.25	.755	.73	.71
In	1.80	.85	.82	.81
	2.50	.75	.71	.70
Sn	2.25	.70	.68	.66

(1) $\Delta_0(v)/\Delta_0(0)$ calculated using equation (3.58).

(2) $\Delta_0(v)/\Delta_0(0)$ calculated by solving the integral equations (3.61) and (3.62).

(3) $\Delta_0(v)/\Delta_0(0)$ calculated by solving the Eliashberg gap equations.

It seems safe to conclude that, for an investigation of the effect of pressure on the energy gap Δ_0 of a weak coupling superconductor, the simple expression (3.58) is adequate. Equations (3.61) and (3.62) could be used for slightly improved accuracy. For a qualitative study of the effect of pressure on medium coupling superconductors equation (3.58) is completely adequate, but for a quantitative study the integral equations (3.61) and (3.62) should be used. In fact, for some calculations these latter equations may be preferable to the Eliashberg equations because of the huge saving in computer time with, it appears, little loss in accuracy.

(ii) Pressure Dependence of the Directional Energy Gaps in a Pure Single-Crystal Superconductor

We readily extend to finite pressure the one iteration result, equation (3.34), for the directional energy gap at the gap edge in a pure single-crystal weak coupling superconductor. We obtain

$$\Delta_0(\theta, \phi, v) = \frac{1}{1 + \lambda(\theta, \phi, v)} \left\{ \int_0^{\omega_c(v)} dv [\alpha^2 F(v, \theta, \phi)]_v K(v, \omega_c(v), \Delta_0(v)) - \mu^* \log\left(\frac{2\omega_c(v)}{\Delta_0(v)}\right) \right\} \Delta_0(v) \quad (3.63)$$

where $\Delta_0(v)$ is the isotropic energy gap in the 'dirty' superconductor when subjected to the fractional volume change v .

$\Delta_0(v)$ is given by equations (3.61) and (3.62).

The directional α^2F computer programme, which is discussed in detail in Chapter IV, is easily modified to calculate $[\alpha^2F(v, \theta, \phi)]_v$ for finite v . However the large amount of computer time needed to calculate this function for many directions (θ, ϕ) and several values of v is not warranted by the one iteration approximation. Instead we make the reasonable assumption that the scaling law of Carbotte and Trofimenkoff⁽³⁹⁾ can be extended to the directional case. That is, we assume that

$$[\alpha^2F(v, \theta, \phi)]_v = \frac{B(\theta, \phi, v)}{\gamma^2(v)} [\alpha^2F(v/\gamma(v), \theta, \phi)]_0 \quad (3.64)$$

The expression for $B(v)$, equation (3.54), was derived in detail in reference (51). The analogous expression for $B(\theta, \phi, v)$ is obtained by repeating this derivation with $\alpha^2F(v)$ replaced by $\alpha^2F(v, \theta, \phi)$. It turns out that, with our approximations of a spherical Fermi surface and a local pseudo-potential, $B(\theta, \phi, v)$ is independent of direction. That is

$$B(\theta, \phi, v) = B(v) \quad (3.65)$$

Hence (3.63) becomes

$$\Delta_0(\theta, \phi, v) = \frac{1}{1 + \frac{B(v)}{\gamma^2(v)}} \frac{1}{\lambda(\theta, \phi, 0)} \left\{ \frac{B(v)}{\gamma(v)} \int_0^{\omega_c(0)} dv [\alpha^2F(v, \theta, \phi)]_0 \right. \\ \left. \times K(\gamma(v)v, \gamma(v)\omega_c(0), \Delta_0(v))^{-\mu} \log\left(\frac{2\gamma(v)\omega_c(0)}{\Delta_0(v)}\right) \right\} \Delta_0(v) \quad (3.66)$$

For Al, replacing K by \tilde{K} is a very good approximation. We do this and obtain

$$\Delta_0(\theta, \phi, \nu) = \frac{1}{1 + \eta(\nu) \bar{\lambda}(\theta, \phi, 0)} \{ \eta(\nu) \bar{\lambda}(\theta, \phi, 0) + [\eta(\nu) \lambda(\theta, \phi, 0) - \mu^*] \times \log\left(\frac{2\gamma(\nu) \omega_c(0)}{\Delta_0(\nu)}\right) \} \Delta_0(\nu) \quad , (3.67)$$

where $\Delta_0(\nu)$ is now given by equation (3.58). We use equation (3.67) to calculate $\Delta_0(\theta, \phi, \nu)$ for Al for $\nu=0$, .025, and .050. $\lambda(\theta, \phi, 0)$ and $\bar{\lambda}(\theta, \phi, 0)$ are calculated using the theoretical $\alpha^2 F(\nu, \theta, \phi)$'s discussed in detail elsewhere in this thesis. The results for $\Delta_0(\theta, \phi, \nu)$ are shown in figure 3.6.

A measure of the anisotropy in $\Delta_0(\theta, \phi, \nu)$ for a given value of ν is the ratio of the maximum to the minimum directional energy gap occurring for that value of ν . We define an anisotropy parameter $A(\nu)$ accordingly.

$$A(\nu) \equiv \frac{\Delta_0^{\text{MAX}}(\theta, \phi, \nu)}{\Delta_0^{\text{MIN}}(\theta, \phi, \nu)} \quad . (3.68)$$

Table 3.11 contains $\Delta_0^{\text{MAX}}(\theta, \phi, \nu)$, $\Delta_0^{\text{MIN}}(\theta, \phi, \nu)$ and $A(\nu)$ for Al for $\nu=0$, .025 and .050. It is apparent from the tabulated values of $A(\nu)$ that the anisotropy of the energy gap in Al increases with increasing pressure. This very interesting result is not hard to understand physically. The dominant source of anisotropy in the energy gap is the anisotropy in the phonon mediated electron-electron interaction. The set of virtual phonons emitted or absorbed by an electron

FIGURE 3.6 The anisotropy of the energy gap $\Delta_0(\theta, \phi)$
in aluminium for three different fractional
volume changes.

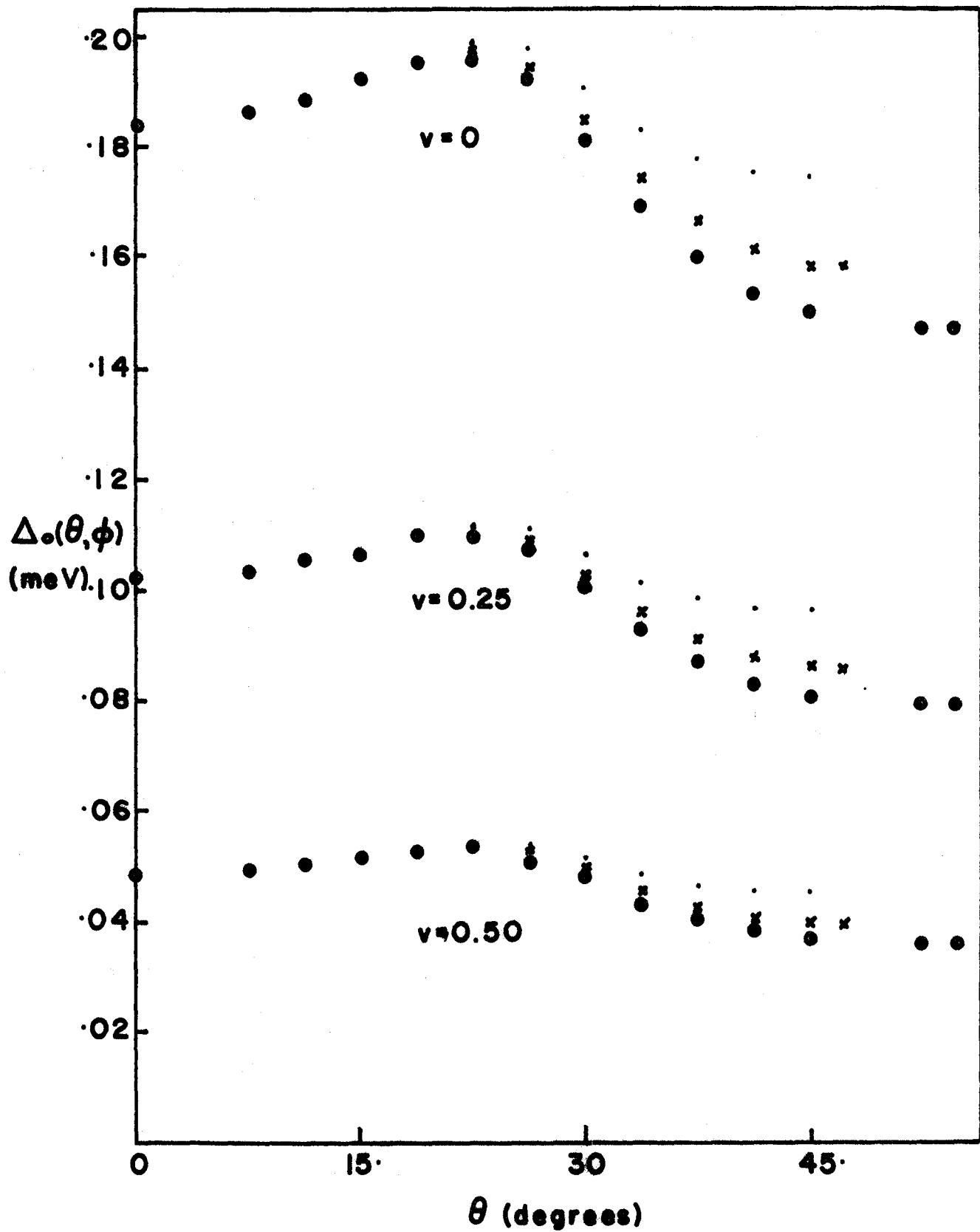


TABLE 3.11
EFFECT OF PRESSURE ON THE ANISOTROPY
OF THE ENERGY GAP IN ALUMINIUM

v	$\Delta_0^{\text{MAX}}(\theta, \phi, v)$ (mev)	$\Delta_0^{\text{MIN}}(\theta, \phi, v)$ (mev)	$A(v)$
0.000	.198	.147	1.35
0.025	.111	.079	1.41
0.050	.054	.036	1.50

making virtual transitions from the state $\underline{k} \equiv (k_F, \theta, \phi)$ to all other points $\underline{k}' \equiv (k_F, \theta', \phi')$ on the Fermi surface depends on the initial state \underline{k} . This is a geometrical effect. In the extended zone scheme the set of all the phonon \underline{q} vectors generated above would terminate on the surface of a sphere of radius k_F . In the reduced zone scheme, which is the physically meaningful representation, the \underline{q} vectors corresponding to umklapp processes would be remapped into the first zone. The parts of the spherical surface lying outside the first zone would be mapped into the first zone forming a complicated two dimensional surface. It is obvious that, unless one had a spherical Brillouin zone or such a small Fermi sphere that there were no umklapp processes, the shape of this surface would depend on the coordinates (θ, ϕ) of the initial state \underline{k} . When the metal is subjected to a hydrostatic pressure the Fermi sphere and the Brillouin zone scale together so that the shape of the complicated surface generated for the initial point (θ, ϕ) does not change (its size does, of course). In the approximation of a mode independent Grüneisen constant we expect the anisotropy in the phonon induced electron-electron interaction to be essentially independent of pressure. But, because this phonon induced interaction decreases with increasing pressure, the anisotropy in the total interaction increases*. Hence the anisotropy in the energy gap increases

The Coulomb pseudopotential parameter μ^ changes very slowly with pressure as compared to the phonon-mediated interaction.

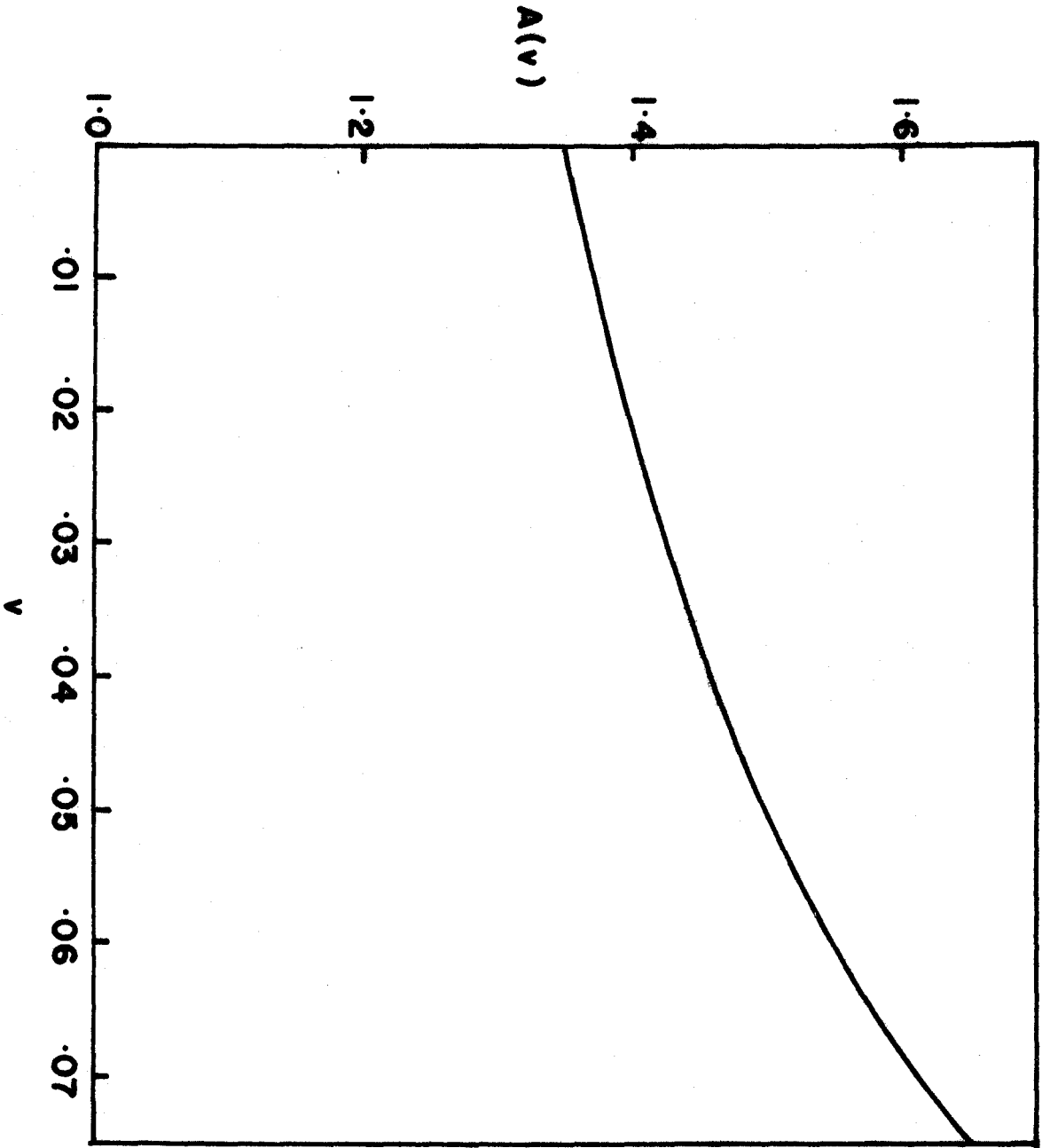
with increasing pressure. Furthermore, the smaller the ratio of the strength of the phonon induced interaction to the strength of the Coulomb interaction the faster will be the increase of the energy gap anisotropy with pressure. Since this ratio decreases with increasing pressure the rate of increase of the anisotropy with increasing pressure will increase as the pressure increases. This qualitative effect is clearly exhibited in figure 3.7 which is a plot of $A(v)$ versus v . The above considerations also lead to the conclusion that the effect of pressure on the anisotropy of the energy gap will be more pronounced for a weak coupling superconductor than for a strong coupling one.

Even if one were to turn off the Coulomb interaction the effect would persist. In this case the anisotropy of the total interaction would be independent of pressure. But the energy gap depends on the total interaction in a very nonlinear way so that the anisotropy of the energy gap would still increase with increasing pressure and the rate of increase would be greater, the greater the pressure. Suppose, for example, that

$$\Delta_0(\theta, \phi, v) = 2\omega_c e^{-1/[N(0)V]_v^{\theta, \phi}} .$$

It is obvious from this equation that even if the anisotropy in $[N(0)V]_v^{\theta, \phi}$ were independent of v the anisotropy in the energy gap would increase with increasing v , i.e. decreasing

FIGURE 3.7 The dependence of the anisotropy parameter
A(v) on the fractional volume change v for
aluminium.



$N(0)V$, and the rate of increase would be larger, the smaller the interaction. The effects predicted above should be accessible to experimentalists because many thermodynamic properties depend on gross features of the anisotropy, such as the mean squared anisotropy. The qualitative arguments given above indicate that it would be best to look for an increase in the anisotropy of the energy gap with pressure in a weak coupling superconductor. Our calculations for aluminium indicate that the effect is quite large. The anisotropy parameter $A(v)$ increases by slightly more than 10% for a fractional volume change of 5%.

3.5 THE TRANSITION TEMPERATURE OF AN ISOTROPIC WEAK COUPLING SUPERCONDUCTOR

The BCS integral equation for the energy gap of an isotropic superconductor at zero temperature is⁽¹¹⁾

$$\Delta_0(0) = N(0) \iint \frac{d\Omega_{\mathbf{k}}}{4\pi} \frac{d\Omega_{\mathbf{k}'}}{4\pi} \int_0^{\omega_D} \frac{d\varepsilon'}{E'} v_{\mathbf{k}\mathbf{k}'} \Delta_0(0) \quad (3.69)$$

The weak coupling version of equation (3.1) can be written in this form. We obtain

$$\Delta_0(0) = \frac{N(0)}{Z_S(\Delta_0(0), 0)} \iint \frac{d\Omega_{\mathbf{k}}}{4\pi} \frac{d\Omega_{\mathbf{k}'}}{4\pi} \int_0^{\omega_c} \frac{d\varepsilon'}{E'} v_{\mathbf{k}\mathbf{k}'} \Delta_0(0), \quad (3.70)$$

where $v_{\mathbf{k}\mathbf{k}'} = 2 \sum_{\lambda} |g_{\mathbf{k}\mathbf{k}'\lambda}|^2 \frac{(E' + \omega_{\mathbf{k}-\mathbf{k}'\lambda})}{(E' + \omega_{\mathbf{k}-\mathbf{k}'\lambda})^2 - \Delta_0^2(0)} - U_c \quad (3.71)$

The phonon-mediated part of $V_{\underline{k}\underline{k}'}$, is known as the Eliashberg interaction.

The BCS result for the energy gap at a finite temperature T is⁽¹¹⁾

$$\Delta_0(T) = N(0) \iint \frac{d\Omega_{\underline{k}}}{4\pi} \frac{d\Omega_{\underline{k}'}}{4\pi} \int_0^{\omega_D} \frac{d\varepsilon'}{E'} V_{\underline{k}\underline{k}'} \tanh(E'/2k_B T) \Delta_0(T) \quad (3.72)$$

where E' is now given by

$$E' \equiv \sqrt{\varepsilon'^2 + \Delta_0^2(T)}$$

We use equations (3.69) and (3.72) to generalize our zero temperature equation, (3.70), to finite temperature. We obtain

$$\Delta_0(T) = \frac{N(0)}{1+\lambda(T)} \iint \frac{d\Omega_{\underline{k}}}{4\pi} \frac{d\Omega_{\underline{k}'}}{4\pi} \int_0^{\omega_c} \frac{d\varepsilon'}{E'} V_{\underline{k}\underline{k}'} \tanh(E'/2k_B T) \Delta_0(T) \quad (3.73)$$

where $V_{\underline{k}\underline{k}'}$, is given by (3.71) with $\Delta_0(0)$ replaced by $\Delta_0(T)$ throughout. We have neglected the effect of thermal phonons in extending (3.71) to finite temperatures. This is a good approximation for weak coupling superconductors because their transition temperatures are very low. Moreover it is the forced vibrations of the ions due to the electrons themselves that are essential in superconductivity, not the thermal vibrations. We have also neglected the very small difference between $Z_s(\Delta_0(T), T)$ and $Z_n(0, T)$. This difference

vanishes at the transition temperature.

The temperature T_c at which the superconducting transition takes place is obtained by letting $\Delta_0(T)$ go to zero as T goes to T_c from below in equation (3.73). We obtain

$$\begin{aligned}
 1 &= \frac{N(0)}{1+\lambda(T_c)} \left\{ 2 \iint \frac{d\Omega_{\underline{k}}}{4\pi} \frac{d\Omega_{\underline{k}'}}{4\pi} \sum_{\lambda} |g_{\underline{k}\underline{k}'\lambda}|^2 \int_0^{\omega_c} \frac{d\varepsilon'}{\varepsilon'} \frac{\tanh(\varepsilon'/2k_B T)}{\varepsilon' + \omega_{\underline{k}-\underline{k}'\lambda}} \right. \\
 &\quad \left. - U_c \int_0^{\omega_c} \frac{d\varepsilon'}{\varepsilon'} \tanh(\varepsilon'/2k_B T_c) \right\} \\
 &= \frac{1}{1+\lambda(T_c)} \left\{ 2 \int_0^{\omega_c} d\nu \alpha^2(\nu) F(\nu) \int_0^{\omega_c} \frac{d\varepsilon'}{\varepsilon'} \frac{\tanh(\varepsilon'/2k_B T_c)}{\varepsilon' + \nu} - \mu^* \right. \\
 &\quad \left. \times \int_0^{\omega_c} \frac{d\varepsilon'}{\varepsilon'} \tanh(\varepsilon'/2k_B T_c) \right\} \quad . (3.74)
 \end{aligned}$$

The last integral is easily evaluated for a weak coupling superconductor⁽⁵³⁾. Changing variables ($x = \varepsilon'/k_B T_c$) and integrating by parts we obtain

$$\begin{aligned}
 \int_0^{\omega_c} \frac{d\varepsilon'}{\varepsilon'} \tanh(\varepsilon'/2k_B T_c) &= \int_0^{\omega_c/k_B T_c} \frac{dx}{x} \tanh(x/2) = \log\left(\frac{\omega_c}{k_B T_c}\right) \\
 &\quad - \int_0^{\infty} dx \log x \frac{d}{dx} \tanh(x/2) \quad . (3.75)
 \end{aligned}$$

We have used the fact that $\tanh(\omega_c/k_B T_c)$ can be replaced by 1 when $\omega_c \gg k_B T_c$ (as it is for a weak coupling superconductor). Since $d/dx \tanh(x/2)$ decreases very rapidly as x increases from zero and since the upper limit, $\omega_c/k_B T_c$, is very large we have replaced it by infinity. The last integral in (3.74) is just a number, $-\log 1.134$. Hence

$$\int_0^{\omega_c} \frac{d\varepsilon'}{\varepsilon'} \tanh(\varepsilon'/2k_B T_c) = \log\left(\frac{1.134 \omega_c}{k_B T_c}\right) \quad (3.76)$$

We evaluate the remaining integral in (3.74) in a similar fashion

$$\begin{aligned} \int_0^{\omega_c} \frac{d\varepsilon'}{\varepsilon'} \frac{\tanh(\varepsilon'/2k_B T_c)}{\varepsilon' + \nu} &= \frac{1}{k_B T_c} \int_0^{\omega_c/k_B T_c} \frac{dx \tanh(x/2)}{x \ x + \nu/k_B T_c} \\ &= \frac{1}{\nu} \left\{ -\tanh\left(\frac{x}{2}\right) \log\left(\frac{x + \nu/k_B T_c}{x}\right) \right\} \Bigg|_0^{\omega_c/k_B T_c} + \int_0^{\omega_c/k_B T_c} dx \log\left(\frac{x + \nu/k_B T_c}{x}\right) \end{aligned}$$

$$\begin{aligned} &\frac{d}{dx} \tanh \frac{x}{2} \Bigg\} \\ &= \frac{1}{\nu} \left\{ \log\left(\frac{\omega_c}{\omega_c + \nu}\right) + \log 1.134 + \int_0^{\omega_c/k_B T_c} dx \log\left(x + \frac{\nu}{k_B T_c}\right) \frac{d}{dx} \tanh \frac{x}{2} \right\}. \end{aligned}$$

Since $\nu/k_B T_c \gg 1$ for those phonon frequencies, ν , which are important in weak coupling superconductivity, and since $\frac{d}{dx} \tanh\left(\frac{x}{2}\right)$ decreases very rapidly as x increases from zero,

we can replace $\log(x+v/k_B T_c)$ by $\log(v/k_B T_c)^*$ in the remaining integral to obtain

$$\int_0^{\omega_c} \frac{d\varepsilon}{\varepsilon} \frac{\tanh(\varepsilon/2k_B T_c)}{\varepsilon+v} = \frac{1}{v} \left[\log\left(\frac{\omega_c}{\omega_c+v}\right) + \log 1.134 + \log\left(\frac{v}{k_B T_c}\right) \right] \quad (3.77)$$

Substituting (3.76) and (3.77) into (3.74) and solving for T_c we obtain

$$k_B T_c = 1.134 \omega_c e^{-\frac{1+\lambda(T_c)-\bar{\lambda}}{\lambda-\mu^*}} \quad (3.78)$$

where $\lambda \equiv \lambda(0)$ and $\bar{\lambda} \equiv \bar{\lambda}(0)$. Equation (3.78) is very similar to the corresponding equation, (3.20), for the zero temperature energy gap. The BCS result for the transition temperature of a weak coupling superconductor is⁽¹¹⁾

$$k_B T_c = 1.134 \omega_D e^{-1/N(0)V} \quad (3.79)$$

A comparison of (3.20) and (3.78) with the corresponding BCS results suggests that the BCS parameter $N(0)V$ should have a temperature dependence given by

$$[N(0)V]_T = \frac{\lambda-\mu^*}{1+\lambda(T)-\bar{\lambda}} \quad (3.80)$$

Recent experimental determinations^(54,55) and

* For $v/k_B T_c \gg 1$ and x small, $\log(x+v/k_B T_c)$ is a very slowly varying function of x .

theoretical calculations^(56,57) of the temperature dependence of the renormalization parameter $\lambda(T)$ indicate that for small T , of the order of a few degrees, $\lambda(T)$ is a very slowly increasing function of T . This implies that the temperature dependence of the BCS parameter is very slight.

We now use equations (3.20) and (3.78) to obtain a small correction to the well known BCS ratio

$$\left(\frac{2\Delta_0(0)}{k_B T_C}\right)^{\text{BCS}} = 3.53 \quad .(3.81)$$

Our result is

$$\left(\frac{2\Delta_0(0)}{k_B T_C}\right) = 3.53 e^{\frac{\lambda(T_C) - \lambda}{\lambda - \mu^*}} \quad .(3.82)$$

Since $\lambda(T_C)$ is slightly larger than λ this equation leads to the result that the ratio $2\Delta_0(0)/k_B T_C$ for a weak coupling superconductor is somewhat larger than the BCS ratio. Our results for Al, Tl, In and Sn are 3.53, 3.585, 3.60 and 3.57 respectively.

We now use the scaling law of Carbotte and Trofimenkoff, equations (3.53) and (3.54), to derive a simple expression for the pressure dependence of the ratio $2\Delta_0(0)/k_B T_C$. The temperature dependence of the renormalization parameter is given by^(58,59)

$$\lambda(T) = 2 \int dE \left(-\frac{\partial f(E)}{\partial E}\right) \int dv \frac{\alpha^2 F(v)}{v+E} \quad , (3.83)$$

where $f(E)$ is the Fermi function

$$f(E) = \frac{1}{e^{E/k_B T} + 1}$$

Within the scaling law approximation the dependence of $\lambda(T)$ on the fractional volume change v is readily found to be

$$\lambda(T, v) = \frac{B(v)}{\gamma^2(v)} \lambda(T/\gamma(v), 0) = \eta(v) \lambda(T/\gamma(v)) \quad .(3.84)$$

We are using the notation: $\lambda(T) \equiv \lambda(T, v=0)$; $\lambda \equiv \lambda(T=0, v=0)$.

It follows from (3.82) and (3.84) that

$$\frac{2\Delta_0(0, v)}{k_B T_c(v)} = 3.53 e^{\eta(v) \frac{[\lambda(T_c(v)/\gamma(v)) - \lambda]}{\eta(v) \lambda^{-\mu^*}}} \quad .(3.85)$$

If $\lambda(T)$ is available for small T this equation can be solved in a fraction of a second on an electronic computer.

The qualitative pressure dependence of (3.85) follows from a simple argument. A calculation of $\lambda(T)$ for low T ($T \ll \theta_D$), using the model⁽⁵⁹⁾

$$\begin{aligned} \alpha^2 F(v) &= \lambda(v/\omega_D)^2 & 0 < v < \omega_D \\ &= 0 & v > \omega_D \end{aligned}$$

leads to the result

$$\frac{\lambda(T) - \lambda}{\lambda} \approx \frac{2\pi^2}{3} \left(\frac{T}{\theta_D}\right)^2 \log\left(\frac{\theta_D}{T}\right) \quad .(3.86)$$

This result is qualitatively correct for a weak coupling superconductor. Now, let us consider equation (3.78) for a moment. Because of the exponential dependence of T_c on $(\lambda - \mu^*)^{-1}$ it is obvious that T_c goes to zero much faster than $(\lambda - \mu^*)$ does. Hence, by equation (3.86), for small T the difference $(\lambda(T) - \lambda)$ goes to zero much faster than $(\lambda - \mu^*)$ does. This means that the factor in the exponential of equation (3.85) decreases with increasing pressure (i.e. decreasing $(\lambda - \mu^*)$) and the ratio of twice the zero temperature energy gap to the transition temperature approaches the BCS result. This effect has been experimentally observed in lead⁽⁶⁰⁾. As a further check equation (3.85) was solved for In and Sn for several values of v using the low temperature values of $\lambda(T)$ calculated in reference (56). For both metals it was found that the ratio of twice the zero temperature energy gap to the transition temperature approaches the BCS value of 3.53 with increasing pressure.

Before proceeding to the next section we observe that our more or less intuitive derivation of equation (3.73) can be justified within the strong coupling formalism. As already mentioned in Chapter II, McMillan⁽³⁰⁾ used the finite temperature Eliashberg gap equations to derive an approximate expression for the transition temperature of a strong coupling superconductor. He assumed, as we have done, a model solution of the form

$$\begin{aligned} \Delta(\omega) &= \Delta_0 & 0 < \omega < \omega_c \\ &= \Delta_c & \omega_c < \omega \end{aligned}$$

He neglected thermal phonons and obtained

$$\Delta^1(0) = \frac{\Delta_0}{Z(0)} \int_0^{\omega_c} \frac{d\omega'}{\omega'} 2 \int_0^{\omega_c} d\nu \alpha^2 F(\nu) \left\{ \frac{f(-\omega')}{\omega'+\nu} - \frac{f(\omega')}{-\omega'+\nu} \right\} \quad (3.87)$$

for the contribution of one-phonon exchange processes to the energy gap. He then neglected ω' relative to ν in the phonon propagators $(\pm\omega'+\nu)^{-1}$ (because the integrand in the ω' integral is heavily weighted at small ω') and obtained

$$\Delta^1(0) \approx \frac{\Delta_0}{Z(0)} \int_0^{\omega_c} \frac{d\omega'}{\omega'} \tanh\left(\frac{\omega'}{2k_B T_c}\right) 2 \int_0^{\omega_c} \frac{d\nu \alpha^2 F(\nu)}{\nu} \quad (3.88)$$

We treat equation (3.87) more accurately. For small T

$f(-\omega')$ is equal to 1 over most of the range of integration $0 < \omega' < \omega_c$ so that it is not a good approximation to neglect ω' relative to ν in the term containing $f(-\omega')/(\omega'+\nu)$.

We leave this term unchanged. For small T $f(\omega')$ decreases very rapidly to zero as ω' increases from zero. For a weak coupling superconductor the important phonon frequencies, ν , are much larger than the values of ω' which are heavily weighted in the term $f(\omega')/(-\omega'+\nu)$. Hence it is a good approximation to replace this last expression by $f(\omega')/(\omega'+\nu)$.

We do this and obtain in place of (3.88)

$$\Delta^1(0) \approx \frac{\Delta(0)}{Z(0)} 2 \int_0^{\omega_c} d\nu \alpha^2 F(\nu) \int_0^{\omega_c} \frac{d\omega'}{\omega'} \frac{\tanh(\omega'/2k_B T_c)}{\omega'+\nu} \quad (3.89)$$

This is precisely the one-phonon exchange contribution to the energy gap occurring in equation (3.74). This justifies our

argument by analogy used in writing down (3.73) and consequently¹⁰⁰ (3.74).

3.6 THE TRANSITION TEMPERATURE OF A PURE SINGLE-CRYSTAL SUPERCONDUCTOR

We can easily generalize equation (3.73) for the isotropic energy gap of a 'dirty' superconductor at a finite temperature T to an equation for the directional energy gap of a pure single-crystal superconductor. We obtain

$$\Delta_0(\underline{k}, T) = \frac{N(0)}{1+\lambda(\underline{k}, T)} \int \frac{d\Omega_{\underline{k}'}}{4\pi} \int_0^{\omega_c} \frac{d\varepsilon'}{\varepsilon'} v_{\underline{k}, \underline{k}'} \Delta_0(\underline{k}', T) \tanh(\varepsilon'/2k_B T) \quad (3.90)$$

where $E' \equiv \sqrt{\varepsilon'^2 + \Delta_0^2(\underline{k}, T)}$. This equation is used in Chapter IV to investigate the temperature dependence of the anisotropy.

Letting the energy gap go to zero as T goes to T_c from below (3.90) becomes

$$\Delta_0(\underline{k}, T_c) = \frac{N(0)}{1+\lambda(\underline{k}, T_c)} \left\{ \int \frac{d\Omega_{\underline{k}'}}{4\pi} 2 \sum_{\lambda} |g_{\underline{k}\underline{k}', \lambda}|^2 \Delta_0(\underline{k}', T_c) \int_0^{\omega_c} \frac{d\varepsilon'}{\varepsilon'} \frac{\tanh(\varepsilon'/2k_B T_c)}{\varepsilon' + \omega_{\underline{k}-\underline{k}', \lambda}} \right. \\ \left. - U_c \int \frac{d\Omega_{\underline{k}'}}{4\pi} \Delta_0(\underline{k}', T_c) \int_0^{\omega_c} \frac{d\varepsilon'}{\varepsilon'} \tanh(\varepsilon'/2k_B T_c) \right\}$$

Using the following results from the previous section,

$$\int_0^{\omega_c} \frac{d\varepsilon'}{\varepsilon'} \tanh(\varepsilon'/2k_B T_c) = \log\left(\frac{1.134\omega_c}{k_B T_c}\right),$$

$$\int_0^{\omega_c} \frac{d\varepsilon'}{\varepsilon'} \frac{\tanh(\varepsilon'/2k_B T_c)}{\varepsilon' + \omega} = \frac{1}{\omega} \left[\log\left(\frac{\omega/\omega_c}{1+\omega/\omega_c}\right) + \log\left(\frac{1.134\omega_c}{k_B T_c}\right) \right],$$

we obtain

$$\Delta_0(\underline{k}, T_c) = \frac{1}{1+\lambda(\underline{k}, T_c)} \left\{ \int \frac{d\Omega_{\underline{k}'}}{4\pi} \Delta_0(\underline{k}', T_c) 2N(0) \Sigma \frac{|g_{\underline{k}\underline{k}'\lambda}|^2}{\lambda \omega_{\underline{k}-\underline{k}'\lambda}} \log\left(\frac{\omega_{\underline{k}-\underline{k}'\lambda}/\omega_c}{1+\omega_{\underline{k}-\underline{k}'\lambda}/\omega_c}\right) \right. \\ \left. + \log\left(\frac{1.134\omega_c}{k_B T_c}\right) \left[\int \frac{d\Omega_{\underline{k}'}}{4\pi} \Delta_0(\underline{k}', T_c) 2N(0) \Sigma \frac{|g_{\underline{k}\underline{k}'\lambda}|^2}{\lambda \omega_{\underline{k}-\underline{k}'\lambda}} - \mu^* \right] \right\} .$$

Integrating over $\Omega_{\underline{k}}$ we obtain

$$\int \frac{d\Omega_{\underline{k}}}{4\pi} \Delta_0(\underline{k}, T_c) (1+\lambda(\underline{k}, T_c)) = \int \frac{d\Omega_{\underline{k}'}}{4\pi} \Delta_0(\underline{k}', T_c) \bar{\lambda}(\underline{k}') + \log\left(\frac{1.134\omega_c}{k_B T_c}\right) \\ \times \left[\int \frac{d\Omega_{\underline{k}'}}{4\pi} \Delta_0(\underline{k}', T_c) \lambda(\underline{k}') - \mu^* \right] \quad (3.91)$$

We let

$$\Delta_0(\underline{k}, T_c) = \langle \Delta_0(\underline{k}, T_c) \rangle (1+a_{\underline{k}})$$

$$\lambda(\underline{k}, T_c) = \lambda(T_c) (1+b_{\underline{k}})$$

$$\lambda(\underline{k}) = \lambda(1+b_{\underline{k}})$$

$$(\lambda(\underline{k}) \equiv \lambda(\underline{k}, 0))$$

$$\bar{\lambda}(\underline{k}) = \bar{\lambda}(1+\bar{b}_{\underline{k}})$$

$$. (3.92)$$

We have assumed that the anisotropy parameters $a_{\underline{k}}$, $b_{\underline{k}}$ and $\bar{b}_{\underline{k}}$ are independent of temperature over the small temperature range from zero to the transition temperature. After substituting (3.92) into (3.91), cancelling $\langle \Delta_0(\underline{k}, T_c) \rangle$ from both sides of the resulting equation, and solving

for $k_B T_c$ we obtain

$$k_B T_c = 1.134 \omega_c e^{-\left(\frac{1 + (1 + \langle ab \rangle) \lambda (T_c) - (1 + \langle a\bar{b} \rangle) \bar{\lambda}}{(1 + \langle ab \rangle) \lambda - \mu^*} \right)} \quad .(3.93)$$

The one iteration results for $\langle ab \rangle$ and $\langle a\bar{b} \rangle$ for Al are used in Chapter IV to estimate the transition temperature of a pure single-crystal of Al using the above equation.

Equation (3.93) is to be compared with the corresponding equation for the average energy gap in a pure single-crystal. We note that

$$\frac{2 \langle \Delta_0(\mathbf{k}, 0) \rangle}{k_B T_c} = 3.53 \exp\left\{ - \frac{(1 + \frac{1}{2} \langle a^2 \rangle + 2 \langle ab \rangle) \lambda - (1 + \langle ab \rangle) \lambda (T_c) - \frac{1}{2} \langle a^2 \rangle \mu^*}{(1 + \langle ab \rangle) \lambda - \mu^*} \right\} \quad .(3.94)$$

In Chapter IV this equation is used to arrive at the very interesting qualitative result that the ratio of twice the average zero temperature energy gap to the transition temperature for a pure single-crystal of Al is smaller than the corresponding ratio for isotropic or 'dirty' Al.

3.7 THE ISOTOPE EFFECT FOR A WEAK COUPLING SUPERCONDUCTOR

We use the equation for the transition temperature of a weak coupling superconductor,

$$k_B T_c = 1.13 \omega_c e^{-\frac{1 + \lambda (T_c) - \bar{\lambda}}{\lambda - \mu^*}} \quad , (3.95)$$

to derive an expression for the isotope effect exponent.

Differentiating the logarithm of both sides of (3.95) with respect to the ionic mass M^* we obtain

$$\frac{d}{dM} \log T_c = \frac{d}{dM} \log \omega_c - \frac{d}{dM} \left(\frac{1 + \lambda(T_c) - \bar{\lambda}}{\lambda - \mu^*} \right) .$$

We assume that $T_c \propto M^{-\beta}$ and recall that $\omega_c \propto M^{-\frac{1}{2}}$ to obtain

$$\beta = \frac{1}{2} + M \left\{ (\lambda - \mu^*) \frac{d\lambda(T_c)}{dM} + (1 + \lambda(T_c) - \bar{\lambda}) \frac{d\mu^*}{dM} \right\} / (\lambda - \mu^*)^2 . \quad (3.96)$$

Now

$$\mu^* = \frac{N(0)V_c}{1 + N(0)V_c \log(E_F/\omega_c)} .$$

Hence

$$\frac{d\mu^*}{dM} = - \frac{(\frac{1}{2})}{M} \left[\frac{N(0)V_c}{1 + N(0)V_c \log(E_F/\omega_c)} \right]^2 = - \frac{(\frac{1}{2})}{M} \mu^{*2} . \quad (3.97)$$

$$\frac{d}{dM} \lambda(T_c) = \frac{d\lambda(T_c)}{d \log T_c} \frac{d \log T_c}{dM} = - \frac{\beta}{M} T_c \frac{d\lambda(T_c)}{dT_c} . \quad (3.98)$$

Substituting (3.97) and (3.98) into (3.96) and solving for the isotope effect exponent, β , we obtain

$$\beta = \frac{1}{2} \frac{\left(1 - \frac{(1 + \lambda(T_c) - \bar{\lambda})}{(\lambda - \mu^*)^2} \mu^{*2} \right)}{\left(1 + T_c \frac{d\lambda(T_c)}{dT_c} / (\lambda - \mu^*) \right)} . \quad (3.99)$$

If we assume that $\Delta_0 \propto M^{-\beta'}$ (Δ_0 is the zero temperature

* M is the average ionic mass of a superconductor consisting of a single element.

energy gap given by equation (3.20)) we find in the same way that

$$\begin{aligned}\beta' &= \frac{1}{2} \left(1 - \frac{(1+\lambda-\bar{\lambda})}{(\lambda-\mu^*)^2} \mu^{*2} \right) \\ &= \frac{1}{2} \left(1 - \frac{1}{1+\lambda-\bar{\lambda}} \left[\frac{\mu^*}{N(0)V} \right]^2 \right),\end{aligned}\quad (3.100)$$

where $N(0)V$ is given by (3.22). $\lambda(T)$ is a slowly increasing function of T for values of T of the order of the superconducting transition temperature of a weak coupling superconductor^(56,57) so that (3.99) and (3.100) lead to the conclusion that β is slightly smaller than β' . To a good approximation they are the same.

We can readily apply the results of section 3.4 on the pressure dependence of the energy gap to a brief study of the pressure dependence of the isotope effect. Using the scaling law of Carbotte and Trofimenkoff we obtain

$$\beta'(v) = \frac{1}{2} \left(1 - \frac{(1+\eta(v)[\lambda(0)-\bar{\lambda}(0)])}{(\eta(v)\lambda(0)-\mu^*(0))^2} \mu^*(0)^2 \right), \quad (3.101)$$

where
$$\eta(v) = \frac{B(v)}{\gamma^2(v)}$$

Table 3.12 contains $\beta'(v)$ calculated, using the above equation, for $v=0, .025, .050$ and $.075$ for Al, Tl, In and Sn. The values of $\lambda, \bar{\lambda}, \omega_c, \mu^*, B(v)$ and $\gamma(v)$ used in this section are the same as those used in section 3.4 to calculate the

TABLE 3.12
PRESSURE DEPENDENCE OF THE ISOTOPE EFFECT EXPONENT

ELEMENT	γ_G	$\beta'(0)$	$\beta'(.025)$	$\beta'(.050)$	$\beta'(.075)$
Al	2.22	.325	.283	.229	.155
Tl	2.25	.469	.4645	.458	.450
In	1.80	.466	.462	.458	.453
Sn	2.25	.443	.432	.419	.403

TABLE 3.13
COMPARISON OF OUR RESULTS FOR THE ISOTOPE
EFFECT WITH THOSE OF GARLAND

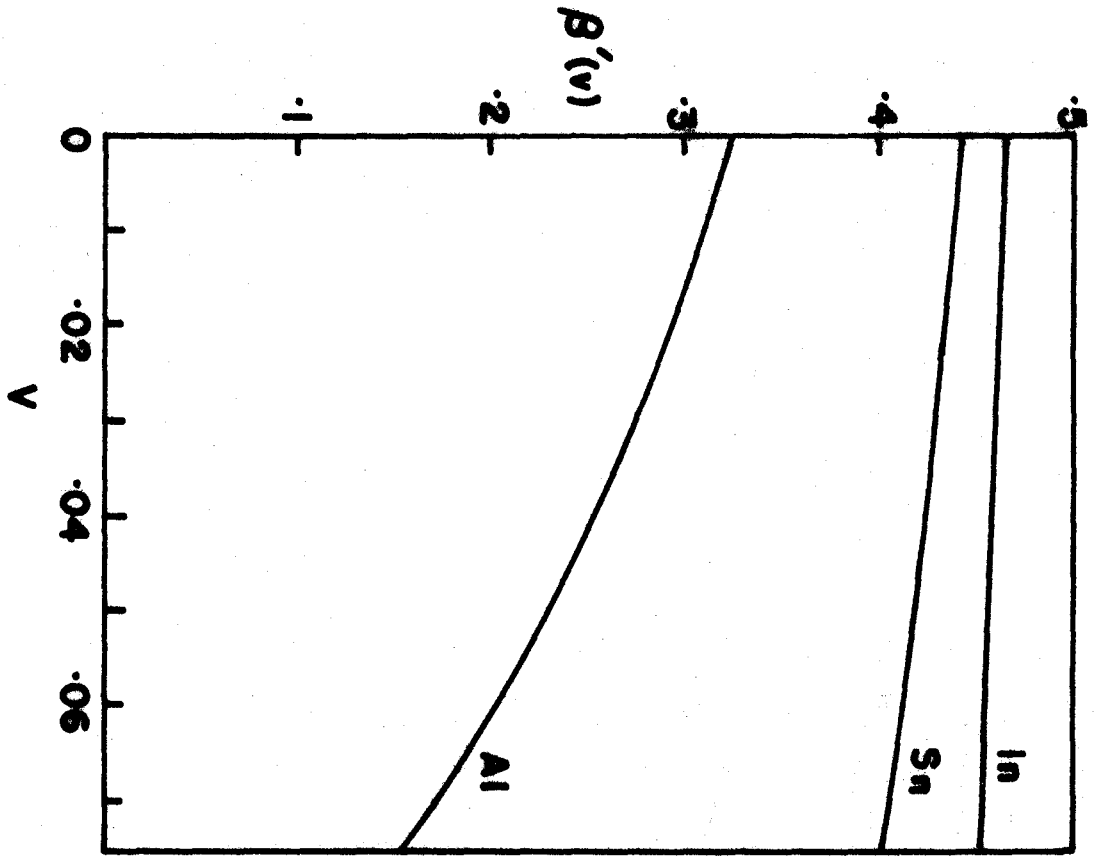
ELEMENT	β'	β_{GARLAND}
Al	.325	.37
Tl	.469	.48
Sn	.443	.455

pressure dependence of the energy gap. Figure 3.8 is a plot of $\beta'(v)$ versus v for Al, Sn and In. Two qualitative features are to be noted: (1) the isotope effect exponent β' is smaller for a weak coupling superconductor than for a medium coupling one; (2) β' decreases with increasing pressure (the weaker the phonon induced electron-electron interaction the greater is the rate of decrease of β' with increasing pressure). These qualitative effects are not unexpected because it is well known that deviations of the isotope effect exponent from $\frac{1}{2}$ are a measure of the relative strengths of the Coulomb and phonon-mediated electron-electron interactions⁽²¹⁾.

We do not compare the calculated zero pressure isotope effect exponents with experiment because the experimental situation is far from clear at the present time. The early experimental results for the simple metals were all close to the BCS value of .5. In particular the experimental value of β for Z_n was $.45 \pm .01$ ⁽⁶¹⁾. A recent measurement gave $.30 \pm .01$ ⁽⁶²⁾.

In table 3.13 we compare our results for β' with the latest results of Garland⁽⁶³⁾ for β . Our results are consistently lower than Garland's. Garland cuts the Coulomb interaction off at $4E_F$ thus obtaining a smaller value of μ^* than is obtained using the usual cut-off at E_F . This cut-off has been criticized because there appears to be no sound physical basis for such a large cut-off.

FIGURE 3.8 The dependence of the isotope effect exponent $\beta'(v)$ on the fractional volume change v for Al, Sn and In.



A good criterion for the correctness of any theoretical expression for the zero temperature energy gap (or the transition temperature) is that it simultaneously gives the correct energy gap and the correct isotope factor β' . Hence, it will be very interesting and illuminating to compare our results for the isotope effect exponent with experiment when reliable experimental values for weak and medium coupling superconductors are made available.

CHAPTER IV

THE ANISOTROPY OF THE ENERGY GAP IN SUPERCONDUCTING ALUMINIUM ARISING FROM THE ANISOTROPY OF THE PHONON DENSITY OF STATES

4.1 CALCULATION OF DIRECTIONAL ELECTRON-PHONON MASS-ENHANCEMENT PARAMETERS

For a pure single-crystal superconductor the essential information about the electron-phonon interaction and the phonon density of states is contained in the function

$$\alpha^2 F(\nu, \theta, \phi) = N(0) \int \frac{d\Omega_{\mathbf{k}'}}{4\pi} \sum_{\lambda} |g_{\mathbf{k}\mathbf{k}',\lambda}|^2 \delta(\nu - \omega_{\mathbf{k}-\mathbf{k}',\lambda}) \quad (4.1)$$

We emphasize again that we are neglecting any anisotropy in the Fermi surface and in the electronic single spin density of states at the Fermi surface. Hence $\mathbf{k} \equiv (k_F, \theta, \phi)$, where k_F is the free electron Fermi wave vector (related to the conduction electron density by $k_F = (3\pi^2 n)^{1/3}$), and $N(0)$ is the isotropic average of $N_{\mathbf{k}}(0)$. We employ the one OPW approximation and a local pseudopotential so that the electron-phonon coupling constant is given by⁽²⁵⁾

$$g_{\mathbf{k}\mathbf{k}',\lambda} = -i \frac{\mathbf{q} \cdot \boldsymbol{\varepsilon}(\mathbf{q}, \lambda)}{\sqrt{2MN\omega_{\mathbf{q}\lambda}}} W(\mathbf{q}) \quad (4.2)$$

where $\mathbf{q} \equiv \mathbf{k} - \mathbf{k}'$.

Equation (4.1) then becomes

$$\alpha^2 F(\nu, \theta, \phi) = \int \frac{d\Omega_{\mathbf{k}'}}{4\pi} \sum_{\lambda} L_{\lambda}(\underline{\mathbf{q}}) \delta(\nu - \omega_{\underline{\mathbf{q}}\lambda}) \quad , (4.3)$$

where

$$L_{\lambda}(\underline{\mathbf{q}}) = \frac{3z}{4k_F^2} \left(\frac{m}{M}\right) \frac{|\underline{\mathbf{q}} \cdot \underline{\boldsymbol{\epsilon}}(\underline{\mathbf{q}}, \lambda)|^2}{\omega_{\underline{\mathbf{q}}\lambda}} W^2(\underline{\mathbf{q}}) \quad . (4.4)$$

In (4.4) z is the number of conduction electrons per ion.

At first sight it might appear that the calculation of the isotropic function, $\alpha^2 F(\nu)$, is more difficult or at least much more time consuming than the calculation of the directional function, $\alpha^2 F(\nu, \theta, \phi)$, because the former involves a double surface integral while the latter involves only a single one. This is not the case. For a spherical Fermi surface and a local pseudopotential the double surface integral can be transformed into a volume integral over a sphere of radius $2k_F$. Symmetry considerations further reduce the range of integration to the irreducible part of the first Brillouin zone. This enables one to use the computer techniques developed by Gilat and Raubenheimer⁽⁶⁴⁾ so that the calculation of the isotropic $\alpha^2 F$ actually involves only a modest amount of computer time⁽²⁵⁾. The calculation of the anisotropic function $\alpha^2 F(\nu, \theta, \phi)$ for an arbitrary point (θ, ϕ) requires a great deal of computer time. Moreover, one needs the function for a large number of directions (θ, ϕ) for a meaningful study of anisotropy.

We now describe in some detail the method of calculating $\alpha^2 F(\nu, \theta, \phi)$ used in this work. The essential information about the lattice vibrations in Al (i.e. the phonon eigenfrequencies $\omega_{\underline{q}\lambda}$ and polarization vectors $\underline{\epsilon}_{\underline{q}\lambda}$ at every point \underline{q} in the first Brillouin zone) is readily available in the literature in the form of a Born-von Kármán force-constant fit to the dispersion curves measured in high symmetry directions by means of inelastic neutron scattering⁽⁶⁵⁾. The electron-ion pseudopotential form factor $W(\underline{q})$ is taken to be that of Heine and Abarenkov⁽⁶⁶⁾ as tabulated in reference (67). With this information the numerical evaluation of $\alpha^2 F(\nu, \theta, \phi)$ in histogram form is quite straightforward. The range of frequencies $0 < \nu < \omega_c$ is divided up into 100 channels, each of width $\omega_c/100$. The surface of the Fermi sphere is divided into $90 \times 180 = 16,200$ small areas by ninety lines of latitude, 2° apart, and 180 lines of longitude, also 2° apart. A random point (k_F, θ', ϕ') is selected from each of the 16,200 small areas and for each of these points the frequencies and eigenvectors $\omega_{\underline{q}\lambda}$ and $\underline{\epsilon}(\underline{q}\lambda)$, and then the weight factors, $L_\lambda(\underline{q}) \sin \theta'$ are calculated. The weight factors are then added to the appropriate frequency channels as specified by the delta functions $\delta(\nu - \omega_{\underline{q}\lambda})$. The resulting histogram is not normalized. For normalization purposes we define the function

$$N(\nu, \theta, \phi) = \int \frac{d\Omega_{\underline{k}'}}{4\pi} \sum_{\lambda} \delta(\nu - \omega_{\underline{q}\lambda}) \quad .(4.5)$$

This is a directional phonon frequency distribution function; it gives the phonon frequency distribution for the set of virtual processes in which an electron in the initial state (k_F, θ, ϕ) scatters to every point (k_F, θ', ϕ') on the surface of the Fermi sphere with the emission of a phonon of wave-vector $\underline{q} = \underline{k} - \underline{k}'$. Although this function is interesting in its own right we have introduced it primarily because of the useful property

$$\int d\nu N(\nu, \theta, \phi) = 3 \quad .(4.6)$$

The normalization procedure is now obvious. $N(\nu, \theta, \phi)$ is calculated simultaneously with $\alpha^2 F(\nu, \theta, \phi)$ in exactly the same manner (except for the difference in weight factor, of course). The resulting (unnormalized) histogram for $N(\nu, \theta, \phi)$ is then used to calculate the integral (4.6). Since the correct result is 3 the normalization constant is 3 divided by the unnormalized value of the integral. This normalization constant depends only on the procedure adopted for choosing the points (k_F, θ', ϕ') and hence applies to the function $\alpha^2 F(\nu, \theta, \phi)$ also. We further note that it is independent of (θ, ϕ) if the same set of points (θ', ϕ') is used for all values of (θ, ϕ) .

Our results for $\alpha^2 F(\nu, \theta, \phi)$ for the high symmetry directions will be presented later.

The phonon renormalized effective mass for an electron

in the state (k_F, θ, ϕ) is given by⁽⁶⁸⁾

$$m^*(\theta, \phi) = 1 + \lambda(\theta, \phi) \quad , (4.7)$$

where

$$\lambda(\theta, \phi) \equiv 2 \int_0^{\infty} \frac{dv}{v} \alpha^2 F(v, \theta, \phi) \quad (4.8)$$

is the electron-phonon mass-enhancement parameter for the direction (θ, ϕ) .

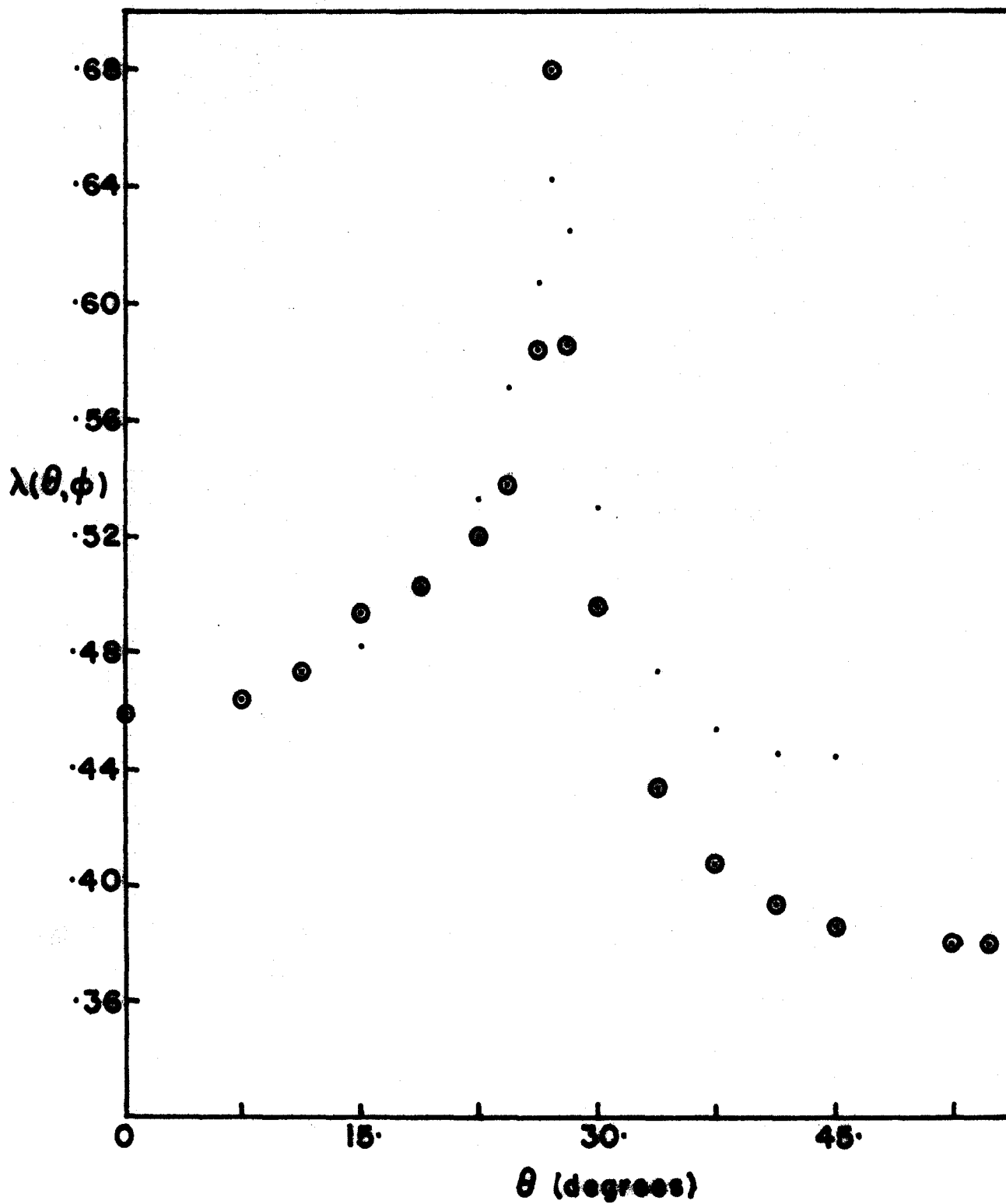
The results of our calculation of $\lambda(\theta, \phi)$ for about 30 directions in Al are presented in figure 4.1. The most obvious feature of this graph is the singular behaviour of $\lambda(\theta, \phi)$ for values of θ near 27° . This singularity is unphysical and arises solely because the one OPW approximation is not valid for an electronic state near a Bragg plane. This shows up in the fact that the one OPW electron-phonon coupling constant, (4.2), is singular if the momentum transfer \underline{q} is equal to a reciprocal lattice vector $\underline{K} \neq 0$. If $\underline{q} = \underline{K}$ then $\omega_{\underline{q}} = \omega_{\underline{K}} = \omega_0 = 0$ and the coupling constant becomes infinite.

The obvious way out of this difficulty is to do a many OPW calculation. This involves mixing into the plane wave state $|\underline{k}\rangle$ those plane wave states, $|\underline{k} + \underline{K}\rangle$ (\underline{K} is a reciprocal lattice vector), which have roughly the same energy as $|\underline{k}\rangle$. An expression for the many OPW coupling constant is easy to derive⁽⁶⁹⁾. However, before this expression can be used, the many OPW Fermi surface must be calculated and, for every vector, \underline{k} or \underline{k}' , terminating on this surface in a

FIGURE 4.1 The directional electron-phonon mass-enhancement parameter, $\lambda(\theta, \phi)$, for Al as calculated within the one OPW approximation.

The results for the two arcs $\phi=0^\circ$ and 45° on the irreducible $(\frac{1}{48})$ th are to be distinguished as follows:

- . $\phi = 0^\circ$
- ⊙ $\phi = 45^\circ$.



region near a Bragg plane, the appropriate mixing coefficients must be calculated. This is easy to do in principle but would extend the amount of computer time needed to calculate $\alpha^2 F(\nu, \theta, \phi)$ beyond the limit of practicability.

It is the low frequency part of $\alpha^2 F$ which is causing all the difficulty. For example, the low frequency portion of the isotropic $\alpha^2 F(\nu)$ for Al calculated within the one OPW approximation⁽²⁵⁾ is linear in ν while it is believed that $\alpha^2 F(\nu)$ should go to zero as ν^2 ⁽²²⁾ or faster⁽⁷⁰⁾ for small ν . This means that the low frequency region of the correct $\alpha^2 F(\nu)$ is unimportant in calculating the mass-enhancement λ or superconducting properties because the strongest weight given to low frequencies in these calculations is considerably weaker than ν^{-2} . Hence, as long as the calculated $\alpha^2 F(\nu)$ is roughly correct in the low frequency region there is no cause for concern. It is only when it is completely wrong that trouble arises. Even the linear behaviour of the low frequency region of the calculated $\alpha^2 F(\nu)$ for Al does not lead to serious errors in calculating λ or the isotropic superconducting energy gap.

The low frequency behaviour of the calculated $\alpha^2 F(\nu, \theta, \phi)$'s is critical as evidenced by the singularity in figure 4.1. The reason for this is easy to understand. In

an investigation of anisotropy what is important are the differences between $\alpha^2 F(\nu, \theta, \phi)$'s in different directions (θ, ϕ) . In calculating anisotropy in the mass-enhancement parameter, $\lambda(\theta, \phi)$, the anisotropy in $\alpha^2 F$ is weighted with a factor ν^{-1} so that the low frequency region is important unless $\alpha^2 F(\lambda, \theta, \phi)$ is very small in that region for all directions. This is the case for the correct $\alpha^2 F(\nu, \theta, \phi)$'s; unfortunately it is not the case for the $\alpha^2 F(\nu, \theta, \phi)$'s calculated within the one OPW approximation. There are some points (θ, ϕ) on the Fermi surface such that in scattering from them to all other points (θ', ϕ') on the Fermi surface no momentum transfers are encountered which are approximately equal to reciprocal lattice vectors. For these directions

(θ, ϕ) the low frequency behaviour of $\alpha^2 F(\nu, \theta, \phi)$ is correct. In other directions (θ, ϕ) momentum transfers are encountered which are approximately equal to reciprocal lattice vectors so that the low frequency behaviour of $\alpha^2 F(\nu, \theta, \phi)$ for these directions is completely wrong. Hence, it is evident that the low frequency singularity in the coupling constant can lead to large unphysical differences between $\alpha^2 F(\nu, \theta, \phi)$'s calculated for different directions. This is a serious difficulty. The above considerations are illustrated schematically in figure 4.2 where we have sketched the qualitative low frequency behaviour of the coupling function

$$\alpha^2(\nu, \Omega) \equiv \alpha^2 F(\nu, \Omega) / N(\nu, \Omega)$$

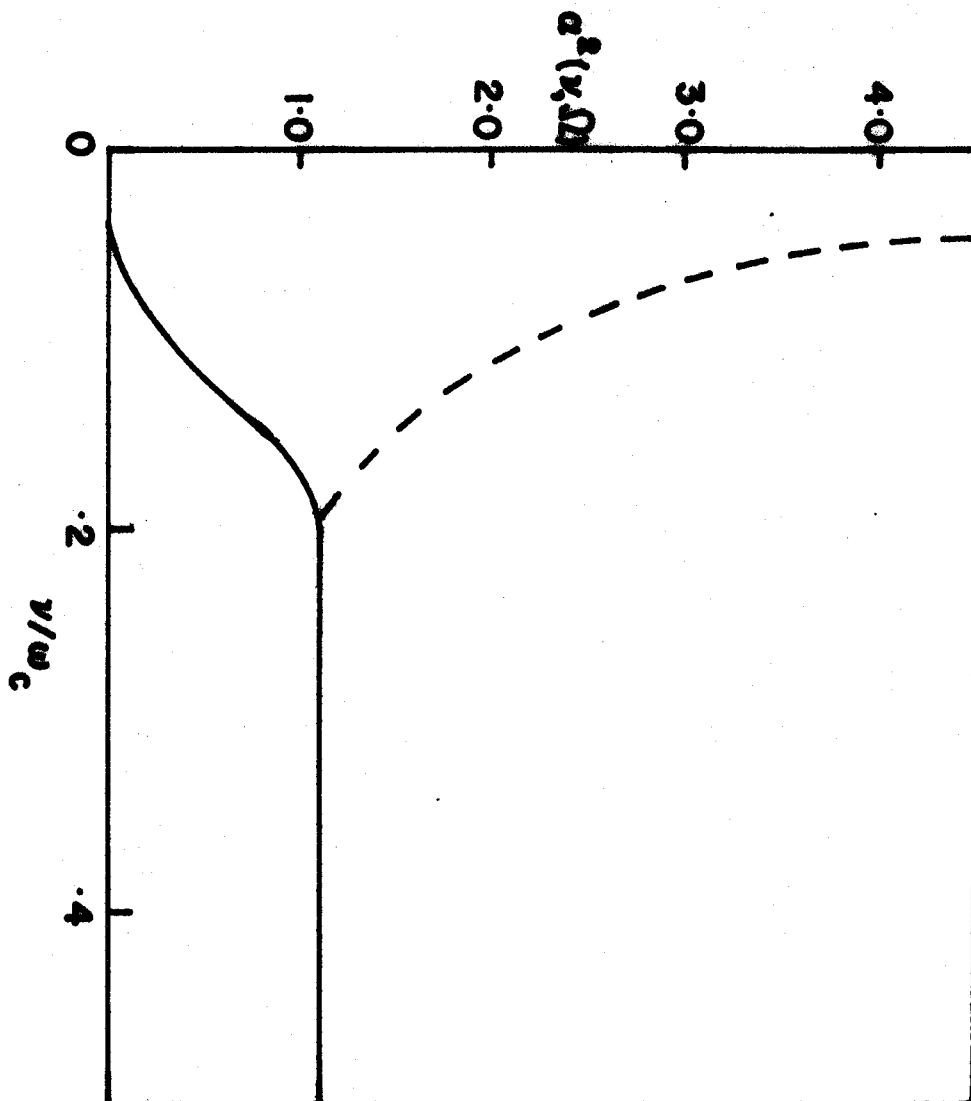
for two different directions $\Omega \equiv (\theta, \phi)$. The solid curve is representative of the behaviour of $\alpha^2(\nu, \Omega)$ for a direction in which the one OPW approximation is good for all the momentum transfers encountered in scattering from Ω to all points Ω' on the Fermi surface. The broken curve is representative of the behaviour for a direction in which the one OPW approximation leads to a divergent electron-phonon coupling constant for some of the scattering processes $\Omega \rightarrow \Omega'$.

In a recent calculation⁽⁶⁸⁾ of the temperature dependence of the mass-enhancement parameter λ Allan and Cohen corrected their calculated isotropic $\alpha^2 F$'s by replacing the divergent one OPW coupling constant by a frequency

FIGURE 4.2 Qualitative low frequency behaviour of the coupling function

$$\alpha^2(\nu, \Omega) \equiv \alpha^2 F(\nu, \Omega) / N(\nu, \Omega)$$

for two different directions. The solid curve is representative of a direction in which the one OPW approximation is valid for all momentum transfers; the broken curve, for a direction in which it is not.



independent coupling constant in the low frequency region $0 < \nu < \omega_D/5$. This is a reasonable procedure. We apply essentially the same correction to the isotropic $\alpha^2 F(\nu)$ for Al (calculated by Carbotte and Dynes) by multiplying it by $(5\nu/\omega_c)$ in the low frequency region below $\omega_c/5$. This corrected function is denoted by $\alpha_c^2 F(\nu)$. It has the correct low frequency behaviour, going to zero as ν^2 as ν goes to zero. We also apply this same correction procedure to the directional one OPW functions. This correction makes very little change in those functions which were essentially correct to begin with and at the same time it makes a drastic change in those that were incorrect. The result is that $\alpha_c^2 F(\nu, \theta, \phi)$ is at least qualitatively correct at low frequencies for all directions. This is all that is required since the low frequency part of $\alpha^2 F$ is unimportant as long as it is roughly correct.

Figure 4.3 is a graph of the corrected isotropic $\alpha_c^2 F$ for Al. Figure 4.4 is a graph of $\alpha_c^2 F(\nu, \theta, \phi)$ for the three high symmetry directions in Al. The important thing to notice in the latter figure is that the anisotropy in the low frequency region ($\nu < 2 \times 10^{12}$ c.p.s.) is negligible compared with that in the high frequency region ($\nu > 2 \times 10^{12}$ c.p.s.).

Figure 4.5 is a graph of the directional electron-phonon mass-enhancement parameter $\lambda(\theta, \phi)$ calculated from the corrected function $\alpha_c^2 F(\nu, \theta, \phi)$. This graph is plotted on the same scale as figure 4.1 to facilitate comparison of the

FIGURE 4.3

The corrected $\alpha^2 F(\nu)$ for Al,

$$\alpha_c^2 F(\nu) = \left(\frac{5\nu}{\omega_c}\right) \alpha^2 F(\nu), \quad 0 < \nu < \frac{\omega_c}{5},$$

$$= \alpha^2 F(\nu), \quad \nu > \frac{\omega_c}{5},$$

versus frequency.

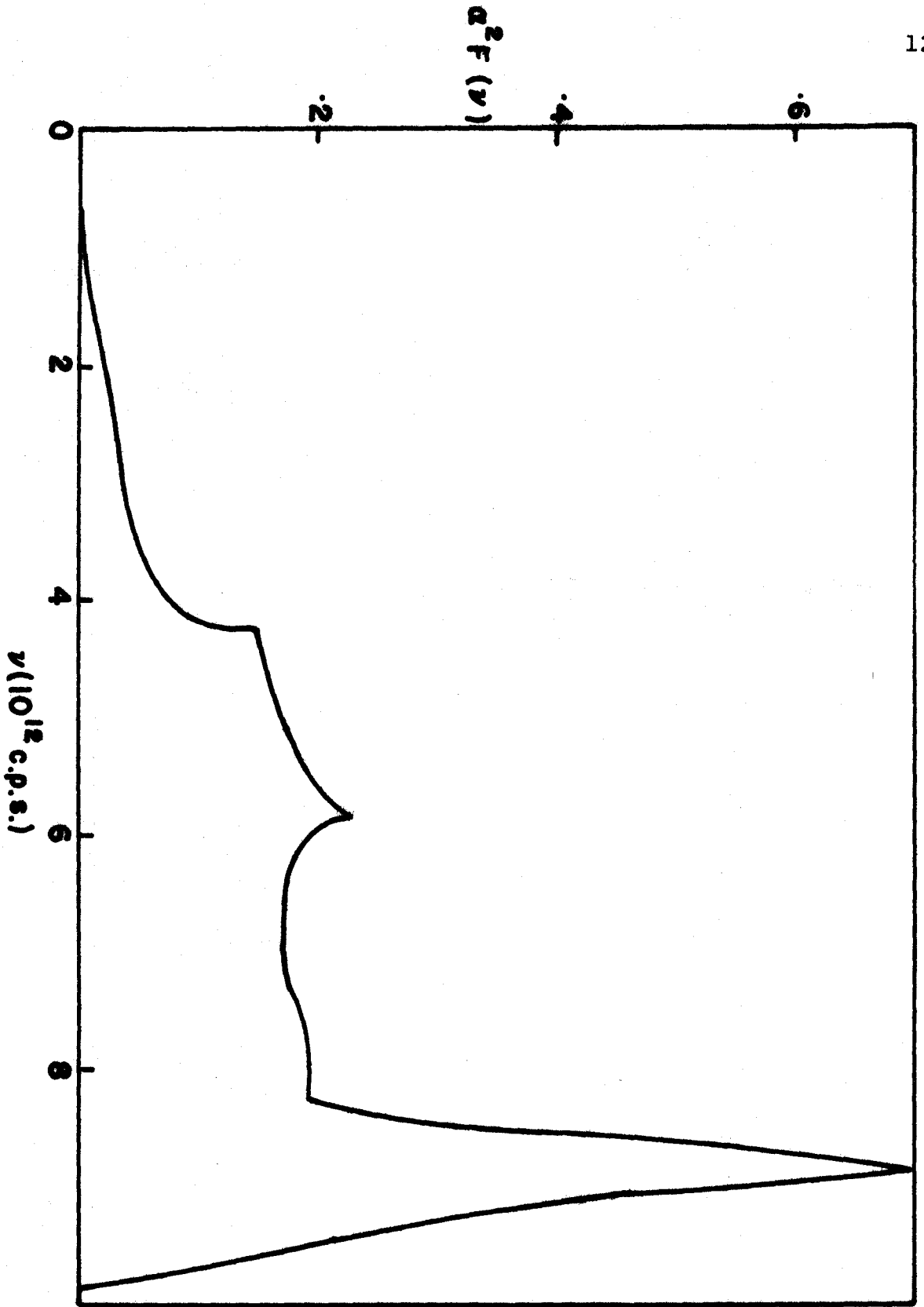


FIGURE 4.4 $\alpha_c^2 F(\nu, \theta, \phi)$ for the three high symmetry directions in Al versus phonon frequency ν .

The three curves are displaced vertically from each other to facilitate comparison. The lower curve is for the [100] direction, the middle curve is for the [110] direction, and the upper curve is for the [111] direction.

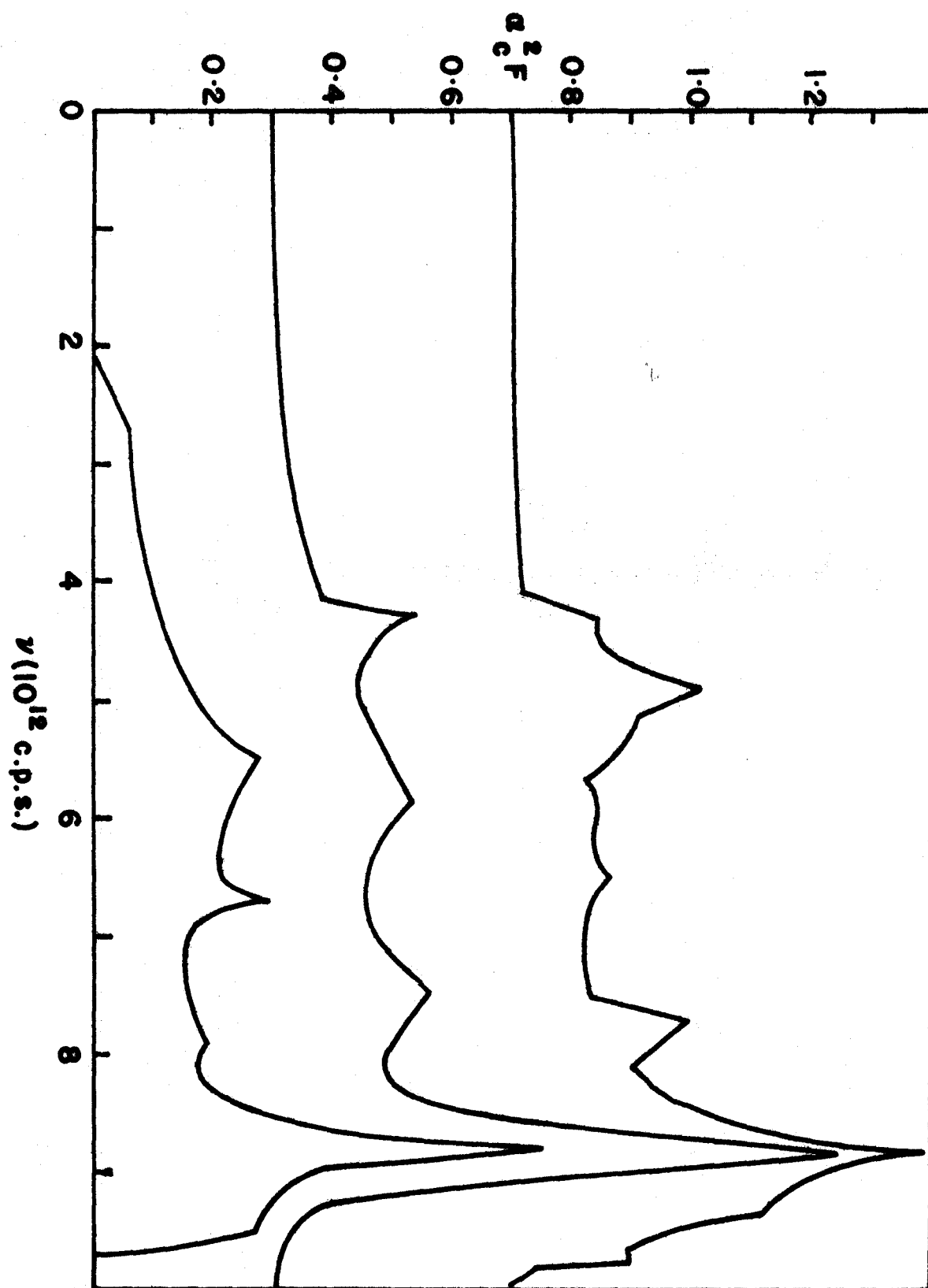
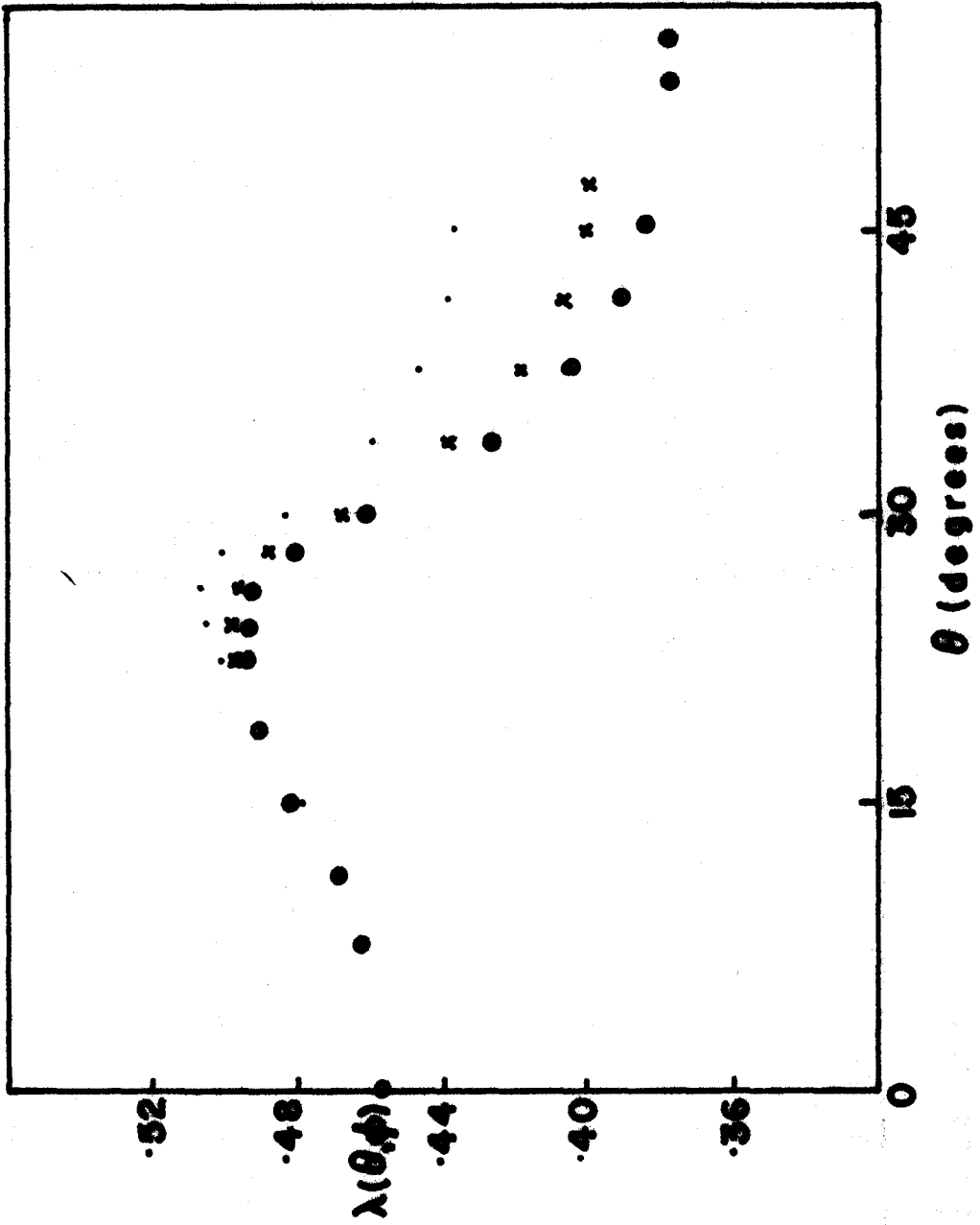


FIGURE 4.5 The directional electron-phonon mass-enhancement parameter, $\lambda(\theta, \phi)$, for Al calculated with the corrected function $\alpha_C^2 F(\nu, \theta, \phi)$.

The results for the three arcs $\phi=0^\circ$, $22\frac{1}{2}^\circ$ and 45° on the irreducible $(\frac{1}{48})$ th are to be distinguished as follows:

- . $\phi=0^\circ$
- x $\phi=22\frac{1}{2}^\circ$
- ⊙ $\phi=45^\circ$.



corrected and uncorrected $\lambda(\theta, \phi)$'s. Although the correction has made a rather drastic change in $\lambda(\theta, \phi)$ for values of θ between roughly 20° and 30° the change in the average value of λ is quite small (approximately 4%). This substantiates our assertion that the low frequency behaviour of $\alpha^2 F$ must be essentially correct for a meaningful study of an anisotropic superconductor even though the properties of an isotropic superconductor are not too sensitive to the low frequency behaviour of this function.

In section 4.3 we use the corrected functions, $\alpha_c^2 F(\nu, \theta, \phi)$, to calculate directional energy gaps using Bennett's one iteration procedure. Before doing this we investigate the importance of further iterations using a simple model for the anisotropic electron-electron interaction. This is the subject of the next section.

4.2 A MODEL INVESTIGATION OF BENNETT'S ONE ITERATION PROCEDURE FOR CALCULATING DIRECTIONAL ENERGY GAPS

In this section we use an unrealistic but mathematically convenient model for the effective electron-electron interaction matrix element, $V_{\underline{k}\underline{k}'}$, to study the convergence of the iteration procedure for calculating directional energy gaps. We assume the simplest possible model for $V_{\underline{k}\underline{k}'}$ which exhibits anisotropy. This is the factorable interaction matrix element,

$$V_{\underline{k}\underline{k}'} = V_M(\Omega, \Omega') = (1+a(\Omega)) V(1+a(\Omega')) \quad , (4.9)$$

of Markowitz and Kadanoff⁽³¹⁾. The anisotropy function $a(\Omega)$ depends only upon the direction, $\Omega \equiv (\theta, \phi)$, of \underline{k} with respect to the crystal axes. If we substitute (4.9) into the zero temperature BCS integral equation we obtain⁽³⁵⁾

$$\Delta(\Omega) = \langle \Delta(\Omega) \rangle (1+a(\Omega)) \quad (4.10)$$

where, in the weak coupling limit, $\langle \Delta(\Omega) \rangle$ is given by

$$1 = N(0)V \int \frac{d\Omega'}{4\pi} (1+a(\Omega'))^2 \log\left(\frac{2\omega_D}{\langle \Delta(\Omega') \rangle (1+a(\Omega'))}\right) \quad (4.11)$$

Clem⁽³⁵⁾ obtained an approximate analytical expression for the average energy gap in terms of the mean squared anisotropy by expanding the right hand side of equation (4.11) in powers of the small parameter $a(\Omega')$, performing the angular averages and neglecting terms of order $\langle a^3 \rangle$. His result is

$$\langle \Delta(\Omega) \rangle = \left[1 + \left(\frac{1}{N(0)V} - \frac{3}{2}\right) \langle a^2 \rangle\right] \Delta \quad (4.12)$$

where

$$\Delta = 2\omega_D e^{-1/N(0)V}$$

is the energy gap in the isotropic or 'dirty' superconductor ($\langle a^2 \rangle = 0$).

The BCS integral equation for the directional energy gap $\Delta(\Omega)$, of an anisotropic superconductor is

$$\Delta(\Omega) = N(0) \int \frac{d\Omega'}{4\pi} V(\Omega, \Omega') \Delta(\Omega') \log\left(\frac{2\omega_D}{\Delta(\Omega')}\right) \quad .(4.13)$$

Bennett's method of calculating an approximate value for $\Delta(\Omega)$ is to replace $\Delta(\Omega')$ on the right hand side of this equation by the isotropic energy gap of the 'dirty' superconductor. One obtains in this way the one iteration result

$$\frac{\Delta^{(1)}(\Omega)}{\Delta} = \frac{V(\Omega)}{V} \quad , (4.14)$$

where

$$V(\Omega) \equiv \int \frac{d\Omega'}{4\pi} V(\Omega, \Omega') \quad , (4.15)$$

and

$$V \equiv \iint \frac{d\Omega}{4\pi} \frac{d\Omega'}{4\pi} V(\Omega, \Omega') \quad .(4.16)$$

For the special case of a factorable interaction matrix element (4.14) becomes

$$\Delta^{(1)}(\Omega) = \Delta(1+a(\Omega)) \quad .(4.17)$$

Comparing this with equation (4.10) we see that for this special case one iteration leads to the correct anisotropy function but does not give the correct average energy gap. On the basis of this, it is reasonable to assume, as Bennett did, that for a realistic interaction one iteration would produce a fairly good approximation to the energy gap anisotropy function. However the extent to which this assumption

holds should be investigated by iterating the integral equation (4.13) with a realistic interaction until convergence is attained. Whether this is feasible or not depends on how quickly the iteration procedure converges. The rate of convergence should be qualitatively the same for the model interaction of Markowitz and Kadanoff as it is for a realistic interaction. Hence we use the model interaction to calculate the average energy gap to order $\langle a^2 \rangle$ in the anisotropy by iterating the BCS integral equation starting with the trial solution Δ .

We expand the energy gap and the factorable interaction matrix element in terms of Kubic harmonics:

$$\Delta(\Omega) = \sum_{m=0}^{\infty} \Delta^m K_m(\Omega) \quad , (4.18)$$

$$V_M(\Omega, \Omega') = V \sum_n \sum_{n'} \alpha^{nn'} K_n(\Omega) K_{n'}(\Omega'), \quad (\alpha^{00}=1) \quad . (4.19)$$

We emphasize that the latter expansion is not valid for a general interaction matrix element $V(\Omega, \Omega')$. It is easy to show, using the orthonormality property of the Kubic harmonics, that for a factorable matrix element

$$\alpha^{nn'} = \alpha^{n0} \alpha^{n'0} \quad . (4.20)$$

It is also easy to show that the average energy gap, the anisotropy function, and the mean squared anisotropy are

given by

$$\langle \Delta(\Omega) \rangle = \Delta^0 \quad , (4.21)$$

$$a(\Omega) \equiv \frac{\Delta(\Omega) - \langle \Delta(\Omega) \rangle}{\langle \Delta(\Omega) \rangle} = \sum_{m=1}^{\infty} \Delta^m K_m(\Omega) / \Delta^0 \quad (4.22)$$

$$\langle a^2 \rangle \equiv \frac{\langle (\Delta(\Omega) - \langle \Delta(\Omega) \rangle)^2 \rangle}{\langle \Delta(\Omega) \rangle^2} = \sum_{m=1}^{\infty} (\Delta^m)^2 / (\Delta^0)^2 \quad . (4.23)$$

The reason for expressing the factorable interaction of Markowitz and Kadanoff in terms of Kubic harmonics is that to second order in the anisotropy the surface integrals encountered in iterating (4.13) to convergence are trivial to evaluate. This simplification is due to the orthonormality property

$$\int \frac{d\Omega}{4\pi} K_m(\Omega) K_n(\Omega) = \delta_{m,n}$$

of the Kubic harmonics.

We expand the logarithm in equation (4.13) to second order in the small quantity $a(\Omega')$ to obtain

$$\Delta(\Omega) = N(0) \log\left(\frac{2\omega_D}{\Delta^0}\right) \int \frac{d\Omega'}{4\pi} V_M(\Omega, \Omega') \Delta(\Omega') - N(0) \Delta^0 \int \frac{d\Omega'}{4\pi} \\ \times V_M(\Omega, \Omega') \{a(\Omega') + \frac{1}{2}a^2(\Omega')\} \quad . (4.24)$$

We substitute equations (4.18), (4.19) and (4.22) into

equation (4.24) and equate the coefficients of the linearly independent functions $K_m(\Omega)$ on both sides of the resulting equation. We obtain, to second order in the anisotropy, the following set of coupled equations for the expansion coefficients of the directional energy gap:

$$\Delta^m = \frac{\log(2\omega_D/\Delta^0)}{\log(2\omega_D/\Delta)} \sum_{m'=0}^{\infty} \left\{ 1 - \frac{[1-\delta_{m',0}]}{\log(2\omega_D/\Delta^0)} \right\} \alpha^{mm'} \Delta^{m'} - \frac{\alpha^{m0}}{2\Delta^0 \log\left(\frac{2\omega_D}{\Delta}\right)} \sum_{m'=1}^{\infty} (\Delta^{m'})^2 \quad (m=0,1,2,\dots) \quad (4.25)$$

These equations allow us to iterate equation (4.24) to convergence with a minimum of computer time.

For our investigation of the rate of convergence of the iteration procedure we truncate the set of equations at $m=3$. Our (arbitrary) choice for the expansion coefficients of the interaction matrix element is

$$\alpha^{00}=1, \quad \alpha^{01}=.1, \quad \alpha^{02}=.01, \quad \alpha^{03}=.001, \quad \alpha^{04}=0, \quad \dots$$

The rest of the coefficients $\alpha^{mm'}$ follow from equation (4.20). We iterate the set of equations (4.25) starting with the trial set of coefficients

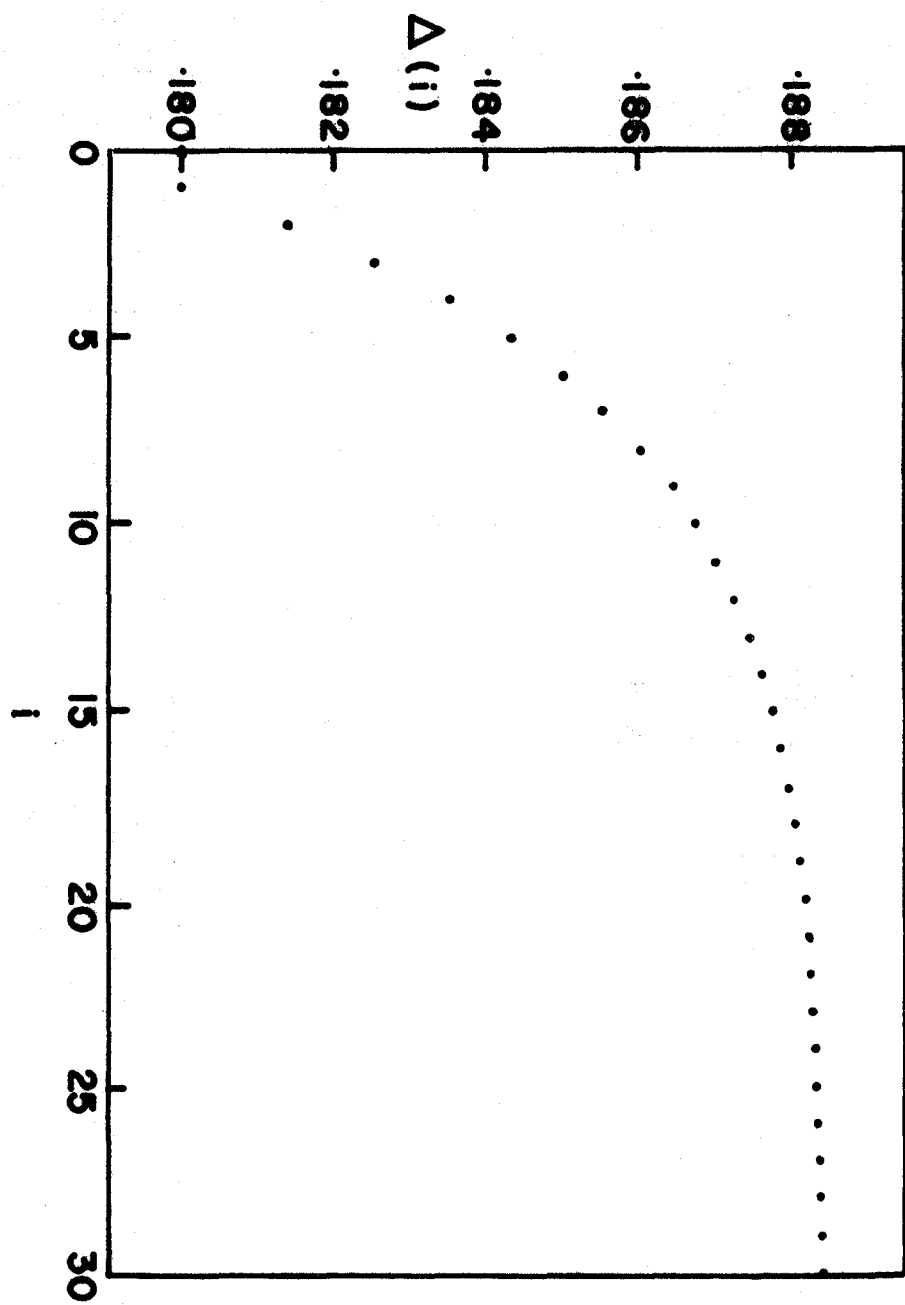
$$\Delta^0 = \Delta, \quad \Delta^1 = \Delta^2 = \Delta^3 = 0$$

As we already know, the first iteration gives the correct anisotropy function, equation (4.22), but does not change

the average energy gap from the isotropic value Δ . The results of successive iterations are shown in figure 4.6 where the average energy gap emerging from the i th iteration, $\Delta^0(i)$, is plotted against i . It is apparent from the figure that the convergence of the average energy gap to the value given by equation (4.12) is very slow. This qualitative conclusion is not changed by using a different set of expansion coefficients $\alpha^{mm'}$.

The results of the model problem investigated above give us some insight into what would be involved in iterating equation (4.13) to convergence with a realistic interaction. There is no reason to believe that the qualitative result obtained above, that the average energy gap converges very slowly from the value Δ appropriate to a dirty superconductor to the value Δ^0 appropriate to a pure single-crystal superconductor, would be any different for the case of a realistic interaction. This means that the labour involved in iterating equation (4.13) to convergence with a physically realistic interaction is formidable. Since the convenient Kubic harmonic expansion, (4.19), holds only for a very restricted class of (unrealistic) interactions, the surface integral in (4.13) would most certainly have to be evaluated numerically. This is very time consuming but is not the most difficult problem. For each iteration after the first, one needs an accurate interpolation scheme for obtaining, from the finite set of directional energy gaps calculated in the previous

FIGURE 4.6 The convergence of the iteration procedure
for calculating the average gap in a pure single-
crystal superconductor. $\Delta^0(i)$ is the result of
the i th iteration.



iteration, the value of $\Delta(\Omega')$ at an arbitrary point Ω' . Clearly, in order to obtain convergence, the errors involved in the interpolation procedure must be less (everywhere on the Fermi surface) than the differences between successive iterations. This is a severe limitation and leads us to conclude that it is unfeasible to iterate the weak coupling integral equation (4.13) to convergence for the case of a physically realistic electron-electron interaction, such as the Eliashberg interaction. Unfortunately many thermodynamic properties such as the low temperature specific heat and nuclear spin-lattice relaxation rate depend on the energy gap essentially exponentially so that the difference between Δ and Δ^0 , although quite small, is important. Hence one needs some scheme for calculating Δ^0 . We use the procedure proposed in section 3.3 and carried out in section 4.4. This method is based upon the assumption that the gross features of the anisotropy, such as the mean squared anisotropy, can be calculated to a good approximation using the one iteration results, $\Delta^{(1)}(\Omega)$, for the directional energy gaps. Since much of the remainder of this chapter is based on the assumption that Bennett's one iteration procedure is valid to a good approximation for calculating the anisotropy in the energy gap (even though it does not give the correct average energy gap), we conclude that it is advisable to obtain some justification for this assumption by performing at least two iterations. This is done in the next section.

4.3 CALCULATION OF THE ANISOTROPIC ENERGY GAP IN SUPER-CONDUCTING ALUMINIUM

In this section the results of our calculation of the directional energy gap at the gap edge,

$$\text{Re}\{\Delta(\omega=\Delta_0(\Omega), \Omega)\} = \Delta_0(\Omega) \quad , (4.26)$$

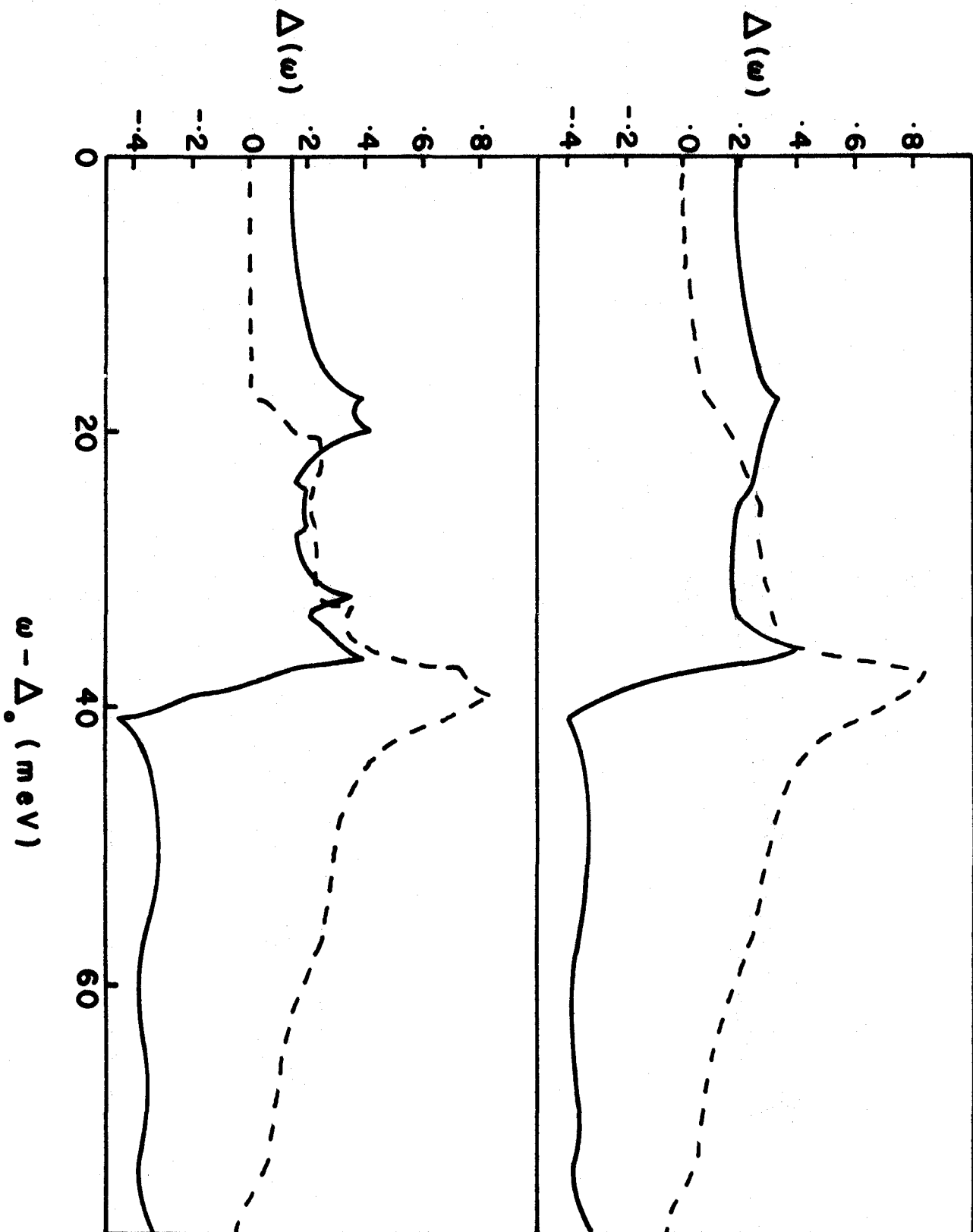
for a large number of points on the irreducible $(\frac{1}{48})$ th of the Fermi surface of aluminium are presented.

Within the strong coupling formalism the procedure used to calculate the directional energy gap $\Delta_0(\Omega)$ was as follows: (1) the Eliashberg gap equations containing the isotropic function $\alpha^2F(\nu)$ and an adjustable Coulomb pseudopotential parameter μ^* were iterated to convergence so as to obtain the experimental energy gap at the gap edge, $\Delta_0 = .18$ meV; (2) the isotropic gap function $\Delta(\omega')$ appearing on the right hand side of the Eliashberg equations and the Coulomb parameter μ^* were fixed once and for all at their converged values; (3) the isotropic function $\alpha^2F(\nu)$ was replaced by the directional function $\alpha^2F(\nu, \Omega)$ in the phonon kernels $K_{\pm}(\omega, \omega')$; (4) one more iteration of the gap equations was performed to generate the approximate directional solution $\Delta^{(1)}(\omega, \Omega)$ and the gap edge $\Delta_0^{(1)}(\Omega)$. The calculation of $\Delta_0^{(1)}(\Omega)$ within the weak coupling formalism of Chapter III followed essentially the same procedure. The only difference was that the simplified integral equations (3.34) and (3.36) were used in place of the Eliashberg equations.

FIGURE 4.7 The real (solid line) and imaginary (dashed line) parts of the frequency dependent gap function for aluminium:

(a) $\Delta(\omega)$ versus ω for isotropic or 'dirty' aluminium;

(b) $\Delta(\omega, \Omega)$ versus ω for the [111] direction in a pure single-crystal of aluminium.



The isotropic gap function $\Delta(\omega')$ and the strong coupling value of the Coulomb parameter μ^* were obtained by iterating the Eliashberg equations to convergence using the isotropic function $\alpha^2F(\nu)$ of Carbotte and Dynes⁽²⁵⁾. The final value of μ^* , .166, gave an isotropic gap edge of .181 meV. The real and imaginary parts of the isotropic solution, $\Delta(\omega')$, are shown in the upper half of figure 4.7.

It was not until after the isotropic solution had been generated that the full importance of the low frequency region of the function α^2F , for an investigation of anisotropy, was appreciated. Hence much of the work of this section was originally based on the uncorrected $\alpha^2F(\nu, \Omega)$'s. For some of this work, this is of no importance whatsoever and the calculations have not been repeated with the corrected $\alpha^2F(\nu, \Omega)$'s. In this category falls the comparison of the directional energy gaps calculated using the Eliashberg equations with those calculated using equations (3.34) and (3.36). Since the agreement is very good for the uncorrected $\alpha^2F(\nu, \Omega)$'s it most certainly would be at least as good for the (less anisotropic) corrected $\alpha^2F(\nu, \Omega)$'s. Hence the qualitative result of this particular investigation would remain unchanged. Also in this category is the comparison of the second iteration values of the directional energy gap with those of the first iteration. On the other hand, the first iteration results for the directional energy gaps were recalculated with the corrected directional α^2F 's.

However, the isotropic solution $\Delta(\omega')$ was not recalculated. There are three reasons for this: (1) the calculation of the isotropic energy gap $\Delta(\omega')$ is extremely time consuming; (2) the low frequency behaviour of $\alpha^2 F(\nu)$ is not very important in calculating an isotropic property and would have led to only a few percent reduction in the gap edge; (3) the gap function $\Delta(\omega')$ calculated with the uncorrected $\alpha^2 F(\nu)$ is actually a better trial solution for the iteration procedure than that calculated with the corrected $\alpha^2 F(\nu)$ because the average energy gap in a pure single-crystal is a few percent larger than the isotropic energy gap of the corresponding 'dirty' crystal. For these reasons the isotropic solution $\Delta(\omega')$ generated with the uncorrected $\alpha^2 F(\nu)$ of Carbotte and Dynes was used as the trial solution in calculating the directional energy gaps with the corrected $\alpha^2 F(\nu, \Omega)$'s.

The real and imaginary parts of the directional gap function, $\Delta(\omega, \Omega)$, for the [111] direction are shown in the bottom half of figure 4.7. This particular example was chosen because $\alpha^2 F(\nu, \Omega)$ is essentially the same as $\alpha_C^2 F(\nu, \Omega)$ for the [111] direction. The important point to note in figure 4.7 is that while the directional and isotropic solutions are quite different for first order processes ($\nu < \omega_C$), they are very much the same for higher order processes ($\nu > \omega_C$). This is easily explained⁽⁷¹⁾. The anisotropy of the effective phonon density of states is washed out to a large extent by the average over all possible intermediate states for

multi-phonon processes.

The directional energy gaps calculated using the weak coupling integral equations (3.34) and (3.36) were compared with those calculated using the Eliashberg equations in section 3.2. The very good agreement between these two calculations is sufficient justification for performing a second iteration with the weak coupling directional integral equations (3.40) and (3.41). Since it is completely out of the question to perform a second iteration within the strong coupling formalism (i.e. using the three dimensional directional Eliashberg equations) the usefulness of the simplified integral equations of Chapter III should be very evident. As pointed out in section 3.2, a second iteration of the directional equations (3.40) and (3.41) is not difficult since it involves little more than a trivial modification of the weight factor in the directional $\alpha^2 F(\nu, \Omega)$ computer programme. One does need, however, an interpolation procedure for obtaining $\Delta_0^{(1)}(\Omega')$ at each of the 16,200 points Ω' used in evaluating the surface integrals occurring on the right hand sides of equations (3.40) and (3.41). A procedure that was found to work quite satisfactorily is now outlined. The first iteration was carried out for about forty points $\Omega \equiv (\theta, \phi)$ on the irreducible $(\frac{1}{48})$ th of the Fermi surface ($0 < \theta < \tan^{-1}(1/\cos\phi)$; $0 < \phi < \pi/4$). These points were chosen so as to obtain a smooth curve for $\Delta_0^{(1)}(\Omega)$ along each of the arcs $\phi = 0^\circ$, $\phi = 22\frac{1}{2}^\circ$ and

$\phi=45^\circ$. A tenth order polynomial fit

$$\Delta_0^{(1)}(\theta, \phi=\text{constant}) = \sum_{i=0}^{10} \alpha_i(\phi=\text{constant}) \theta^i$$

was made for each of the three arcs $\phi=\text{constant}$. A fourth order polynomial fit

$$\alpha_i(\phi) = \sum_{j=0}^4 \beta_{ij} \phi^j \quad (i=0,1,\dots,10)$$

was then made (for each value of i) to the five calculated expansion coefficients $\alpha_i(-22\frac{1}{2}^\circ)$, $\alpha_i(0^\circ)$, $\alpha_i(22\frac{1}{2}^\circ)$, $\alpha_i(45^\circ)$ and $\alpha_i(67\frac{1}{2}^\circ)$. We have used the fact that $\alpha_i(-22\frac{1}{2}^\circ) = \alpha_i(22\frac{1}{2}^\circ) = \alpha_i(67\frac{1}{2}^\circ)$ (this follows readily from the cubic symmetry of a pure single-crystal of aluminium) to improve the polynomial fit without any additional labour. The resulting interpolation formula,

$$\Delta_0^{(1)}(\theta, \phi) = \sum_{i=0}^{10} \sum_{j=0}^4 \beta_{ij} \theta^i \phi^j \quad , (4.27)$$

was used to obtain $\Delta_0^{(1)}(\theta, \phi)$ at any point (θ, ϕ) on the irreducible $(\frac{1}{48})$ th of the Fermi surface. In our actual calculations the irreducible $(\frac{1}{48})$ th was broken up into two regions by a line of latitude ($\theta \sim 30^\circ$) and the above interpolation procedure was applied to each region separately. To test this formula we calculated $\Delta_0^{(1)}(\Omega)$ (using the Eliashberg equations) for a few additional points in the region where the ϕ variation of $\Delta_0^{(1)}(\theta, \phi)$ was largest. These

values are compared in table 4.1 with the interpolated values obtained using equation (4.27). The very good agreement indicates that the interpolation formula is more than adequate for our purposes.

TABLE 4.1

A TEST OF THE INTERPOLATION FORMULA, EQUATION (4.27)

DIRECTION		$\Delta_0^{(1)}(\theta, \phi)$	
θ	ϕ	actual value	interpolated value
45°	7.5°	.1738	.1719
45°	15 °	.1656	.1655
45°	30 °	.1541	.1542
45°	37.5°	.1513	.1513

There is one further complication. $\Delta_0^{(1)}(\Omega)$ is needed everywhere on the Fermi surface not just on the irreducible $(\frac{1}{48})$ th of it. It is evident that equation (4.27) is valid only on the $(\frac{1}{48})$ th. Hence a scheme is needed to map any point Ω on the Fermi surface into its equivalent point on the $(\frac{1}{48})$ th so that the interpolation formula can be applied. We used the following procedure: (1) the absolute values of the cartesian components k_x, k_y, k_z of the point (k_F, θ, ϕ) were calculated to generate an equivalent point $(|k_x|, |k_y|, |k_z|)$

on the positive octant of the Fermi surface; (2) the angular coordinates of the point $(|k_x|, |k_y|, |k_z|)$ were calculated and then tested to see if they were in the range $(0 < \theta < \tan^{-1}(1/\cos\phi); 0 < \phi < \pi/4)$; (3) if not, successive permutations of $|k_x|, |k_y|, |k_z|$ were performed until the corresponding angular coordinates were found to belong to the irreducible $(\frac{1}{48})$ th (this required a maximum of 5 permutations).

With these difficulties cleared up a second iteration of equations (3.40) and (3.41) was straightforward. Our results for the second iteration are presented in table 4.2 where $\Delta_0^{(2)}(\Omega)$ is compared with $\Delta_0^{(1)}(\Omega)$ for several directions Ω . The values for $\Delta_0^{(1)}(\Omega)$ are those which were calculated using the Eliashberg equations. It is evident from this table that the main effect of the second iteration is to shift the energy gaps for all directions upwards by a small amount without changing the anisotropy very much. This is what the simple model of section 4.2 led us to expect. For the model interaction of Markowitz and Kadanoff the only effect of successive iterations was to increase the average energy gap by a small amount leaving the anisotropy function $a(\Omega)$ unchanged. We further note that the largest differences between the first and second iteration results occur in those directions where the one OPW approximation is suspect. If we had used the corrected $\alpha^2 F(\nu, \Omega)$'s these differences would have been smaller.

Although we have not proved that Bennett's one iteration

TABLE 4.2

A COMPARISON OF THE FIRST AND SECOND ITERATION RESULTS
FOR THE DIRECTIONAL GAP EDGE $\Delta_0(\Omega)$

θ (degrees)	ϕ (degrees)	$\Delta_0^{(0)}(\Omega) \equiv \Delta_0$	$\Delta_0^{(1)}(\Omega)$	$\Delta_0^{(2)}(\Omega)$
0.	0.	.181	.185	.185
7.5	0.	.181	.187	.187
15.	0.	.181	.193	.194
22.5	0.	.181	.208	.211
30.	0.	.181	.2035	.207
37.5	0.	.181	.181	.182
45.	0.	.181	.177	.178
15.	22.5	.181	.195	.196
22.5	22.5	.181	.205	.208
30.	22.5	.181	.195	.198
37.5	22.5	.181	.167	.168
45.	22.5	.181	.159	.160
15.	45.	.181	.196	.196
22.5	45.	.181	.204	.207
30.	45.	.181	.192	.195
37.5	45.	.181	.161	.162
45.	45.	.181	.150	.152
52.5	45.	.181	.148	.150
54.75	45.	.181	.147	.149

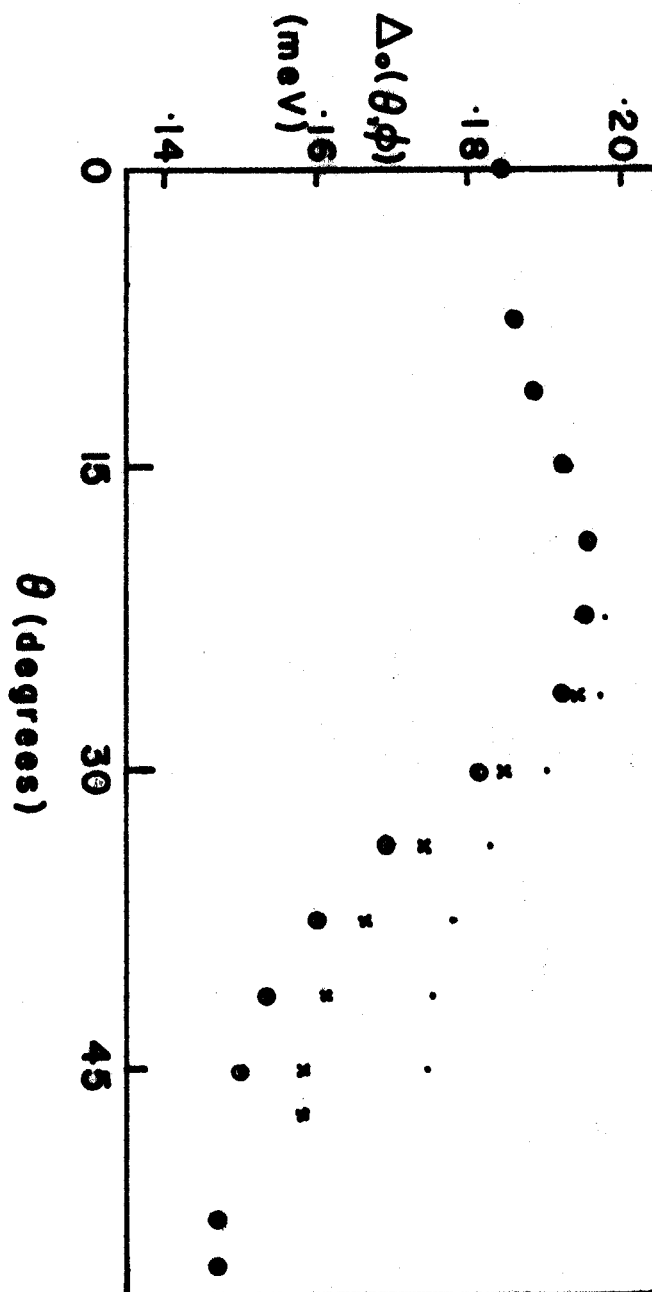
procedure is a good approximation we have obtained some justification for it by showing that nothing drastic happens when a further iteration is performed. We did not perform further iterations for the following reasons: (1) it would take a large number of iterations for the average energy gap to converge (section 4.2); (2) each iteration requires a very large amount of computer time; (3) the interpolation procedure would have to be made more accurate as the differences between successive iterations became smaller; (4) we did not expect that the anisotropy function $a(\Omega)$ would change very much with further iterations; (5) we did not need the converged value of the average energy gap because an approximate result for the average energy gap in terms of quantities calculated from the first iteration anisotropy function, $a^{(1)}(\Omega)$, was available (section 3.3).

The one iteration calculation of the directional energy gaps $\Delta_0(\Omega)$ was repeated using the Eliashberg equations for the corrected $\alpha^2F(\nu, \Omega)$'s. The results are shown in figure 4.8. From the figure it is obvious that the anisotropy of the energy gap in aluminium is considerable and should have an appreciable effect on many superconducting properties. This is investigated in some detail in the next section where the directional energy gaps of figure 4.8 are used in a calculation of the low temperature electronic specific heat and nuclear spin-lattice relaxation rate for a pure single-crystal of aluminium.

FIGURE 4.8 The directional energy gap $\Delta_0(\Omega)$ for Al
as calculated with the corrected function
 $\alpha_c^2 F(\nu, \Omega)$.

The results for the three arcs $\phi=0^\circ$, $22\frac{1}{2}^\circ$
and 45° on the irreducible $(\frac{1}{48})$ th are to be
distinguished as follows:

- . $\phi=0^\circ$
- x $\phi=22\frac{1}{2}^\circ$
- ⊙ $\phi=45^\circ$.



4.4 SOME EFFECTS OF THE ANISOTROPY OF THE ENERGY GAP IN ALUMINIUM

In this section we present the results of our calculation of the low temperature behaviour of the specific heat and the nuclear spin-lattice relaxation rate for a pure single-crystal of aluminium.

In the temperature regime $T < .25 T_c$ the temperature dependence of the energy gap can be neglected and the expressions for the electronic specific heat and the nuclear spin-lattice relaxation rate of an anisotropic weak coupling superconductor are given by⁽³⁵⁾

$$C_S(T) = 2N(0)k_B \beta^2 \int_{-\infty}^{\infty} d\omega \omega^2 f(\omega) [1-f(\omega)] \langle n(\Omega, \omega) \rangle \quad (\beta=1/k_B T) \quad (4.28)$$

and

$$\frac{R_S(T)}{R_n(T_c)} = \frac{1}{k_B T_c} \int_{-\infty}^{\infty} d\omega f(\omega) [1-f(\omega)] \{ \langle n(\Omega, \omega) \rangle^2 + \langle \bar{n}(\Omega, \omega) \rangle^2 \} \quad (4.29)$$

respectively. In (4.28) and (4.29) $n(\Omega, \omega)$ is the anisotropic quasiparticle density of states,

$$n(\Omega, \omega) \equiv \text{Re} \left\{ \frac{\omega}{\sqrt{\omega^2 - \Delta_0^2(\Omega)}} \right\} \quad , (4.30)$$

and $\bar{n}(\Omega, \omega)$ is given by

$$\bar{n}(\Omega, \omega) \equiv \text{Re} \left\{ \frac{\Delta_0(\Omega)}{\sqrt{\omega^2 - \Delta_0^2(\Omega)}} \right\} \quad , (4.31)$$

where the energy variable ω is measured relative to the Fermi level and the sign of the square root is such that

$$\sqrt{\omega^2 - \Delta_0^2(\Omega)} \rightarrow \omega \quad \text{as} \quad |\omega| \rightarrow \infty .$$

The angular brackets denote a Fermi surface average, i.e.

$$\langle F(\Omega, \omega) \rangle \equiv \int \frac{d\Omega}{4\pi} F(\Omega, \omega)$$

for any function $F(\Omega, \omega)$.

Clem introduced the anisotropy distribution function, $P(a)$, which has the property that $P(a)da$ is the fraction of the Fermi surface for which the anisotropy function $a(\Omega)$ has a value between a and $a+da$. Since a is known to be small the first three moments of $P(a)$ are often useful. They are

$$\begin{aligned} \int da P(a) &= 1 & , \\ \int da P(a) a &= 0 & , \\ \int da P(a) a^2 &= \langle a^2 \rangle & . \end{aligned}$$

This distribution function enables one to reduce a two dimensional Fermi surface integral to a one dimensional integral over a . Since $\Delta_0(\Omega) = \langle \Delta_0(\Omega) \rangle (1+a(\Omega))$ it follows immediately from the definition of $P(a)$ that

$$\langle G(\Delta_0(\Omega), \omega) \rangle = \int da P(a) G(\langle \Delta_0(\Omega) \rangle (1+a), \omega) \quad (4.33)$$

for any function $G(\Delta_0(\Omega), \omega)$.

In his theoretical investigation of the effects of anisotropy, Clem⁽³⁵⁾ used a rectangular model for the anisotropy distribution function. That is, he assumed that $P(a)$ could be approximated by

$$P(a) = \begin{cases} \overline{(2\sqrt{3}\langle a^2 \rangle)}^{-1} & a_{\min} < a < a_{\max} \\ 0 & \text{otherwise} \end{cases}, \quad (4.34)$$

where a_{\min} and a_{\max} are the minimum and maximum values of the anisotropy. For this model, $a_{\min} = -a_{\max}$. Clem also used, for the average energy gap and the transition temperature of a pure single-crystal, the values obtained by solving the BCS integral equation with the factorable interaction, $V(\Omega, \Omega') = (1+a(\Omega)) V(1+a(\Omega'))$, of Markowitz and Kadanoff⁽³¹⁾. These are

$$\begin{aligned} \langle \Delta_0(\Omega) \rangle &= \left[1 + \left(\frac{1}{N(0)V} - \frac{3}{2} \right) \langle a^2 \rangle \right] 2\omega_D e^{-1/N(0)V} \\ &= \left[1 + \left(\frac{1}{N(0)V} - \frac{3}{2} \right) \langle a^2 \rangle \right] \Delta_0^{\text{BCS}}, \end{aligned} \quad (4.35)$$

$$\begin{aligned} k_B T_c &= \left[1 + \frac{\langle a^2 \rangle}{N(0)V} \right] 1.134 \omega_D e^{-1/N(0)V} \\ &= \left[1 + \frac{\langle a^2 \rangle}{N(0)V} \right] k_B T_c^{\text{BCS}}, \end{aligned} \quad (4.36)$$

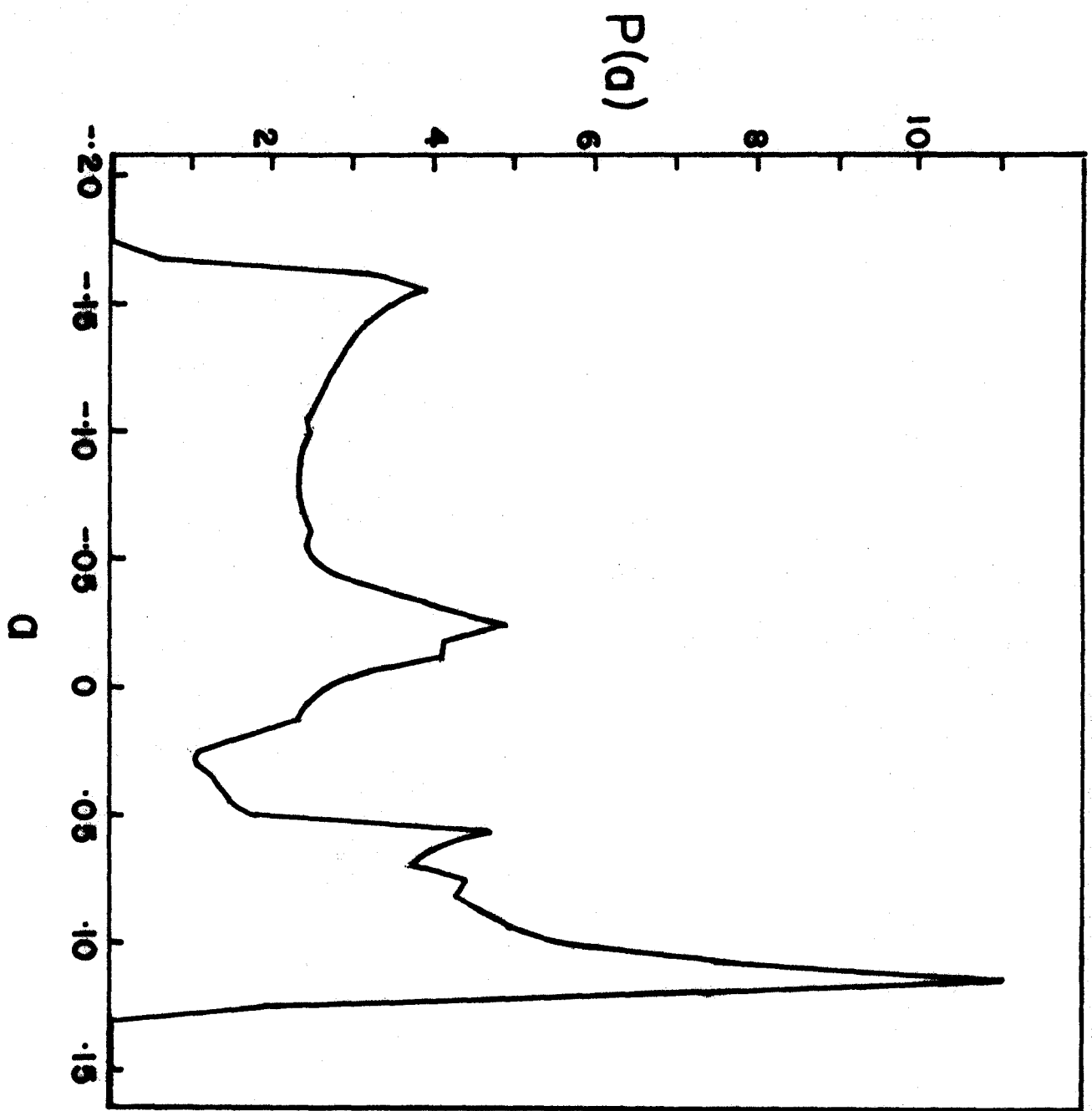
where Δ_0^{BCS} and T_c^{BCS} are the usual BCS results for the isotropic energy gap and the transition temperature of an

isotropic or 'dirty' superconductor. Clem's model is a one parameter model; the single parameter is the mean squared anisotropy $\langle a^2 \rangle$.

Cheeke and Ducla-Soares⁽³⁶⁾ analyzed their low temperature specific heat data for pure superconducting Al using a model which gave results very similar to those for Clem's model (to within 0.5% at $T_c/T=6$). They concluded that, within their model, $\langle a^2 \rangle = 0.010 \pm .003$ for pure Al.

We now use our one iteration results for the directional energy gaps in pure Al to calculate the anisotropy distribution function and the anisotropy parameters $\langle a^2 \rangle$, $\langle ab \rangle$ and $\langle a\bar{b} \rangle$. The procedure is simple. For example, to calculate $P(a)$, the directional energy gaps are calculated, using the polynomial interpolation scheme, for a fine mesh of points on the irreducible ($\frac{1}{48}$)th of the Fermi surface ($0 < \theta < \tan^{-1}(1/\cos\phi)$, $0 < \phi < \pi/4$) and these calculated gaps are sorted into their appropriate histogram channels. From this directional energy gap distribution function we readily obtain the average gap and hence the anisotropy distribution function. Figure 4.9 is a plot of the anisotropy distribution obtained in this way for Al. We note that its shape is far from rectangular and that it is not symmetric about $a=0$ as a rectangular distribution function must be. Of course, our distribution function and that of Clem do not represent quite the same thing. We have determined the anisotropy in the energy gap arising from the anisotropy in the phonon

FIGURE 4.9 The anisotropy distribution function, $P(a)$,
for Al, calculated assuming that the anisotropy
in the phonon density of states is the only
source of anisotropy in the superconducting
energy gap.



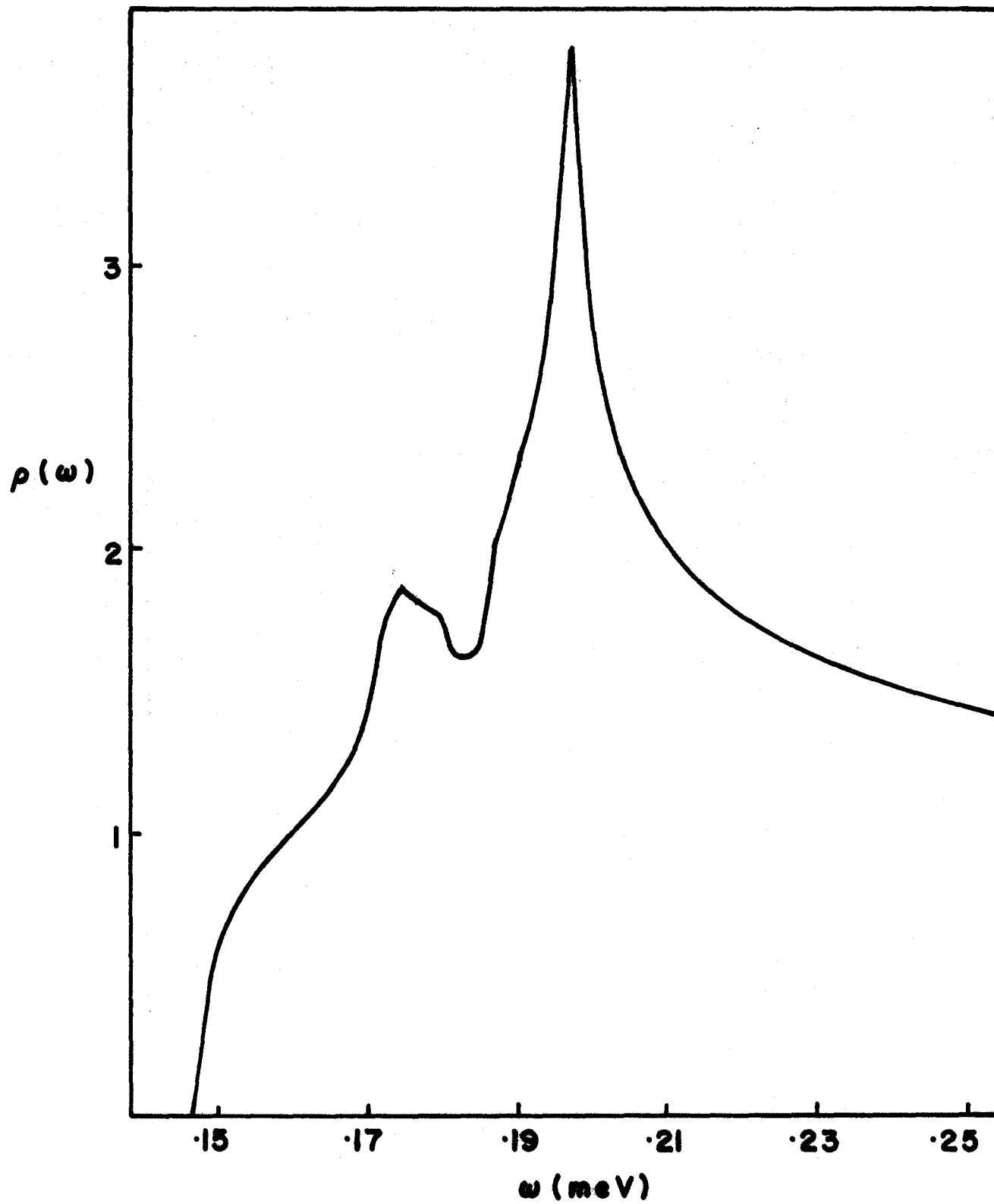
spectra and have neglected all other sources of anisotropy. Clem's rectangular distribution function is a model for the anisotropy in the energy gap arising from all sources. If the anisotropy in the phonon density of states is the dominant source of anisotropy in the energy gap, then the actual $P(a)$ for Al must be qualitatively similar to the one that we have calculated. It most certainly will exhibit the 2 dimensional types of Van Hove singularities, an upward step, a downward step and a logarithmic infinity, all of which are evident in figure 4.9, although they are somewhat smeared by the finite histogram channel width and the polynomial interpolation scheme. Figure 4.10 is a graph of the averaged quasiparticle density of states function,

$$\rho(\omega) \equiv \langle n(\Omega, \omega) \rangle = \int da P(a) \operatorname{Re} \left\{ \frac{\omega}{\sqrt{\omega^2 - \langle \Delta_0(\Omega) \rangle^2} (1+a)^2} \right\},$$

calculated with the anisotropy distribution function of figure 4.9. The dominant features of $P(a)$ are reflected in $\rho(\omega)$ although they are smeared considerably.

The mean squared anisotropy calculated using the $P(a)$ of figure 4.9 is $\langle a^2 \rangle = .0084$. We note, in passing, that the value of $\langle a^2 \rangle$ obtained using the uncorrected $\alpha^2 F(\nu, \theta, \phi)$'s to calculate the directional energy gaps is .013. This value certainly represents an upper limit to the phonon density of states contribution to the anisotropy of the energy gap.

FIGURE 4.10 The averaged quasiparticle density of states calculated with the anisotropy distribution function of figure 4.9.



Substituting the one iteration results for $\langle ab \rangle$ and $\langle a\bar{b} \rangle$, .0081 and .0142 respectively, into equations (3.45) and (3.93) we obtain

$$\langle \Delta_0(\Omega) \rangle / \Delta_0 = 1.022 \quad (1.027) \quad ,$$

$$T_c^{\text{PSC}} / T_c = 1.039 \quad (1.056) \quad ,$$

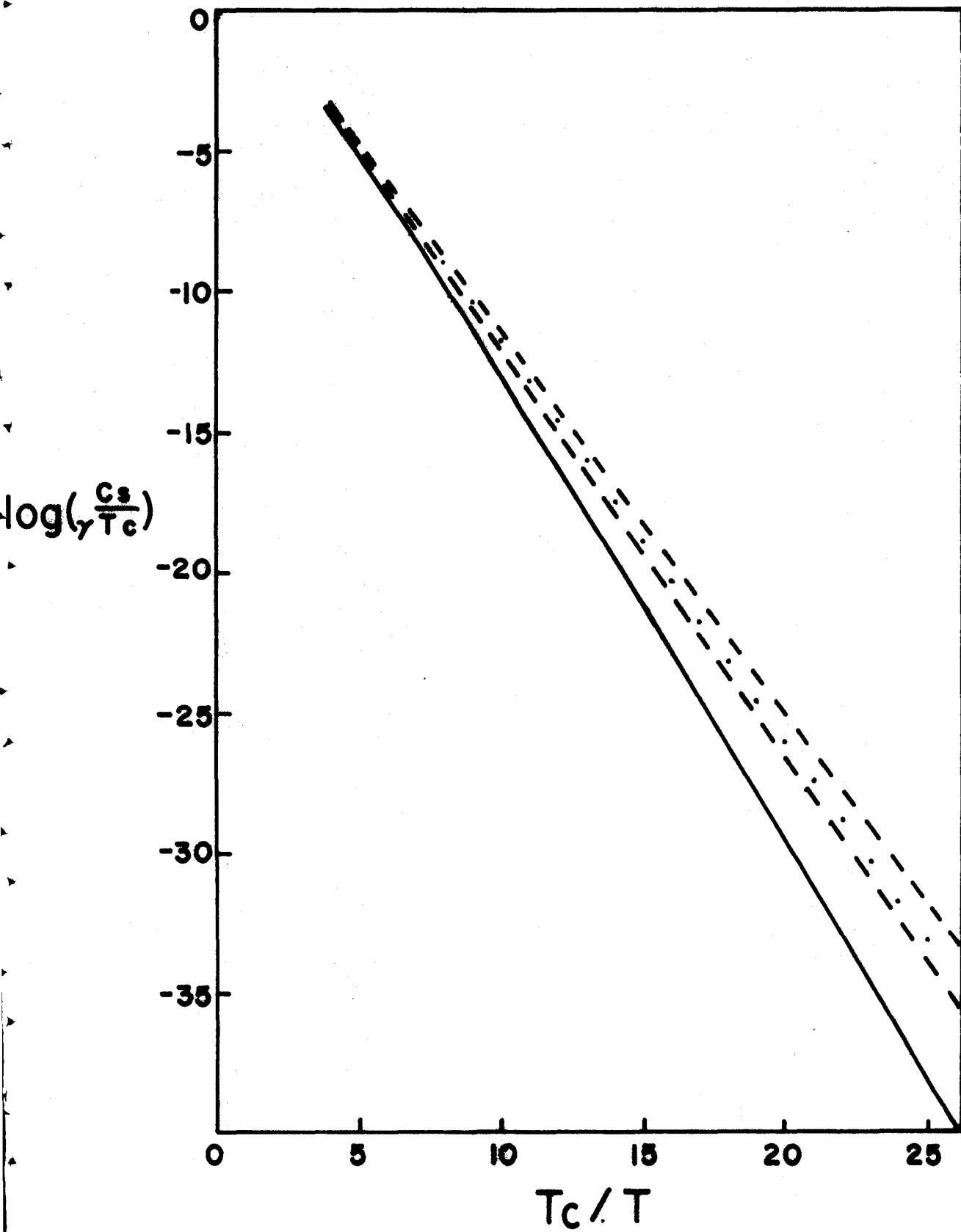
where T_c^{PSC} is the transition temperature of a pure single-crystal and where Δ_0 and T_c refer to the isotropic superconductor. The values in brackets represent upper limits and were calculated using the uncorrected directional $\alpha^2 F(\nu, \theta, \phi)$'s. The experimental values of Cheeke and Duclaux-Soares for the transition temperatures of pure and 'dirty' Al are 1.19°K and 1.132°K respectively. Hence the experimental ratio of the transition temperatures is

$$(T_c^{\text{PSC}} / T_c)^{\text{EXP}} = 1.051 \quad .$$

We see that the anisotropy of the phonon density of states accounts for roughly 80% of this effect.

Results for the low temperature behaviour of the electronic contribution to the specific heat in Al are shown in figure 4.11 where $\log(C_s / \gamma T_c)$ is plotted against T_c / T . (γT_c is the normal state electronic contribution to the specific heat at the transition temperature.) The solid curve is the BCS result for the isotropic crystal. The two dashed

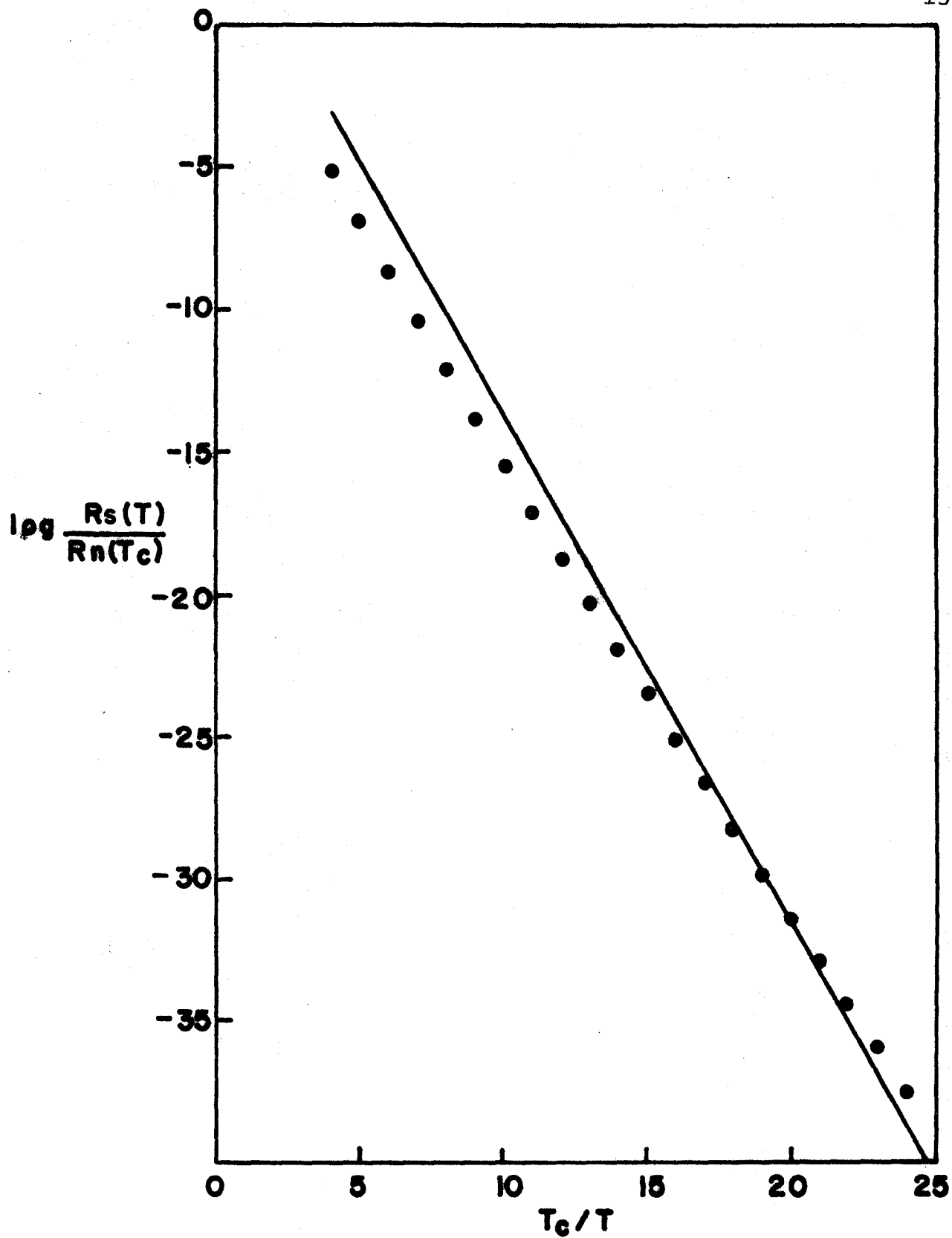
FIGURE 4.11 Low temperature behaviour of the electronic contribution to the specific heat of aluminium. The solid curve is the BCS result for the isotropic superconductor. The lower (upper) dashed curve was calculated using Clem's one parameter model with $\langle a^2 \rangle = .007$ (.013). The points are our results for a pure single-crystal of aluminium.



lines are results for the pure single-crystal calculated using Clem's rectangular model for the distribution function $P(a)$ and using equations (4.35) and (4.36) to determine the average energy gap and the transition temperature. The upper dashed curve is for $\langle a^2 \rangle = .013$ and the lower dashed curve is for $\langle a^2 \rangle = .007$. The points lying between the two dashed lines are our results calculated using the anisotropy distribution function of figure 4.9 and using equations (3.45) and (3.93) to calculate the average energy gap and transition temperature. It is evident from the graph that our results fall within the experimental limits set by Cheeke and Ducla-Soares. If the best fit curve were included in the figure our results would lie somewhat below it. We conclude that the anisotropy of the phonon density of states can account for most of the low temperature enhancement of the electronic contribution to the specific heat in a pure single-crystal superconductor.

In figure 4.12 we present results for the low temperature nuclear spin-lattice relaxation rate. The solid curve is the usual BCS result for an isotropic superconductor. The circled points are our results for anisotropic aluminium calculated using the anisotropy distribution function of figure 4.9. It is to be noted that the curve for the isotropic superconductor lies below that of the anisotropic superconductor at very low temperatures but rises above it as the temperature is increased. This reflects the fact

FIGURE 4.12 Low temperature behaviour of the nuclear spin-lattice relaxation rate for aluminium. The solid curve is the BCS result for the isotropic superconductor; the points are our results for pure single-crystal aluminium.



that the BCS result for the isotropic case diverges logarithmically as the transition temperature is approached from below. This divergence can be washed out by energy gap anisotropy, spatial inhomogeneities^(72,73) or quasi-particle damping⁽⁷⁴⁾.

In this section we have assumed that the energy gap anisotropy in aluminium is independent of temperature. This assumption is investigated in the next section.

4.5 TEMPERATURE DEPENDENCE OF THE ENERGY GAP ANISOTROPY IN ALUMINIUM

In section 4.4 it was assumed that the energy gap anisotropy in aluminium was independent of temperature. This is a reasonable assumption to make because the transition temperature of aluminium is very low (1.9°K). In this section we show, within the weak coupling formalism of Chapter III, that this assumption is essentially correct.

The one iteration result for the directional energy gap $\Delta_0(\Omega, T)$ at a finite temperature T follows immediately from equation (3.90) on replacing $\Delta_0(\Omega, T)$ on the right hand side by the isotropic energy gap $\Delta_0(T)$ appropriate to 'dirty' aluminium. We obtain

$$\Delta_0^{(1)}(\Omega, T) = \frac{1}{1+\lambda(\Omega, T)} \left\{ 2 \int_0^{\omega_c} dv \alpha^2 F(v, \Omega) \int_0^{\omega_c} \frac{d\varepsilon'}{E'} \frac{(E'+v) \tanh(E'/2k_B T)}{(E'+v)^2 - \Delta_0^2(T)} \right. \\ \left. - \mu^* \int_0^{\omega_c} \frac{d\varepsilon'}{E'} \tanh(E'/2k_B T) \right\} \Delta_0(T) \quad , (4.37)$$

where $E' \equiv \sqrt{\epsilon'^2 + \Delta_0^2(T)}$. We consider only one temperature, $T = .98 T_c$, in this study. To determine $\Delta_0(T)$ we use the BCS value for the ratio $\Delta_0(T)/\Delta_0(0)$ as calculated by Mühlischlegel⁽⁷⁵⁾. P. Truant⁽⁷⁶⁾ has calculated $\lambda(\Omega, T)$ for Al using our $\alpha^2 F(\nu, \Omega)$'s. It is clear from his results that the temperature dependence of $\lambda(\Omega, T)$ can be neglected to a very good approximation for the temperatures of interest here. The calculation of $\Delta_0^{(1)}(\Omega, T)$ is then straightforward. The integrals occurring in (4.37) are easily performed numerically. Our results are presented in table 4.3. Since the total variation in the ratio $\Delta_0^{(1)}(\Omega, 0)/\Delta_0^{(1)}(\Omega, .98T_c)$ is less than 1% it is safe to conclude that the temperature dependence of the energy gap anisotropy in aluminium can be neglected to a very good approximation.

TABLE 4.3
 TEMPERATURE DEPENDENCE OF THE ENERGY GAP
 ANISOTROPY IN ALUMINIUM. ($T = .98T_c$)

DIRECTION		$\Delta_0^{(1)}(\Omega, 0)$
θ°	ϕ°	$\Delta_0^{(1)}(\Omega, T)$
0.0	0.0	4.08
7.5	0.0	4.08
15.0	0.0	4.08
22.5	0.0	4.07
30.0	0.0	4.09
37.5	0.0	4.08
45.0	0.0	4.08
22.5	45.0	4.07
54.75	45.0	4.11
22.5	22.5	4.07
45.0	22.5	4.09

CHAPTER V

SUMMARY AND CONCLUSIONS

5.1 A CONTRIBUTION TO THE THEORY OF A WEAK COUPLING SUPERCONDUCTOR

For the special case of weak and medium coupling superconductors reasonable approximations were employed to reduce the Eliashberg gap equations for the zero temperature gap edge Δ_0 of an isotropic superconductor to a very much simpler approximate set of integral equations. The fact that for weak coupling superconductors the important phonon energies are much larger than the energy gap was exploited to obtain an approximate analytical solution to the simplified integral equations. The resulting simple expression is formally identical to the BCS result for the zero temperature energy gap and hence the BCS parameter $N(0)V$ can be identified with a certain simple function of the normal state properties. We compared our expression for $N(0)V$ with that of Morel and Anderson for several superconductors for which reliable normal state data was available. It was found that, even after renormalizing the Morel-Anderson expression, our equation gave much better agreement with experiment for all of the metals considered. A careful investigation established, for weak and medium coupling

superconductors, that the gap edge obtained by solving the simplified integral equations is in good quantitative agreement with that obtained by solving the Eliashberg equations. It was also found that the simple analytical expression for Δ_0 is a good approximation to the Eliashberg value for weak coupling superconductors and a fairly good approximation for medium coupling superconductors. The importance of these conclusions lies in the fact that one can save an enormous amount of computer time at the expense of a small loss in accuracy by using the simplified integral equations in place of the Eliashberg equations for certain investigations.

The analytical expression for Δ_0 was applied to a Tl-In alloy series with very satisfactory results.

The simplified integral equations were generalized so as to be suitable for an anisotropic pure single-crystal superconductor. The anisotropic energy gap in aluminium was calculated for several directions and the results found to be in very good agreement with the corresponding results calculated using the Eliashberg equations. An expression was derived for the average energy gap in a pure single-crystal superconductor in terms of certain gross features of the anisotropy. It was found that the average energy gap in a pure single-crystal of aluminium is a few percent larger than the isotropic energy gap in dirty aluminium.

The pressure dependence of the BCS parameter $N(0)V$ was investigated for Al, Tl, In and Sn. It was found for

all of these elements that to a good approximation the decrease of $N(0)V$ was linear in the fractional volume change. The pressure dependence of the isotropic energy gap in dirty Al, Tl, In and Sn was studied using the weak coupling integral equations and the simple analytical expression for Δ_0 . A comparison was made with the pressure work done by P. Vashishta for Tl, In and Sn using the Eliashberg gap equations. The quantitative agreement obtained with the simplified integral equations was very good while that obtained with the analytical expression was satisfactory. The pressure dependence of the anisotropic energy gap in a pure single-crystal of aluminium was calculated. It was found that the anisotropy increased quite markedly with pressure. It is hoped that this effect will be investigated by experimentalists in the near future.

A simple expression was derived for the transition temperature of a weak coupling isotropic superconductor by introducing certain approximations into the finite temperature Eliashberg equations. A correction to the BCS value for the ratio of twice the energy gap to the transition temperature was obtained and it was shown that this correction decreases with increasing pressure so that the BCS ratio is obtained in the limit of very high pressure.

A new expression for the isotope effect was obtained and the pressure dependence of the isotope effect exponent for Al, Tl, In and Sn was studied. It was found that the

exponent decreases with increasing pressure i.e. that the deviation from the BCS value of $\frac{1}{2}$ increases with pressure. This effect should be of interest to experimentalists.

A crucial test of any equation for the transition temperature of a superconductor is that it be capable of giving both the correct transition temperature and the correct isotope effect exponent. It is hoped that reliable experimental values of the isotope effect exponent will be available in the near future for a large number of superconductors so that we can test our simple expression for the transition temperature further.

5.2 ENERGY GAP ANISOTROPY IN ALUMINIUM

The function $\alpha^2 F(\nu, \theta, \phi)$ for aluminium was calculated for a large number of points (θ, ϕ) on the irreducible $(\frac{1}{48})$ th of the Fermi surface. This function was then used to calculate the directional electron-phonon mass-enhancement parameter. We found considerable anisotropy in the mass-enhancement parameter.

We calculated the energy gap anisotropy in aluminium arising from the anisotropy in the phonon spectrum. We neglected all other sources of anisotropy. The Eliashberg gap equations containing the directional $\alpha^2 F(\nu, \theta, \phi)$'s were iterated once (using the isotropic solution as a trial solution) to obtain the gap edge for a large number of points on the $(\frac{1}{48})$ th of the Fermi surface. A procedure was devised

to interpolate between these values so that the directional energy gap could be obtained quite accurately at any point on the Fermi surface. A second iteration was performed using the weak coupling integral equations. The results of the second iteration differed from the first iteration values for the energy gap by only a small amount. This gave some justification for Bennett's one iteration procedure.

An energy gap anisotropy distribution function was calculated and found to be very different from the rectangular model of Clem. The distribution function was used to calculate the mean squared anisotropy $\langle a^2 \rangle$. We found $\langle a^2 \rangle = .0084$. Since experiments indicate that $\langle a^2 \rangle \sim .01$ for aluminium we conclude that the anisotropy in the phonon spectrum is the dominant source of energy gap anisotropy, accounting for roughly 80% of the observed anisotropy. We calculated the average energy gap and the transition temperature of a pure single-crystal of aluminium using the results for the directional mass-enhancement parameter, the one iteration values of the directional energy gap and the theoretical equation derived in Chapter III. It was found that the ratio of the transition temperature of a pure single-crystal of aluminium to that of dirty aluminium was 1.04. The experimental value is 1.05. We again conclude that the anisotropy in the phonon spectrum accounts for most of the experimental effect. The anisotropy distribution function was used to calculate the Fermi surface averaged

quasiparticle density of states and this in turn was used to calculate the low temperature electronic contribution to the specific heat of a pure single-crystal of aluminium. Our results fell well within the experimental limits. In the specific heat calculation it was assumed that the energy gap anisotropy in aluminium was independent of temperature. This assumption was investigated by calculating several directional energy gaps at a temperature very close to the transition temperature ($.98 T_c$) and comparing them with the corresponding zero temperature gaps. It was found that the energy gap anisotropy in aluminium is independent of temperature to a good approximation.

The qualitative conclusions of this investigation can be summarized as follows: the principal source of energy gap anisotropy in superconducting aluminium is the anisotropy in the phonon spectrum; the anisotropy in the energy gap is independent of temperature to a good approximation.

REFERENCES

- (1) H. K. Onnes, Commun. Phys. Lab. Univ. Leiden, No. 119b (1911)
- (2) J. M. Blatt, Theory of Superconductivity (Academic Press Inc., New York, 1964)
- (3) C. J. Gorter and H. Casimir, Physica 1, 306 (1934)
- (4) F. London and H. London, Proc. Roy. Soc. (London) A149, 71 (1935)
- (5) A. B. Pippard, Proc. Roy. Soc. (London) A216, 547 (1953)
- (6) V. L. Ginzburg and L. D. Landau, Zh. Eksperim. i Teor. Fiz. 20, 1064 (1950)
- (7) H. Fröhlich, Phys. Rev. 79, 845 (1950)
- (8) E. Maxwell, Phys. Rev. 78, 477 (1950)
- (9) B. Serin, C. A. Reynolds and L. B. Nesbitt, Phys. Rev. 80, 761 (1950)
- (10) L. N. Cooper, Phys. Rev. 104, 1189 (1956)
- (11) J. Bardeen, L. N. Cooper and J. R. Schrieffer, Phys. Rev. 108, 1175 (1957)
- (12) L. D. Landau, Zh. Eksperim. i Teor. Fiz. 30, 1058 (1956); Soviet Phys. JETP 7, 996 (1958)
- (13) P. W. Anderson, J. Phys. Chem. Solids 11, 26 (1959)
- (14) J. Bardeen and J. R. Schrieffer, in Progress in Low Temperature Physics, Vol. 3, edited by C. J. Gorter (North-Holland, Amsterdam, 1961)

- (15) R. Meservey and B. B. Schwartz, in Superconductivity, edited by R. D. Parks (Marcel Dekker, Inc., New York, 1969)
- (16) D. M. Ginsberg and L. C. Hebel, in Superconductivity, edited by R. D. Parks (Marcel Dekker, Inc., New York, 1969)
- (17) A. B. Migdal, Zh. Eksperim. i Teor. Fiz. 34, 1438 (1958); Soviet Phys. JETP 7, 996 (1958)
- (18) G. M. Eliashberg, Zh. Eksperim. i Teor. Fiz. 38, 996 (1960); Soviet Phys. JETP 11, 696 (1960)
- (19) Y. Nambu, Phys. Rev. 117, 648 (1960)
- (20) D. J. Scalapino, J. R. Schrieffer and J. W. Wilkens, Phys. Rev. 148, 263 (1966)
- (21) D. J. Scalapino, in Superconductivity, edited by R. D. Parks (Marcel Dekker, Inc., New York, 1969)
- (22) W. L. McMillan and J. M. Rowell, in Superconductivity, edited by R. D. Parks (Marcell Dekker, Inc., New York, 1969)
- (23) N. N. Bogoliubov, V. V. Tolmachev and D. V. Shirkov, A New Method in the Theory of Superconductivity (Academy of Science, Moscow, 1958, translation Consultants Bureau, New York, 1959)
- (24) J. R. Schrieffer, Theory of Superconductivity (W. A. Benjamin, Inc., New York, 1964)
- (25) J. P. Carbotte and R. C. Dynes, Phys. Rev. 172, 476 (1968)

- (26) B. N. Brockhouse, E. D. Hallman and S. C. Ng,
in Magnetic and Inelastic Scattering of Neutrons by
Metals, edited by T. J. Rowland and P. A. Beck
(Gordon and Breach Science Publishers, Inc.,
New York, 1969)
- (27) J. M. Ziman, Electrons and Phonons (Oxford University
Press, 1960)
- (28) L. P. Gorkov, Zh. Eksperim. i Teor. Fiz. 34 735 (1958);
Soviet Phys. JETP 7, 505 (1958)
- (29) P. Morel and P. W. Anderson, Phys. Rev. 125, 1263 (1962)
- (30) W. L. McMillan, Phys. Rev. 167, 331 (1968)
- (31) D. Markowitz and L. P. Kadanoff, Phys. Rev.
131, 563 (1963)
- (32) E. A. Lynton, B. Serin and M. Zucker, J. Phys. Chem. Solids
3, 165 (1957);
R. I. Gayley, Jr., E. A. Lynton and B. Serin,
Phys. Rev. 126, 43 (1962)
- (33) G. Chanin, E. A. Lynton and B. Serin, Phys. Rev.
114, 719 (1959)
- (34) D. P. Seraphim, C. Chiou and D. J. Quinn, Acta Met.
9, 861 (1961)
- (35) J. R. Clem, Annals of Physics 40, 268 (1966)
- (36) J. D. N. Cheeke and E. Ducla-Soares, Physics Letters
27A, 264 (1968)
- (37) A. J. Bennett, Phys. Rev. 140, 1902 (1965)

- (38) G. Rickayzen, Theory of Superconductivity (John Wiley and Sons, Inc., New York, 1965) p. 144
- (39) P. N. Trofimenkoff, Ph.D. Thesis, McMaster University, Hamilton, Canada (unpublished) (1969)
- (40) P. Vashishta, private communication
- (41) E. Fermi, Z. Physik 48, 73 (1928);
L. H. Thomas, Proc. Cambridge Phil. Soc. 23, 542 (1927)
- (42) P. B. Allen and M. L. Cohen, Phys. Rev. 187, 525 (1969)
- (43) R. E. Fasnacht and J. R. Dillinger, Phys. Rev. Letters 17, 255 (1966)
- (44) R. C. Dynes, Phys. Rev. (in press)
- (45) R. W. Stark and L. M. Falicov, Phys. Rev. Letters 19, 795 (1967)
- (46) J. A. Young and J. U. Koppel, Phys. Rev. 134, A1476 (1964)
- (47) O. A. E. Cherney and J. Stewchun, Can. J. Phys. 47, 1101 (1969)
- (48) T. T. Chen, J. T. Chen, J. D. Leslie and H. J. T. Smith, Phys. Rev. Letters 22, 526 (1969)
- (49) S. Bermon and D. M. Ginsberg, Phys. Rev. 135, A306 (1964)
- (50) C. Kittel, Introduction to Solid State Physics (John Wiley and Sons, Inc., New York, 1966) p. 183
- (51) P. N. Trofimenkoff and J. P. Carbotte, Phys. Rev. B 1, 1136 (1970);
Solid St. Comm. 7, 661 (1969)
- (52) P. Vashishta, private communication

- (53) G. Rickayzen, Theory of Superconductivity (John Wiley and Sons, Inc., New York, 1965) p. 177
- (54) R. G. Pulsen, private communication
- (55) J. J. Sabo, Jr., Phys. Rev. B 1, 1325 (1970)
- (56) P. Truant, private communication
- (57) P. B. Allen and M. L. Cohen, Phys. Rev. B 1, 1329 (1970)
- (58) G. Grimvall, J. Phys. Chem. Solids 29 1221 (1968)
- (59) J. W. Wilkins, Observable Many-Body Effects in Metals (Nordita, Copenhagen, 1968)
- (60) J. P. Frank and W. J. Keeler, Phys. Rev. Letters 20, 379 (1968)
- (61) T. H. Geballe and B. T. Matthias, IBM J. Res. Develop. 6, 256 (1962)
- (62) R. E. Fasnacht and J. R. Dillinger, Phys. Rev. Letters 17, 255 (1966)
- (63) J. W. Garland, Jr., Phys. Rev. Letters 11, 114 (1963);
Phys. Rev. 153, 460 (1967)
- (64) G. Gilat and L. J. Raubenheimer, Phys Rev. 144, 390 (1966)
- (65) G. Gilat and R. M. Nicklow, Phys. Rev. 143, 487 (1966)
- (66) V. Heine and I. Abarenkov, Phil. Mag. 9, 451 (1964)
- (67) W. A. Harrison, Pseudopotentials in the Theory of Metals (W. A. Benjamin, Inc., New York, 1966)
- (68) P. B. Allen and M. L. Cohen, Phys. Rev. B 1, 1329 (1970)
- (69) L. J. Sham and J. M. Ziman, Solid State Phys. 15, 221 (1963)
- (70) R. Stedman, L. Almqvist and G. Nilsson, Phys. Rev. 162, 599 (1967)

- (71) R. C. Dynes and J. P. Carbotte, in Proceedings of the Conference on Superconductivity at Stanford, 1969
(to be published)
- (72) L. C. Hebel and C. P. Slichter, Phys. Rev. 113, 1504 (1959)
- (73) L. C. Hebel, Phys. Rev. 116, 79 (1959)
- (74) M. Fibich, Phys. Rev. Letters 14, 561 (1965)
- (75) B. Z. Mühlischlegel, Phys. 155, 313 (1959)
- (76) P. Truant, private communication
- (77) P. Nozières, Theory of Interacting Fermi Systems
(W. A. Benjamin, Inc., New York, 1963)
- (78) D. Pines and P. Nozières, The Theory of Quantum Liquids
(W. A. Benjamin, Inc., New York, 1966)
- (79) V. P. Silin, Zh. Eksperim. i Teor. Fiz. 33, 495 (1957);
Soviet Phys. JETP 6, 945 (1958)
- (80) R. E. Prange and A. Sachs, Phys. Rev. 158, 672 (1967)
- (81) For Na, M. J. G. Lee, Proc. Roy. Soc. (London)
A295, 440 (1966);
For K, M. J. G. Lee and L. M. Falicov, *ibid.*
A314, 319 (1968)
- (82) T. M. Rice, Phys. Rev. 175, 858 (1968)
- (83) T. M. Rice, Ann. Phys. (N.Y.) 31, 100 (1965)
- (84) A. D. B. Woods, B. N. Brockhouse, R. H. March,
A. T. Stewart and R. Bowers, Phys. Rev. 128, 112 (1962)
- (85) R. A. Cowley, A. D. B. Woods and G. Dolling, Phys. Rev.
150, 487 (1966)

- (86) J. R. D. Copley, B. N. Brockhouse and S. H. Chen,
in Neutron Inelastic Scattering (International Atomic
Energy Agency, Vienna, 1968)
- (87) N. W. Ashcroft, Phys. Letters 23, 48 (1966)
- (88) B. Hayman, private communication
- (89) R. W. Shaw, Jr. and R. Pynn, Solid St. Phys.
2, 2071 (1969)
- (90) J. K. Darby and N. H. March, Proc. Phys. Soc. (London)
84, 591 (1964)
- (91) G. Grimvall, Physik Kondensierten Materie 6, 15 (1967)
- (92) G. Grimvall, Solid St. Comm. 7, 1630 (1969)
- (93) W. F. Brinkman, P. M. Platzman and T. M. Rice, Phys. Rev.
174, 495 (1968)
- (94) C. C. Grimes and A. F. Kip, Phys. Rev. 132, 1991 (1963)
C. C. Grimes, Bull. Am. Phys. Soc. 12, 414 (1967)

APPENDIX

ANISOTROPY OF THE ELECTRON-PHONON SCATTERING FUNCTION OF FERMI LIQUID THEORY FOR Na, K AND Rb

The Landau theory of a Fermi liquid^(12,77,78) is a semiphenomenological description of a normal Fermi liquid i.e. of a system of strongly interacting fermions whose essential properties are not qualitatively different from those of a system of noninteracting fermions. The great success of the independent particle model of the conduction electrons in a metal in describing qualitatively and even quantitatively a wide variety of experiments implies that the electrons in the conduction band of a metal form a normal Fermi liquid (provided, of course, that the metal is not in the superconducting state). Landau's theory, which described a system of neutral fermions interacting through a short range potential, was extended by Silin⁽⁷⁹⁾ to describe a system of charged fermions interacting through the long ranged Coulomb repulsion. Recently, Prange and Sachs⁽⁸⁰⁾ have extended the theory to describe a system of electrons interacting via the Coulomb repulsion and the virtual exchange of phonons. In a real metal there are modifications due to the periodic crystal potential. However in the alkali metals we can, to a good approximation, ignore these band structure effects (the Fermi surfaces of Na and K are

free electron-like to within .2%⁽⁸¹⁾) and treat the electrons in the one OPW approximation.

The basic ingredients of the Landau theory of an isotropic system are an effective mass, m^* , which relates the quasiparticle velocity at the Fermi surface to the Fermi momentum through the expression

$$\underline{V}_F = \frac{\underline{P}_F}{m^*} \quad (\text{A.1})$$

and the expansion coefficients f_ℓ^s and f_ℓ^a of the Legendre polynomial expansion of the quasiparticle interaction function

$$f(\underline{k}_\underline{\sigma}, \underline{k}'_{\underline{\sigma}'}) = \sum_{\ell=0}^{\infty} (f_\ell^s + f_\ell^a \underline{\sigma} \cdot \underline{\sigma}') P_\ell(\cos \theta_{\underline{k}\underline{k}'}) \quad (\text{A.2})$$

In the above equation $\underline{\sigma}$ and $\underline{\sigma}'$ are the usual spin operators and $\theta_{\underline{k}\underline{k}'}$ is the angle between the wavevectors \underline{k} and \underline{k}' .

For an anisotropic situation one must introduce many additional parameters to describe the anisotropy of the effective mass and the interaction function. The anisotropy of the Fermi surface of an alkali metal is very small and can be ignored to a good approximation. However, the anisotropy in the phonon spectra of the alkali metals is considerable and cannot be ignored a priori since the electrons interact with each other by the virtual exchange of phonons. The anisotropy in the electron-phonon interaction enters the Fermi liquid theory of a real metal through the Legendre

polynomial moments of the directional electron-phonon scattering function⁽⁸²⁾. These moments are given by

$$g_{\ell}^{\text{ep}}(\underline{k}) = \left(\frac{m_{\text{ep}}^*}{m}\right) \left(\frac{m_{\text{ee}}^*}{m^*}\right)^2 \frac{mk_{\text{F}}}{\pi^2} \cdot \frac{1}{2NM} \sum_{\lambda} \int \frac{d\Omega_{\underline{k}'}}{4\pi} \left(\frac{\underline{\epsilon}(\underline{k}-\underline{k}', \lambda) \cdot (\underline{k}-\underline{k}')}{\omega(\underline{k}-\underline{k}', \lambda)} \right)^2 \\ \times W^2(\underline{k}-\underline{k}') P_{\ell}(\cos \theta_{\underline{k}\underline{k}'}) \quad , (A.3)$$

where m_{ee}^* , m_{ep}^* and m^* are, respectively, the Coulomb renormalized, phonon renormalized and fully renormalized electron masses. In (A.3) \underline{k} and \underline{k}' are confined to the Fermi surface; i.e. $\underline{k} \equiv (k_{\text{F}}, \theta, \phi)$, $\underline{k}' \equiv (k_{\text{F}}, \theta', \phi')$. Rice⁽⁸²⁾ suggests that omitting all frequency dependent vertex corrections and all quasiparticle renormalization factors for the Coulomb interaction is better than including the latter but omitting the former. This suggestion is based on the supposition that there is an approximate cancellation between the Coulomb quasiparticle renormalization factors and the Coulomb vertex corrections. This supposition has been borne out by detailed calculations⁽⁸³⁾. If we follow Rice's suggestion by replacing m_{ee}^* by m and m^* by m_{ep}^* in equation (A.3) we obtain

$$g_{\ell}^{\text{ep}}(\underline{k}) = \frac{\lambda_{\ell}^{\text{ep}}(\underline{k})}{1+\lambda} \quad , (A.4)$$

where

$$\lambda_{\ell}^{\text{ep}}(\underline{k}) \equiv 2N(0) \sum_{\lambda} \int \frac{d\Omega_{\underline{k}'}}{4\pi} \frac{|g_{\underline{k}\underline{k}'\lambda}|^2}{\omega_{\underline{k}-\underline{k}'\lambda}} P_{\ell}(\cos \theta_{\underline{k}\underline{k}'}) \quad . (A.5)$$

In writing down equation (A.4) we used the well known expression⁽²¹⁾

$$\frac{m^*_{ep}}{m} = 1 + \lambda \quad (\text{A.6})$$

for the phonon renormalized effective mass.

Although the moments of the directional electron-phonon scattering function are not relevant to superconductivity (particularly for the alkali metals) they are closely related to the directional electron-phonon mass-enhancement parameter, $\lambda(\underline{k})$, which was calculated in Chapter IV for aluminium. If we compare equation (A.5) for $\lambda_{\ell}^{ep}(\underline{k})$ with the equation,

$$\lambda(\underline{k}) = 2N(0) \sum_{\lambda} \int \frac{d\Omega_{\underline{k}'}}{4\pi} \frac{|g_{\underline{k}\underline{k}'\lambda}|^2}{\omega_{\underline{k}-\underline{k}'\lambda}} \quad , (3.42)$$

for the directional mass-enhancement parameter, it is immediately apparent that $\lambda_{\ell}^{ep}(\underline{k})$ can be calculated by multiplying the weight factor in the computer programme for $\lambda(\underline{k})$ by $P_{\ell}(\cos \theta_{\underline{k}\underline{k}'})$. In fact,

$$\lambda_0^{ep}(\underline{k}) = \lambda(\underline{k})$$

can be calculated with no modification whatsoever. Moreover, the average moments,

$$g_{\ell}^{ep} \equiv \int \frac{d\Omega_{\underline{k}}}{4\pi} g_{\ell}^{ep}(\underline{k}) \quad , (A.7)$$

can be calculated by making the same modification in the α^2F computer programme of Carbotte and Dynes⁽²⁵⁾.

To calculate $\lambda_{\ell}^{ep}(\underline{k})$ within the one OPW approximation we need the following information: (1) the phonon frequencies $\omega(\underline{q}, \lambda)$ and polarization vectors $\underline{\epsilon}(\underline{q}, \lambda)$ in the first Brillouin zone; (2) the electron-ion pseudopotential form factor $W(\underline{q})$ for $0 < q < 2k_F$. The information about the lattice dynamics is readily available for each of the metals Na⁽⁸⁴⁾, K⁽⁸⁵⁾ and Rb⁽⁸⁶⁾ in the form of a force constant fit to the phonon dispersion curves measured by the technique of inelastic neutron scattering. The one parameter pseudopotential form factors of Ashcroft⁽⁸⁷⁾ were used in our investigation. B. Hayman⁽⁸⁸⁾ was able to obtain a good fit to the experimental electrical resistivity over a wide temperature range with a single value of the adjustable parameter, r_c , for each of the alkali metals Na, K and Rb. Our calculations were done with his fitted values of r_c . In order to investigate the sensitivity of the directional moments of the electron-phonon scattering function to the exact form of the pseudopotential we repeated the calculation for Na and K with the pseudopotential form factors of Shaw⁽⁸⁹⁾.

We now present our one OPW results for the first few moments of the directional electron-phonon scattering function for the alkali metals Na, K and Rb. Some interesting intermediate results are also presented.

Figures A.1 and A.2 contain our results for $\alpha^2F(\nu, \theta, \phi)$

FIGURE A.1 $\alpha^2 F(\nu, \theta, \phi)$ for the three high symmetry directions in Na. The curves are, from bottom to top, for the [001], [011] and [111] directions. The three curves are displaced vertically from each other to facilitate comparison.

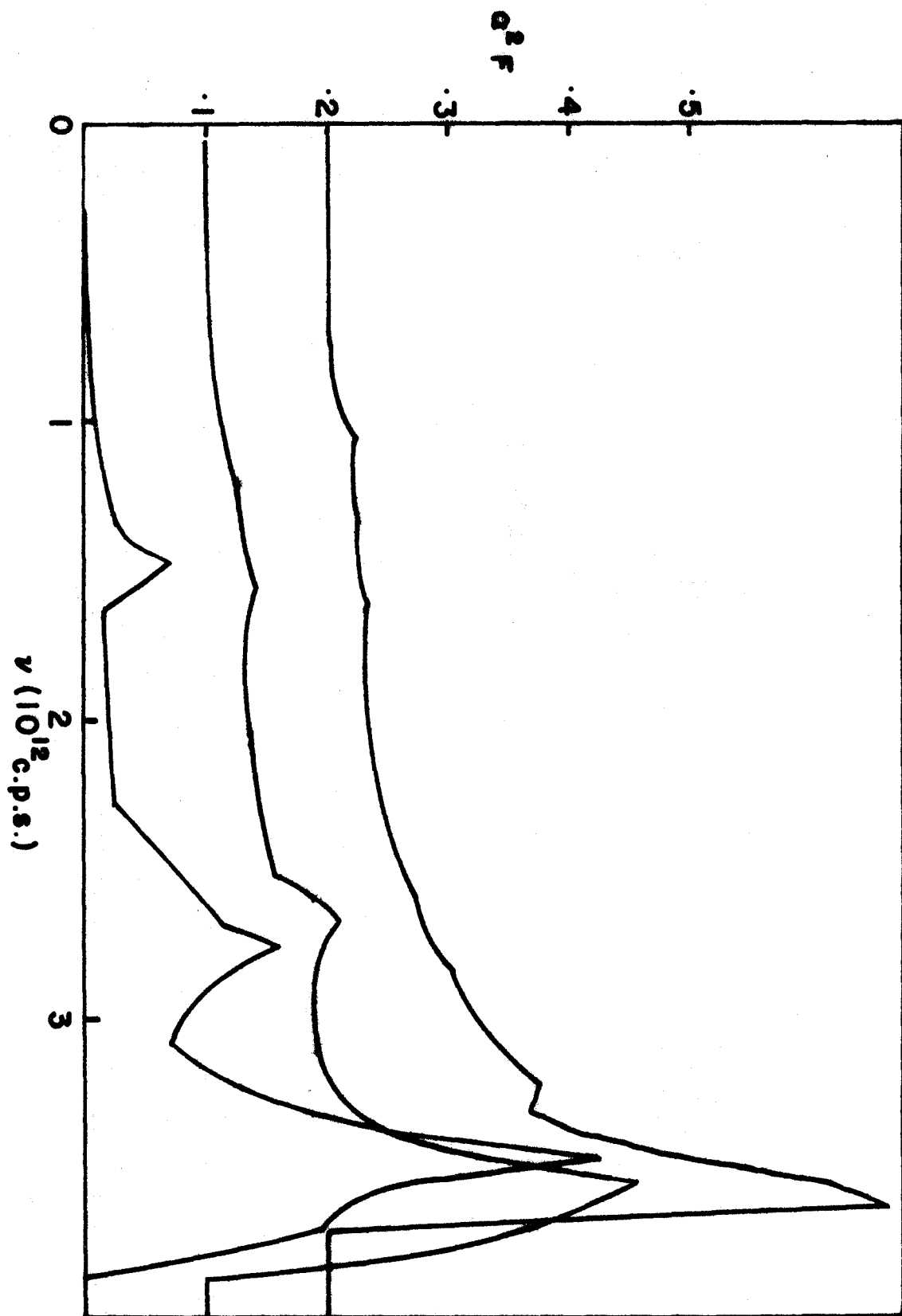
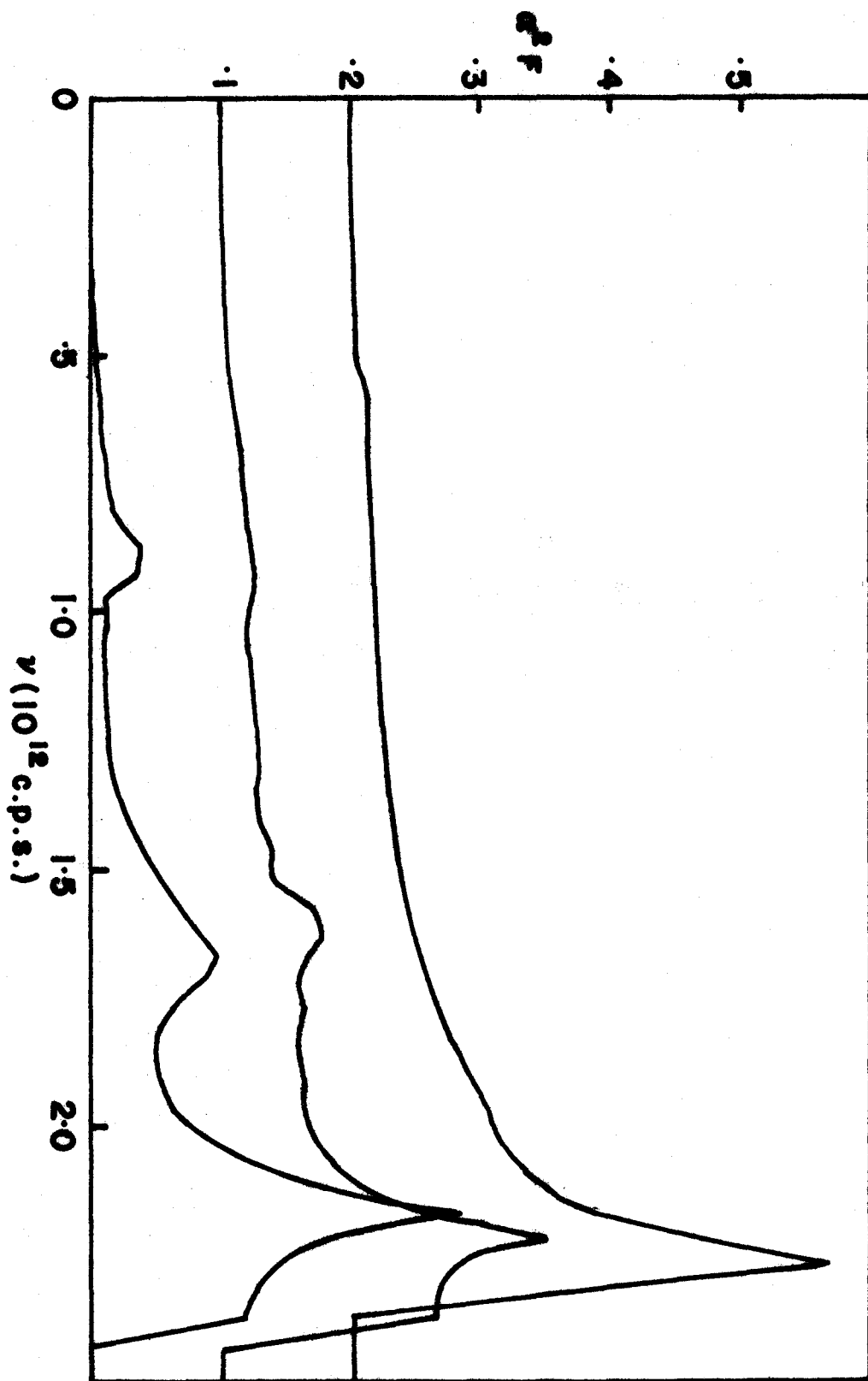


FIGURE A.2 $\alpha^2 F(\nu, \theta, \phi)$ for the three high symmetry directions in K. The curves are, from bottom to top, for the [001], [011] and [111] directions.



for the three high symmetry directions in Na and K respectively. Only fifty histogram channels were used for these calculations so that the two dimensional Van Hove singularities are smeared considerably. However, even with this smearing, the large amount of anisotropy in $\alpha^2 F(\nu, \theta, \phi)$ for the alkali metals is quite evident. It is worth pointing out that the corresponding curves for Na and K are quite similar. We further note that the one OPW approximation does not break down for the alkalis as it does for Al because the Fermi sphere of an alkali metal is small enough that momentum transfers in the range $0 < q < 2k_F$ are all considerably less than any reciprocal lattice vector $K \neq 0$.

In figures A.3, A.4 and A.5 we present our results for the directional functions $\lambda_0^{ep}(\underline{k})$, $\lambda_1^{ep}(\underline{k})$ and $\lambda_2^{ep}(\underline{k})$ for Na, K and Rb respectively. These calculations were all performed with the Ashcroft pseudopotential. Figures A.6 and A.7 contain our results for Na and K respectively using the Shaw pseudopotential.

In order to have a quantitative measure of the amount of anisotropy in the various moments of the directional electron-phonon scattering function we introduce an anisotropy parameter

$$a_\ell \equiv \frac{\text{Max}(g_\ell^{ep}(\underline{k})) - \text{Min}(g_\ell^{ep}(\underline{k}))}{g_\ell^{ep}} \quad .(A.8)$$

Our results for a_ℓ appear in table A.1. A glance at this

FIGURE A.3 The directional functions $\lambda_0^{\text{ep}}(\underline{k})$, $\lambda_1^{\text{ep}}(\underline{k})$
and $\lambda_2^{\text{ep}}(\underline{k})$ for Na as calculated with Ashcroft's
pseudopotential.

The results for the three arcs $\phi=0^\circ$, $22\frac{1}{2}^\circ$
and 45° on the irreducible $(\frac{1}{48})$ th are to be
distinguished as follows:

- . $\phi=0^\circ$
- x $\phi=22\frac{1}{2}^\circ$
- ⊙ $\phi=45^\circ$.

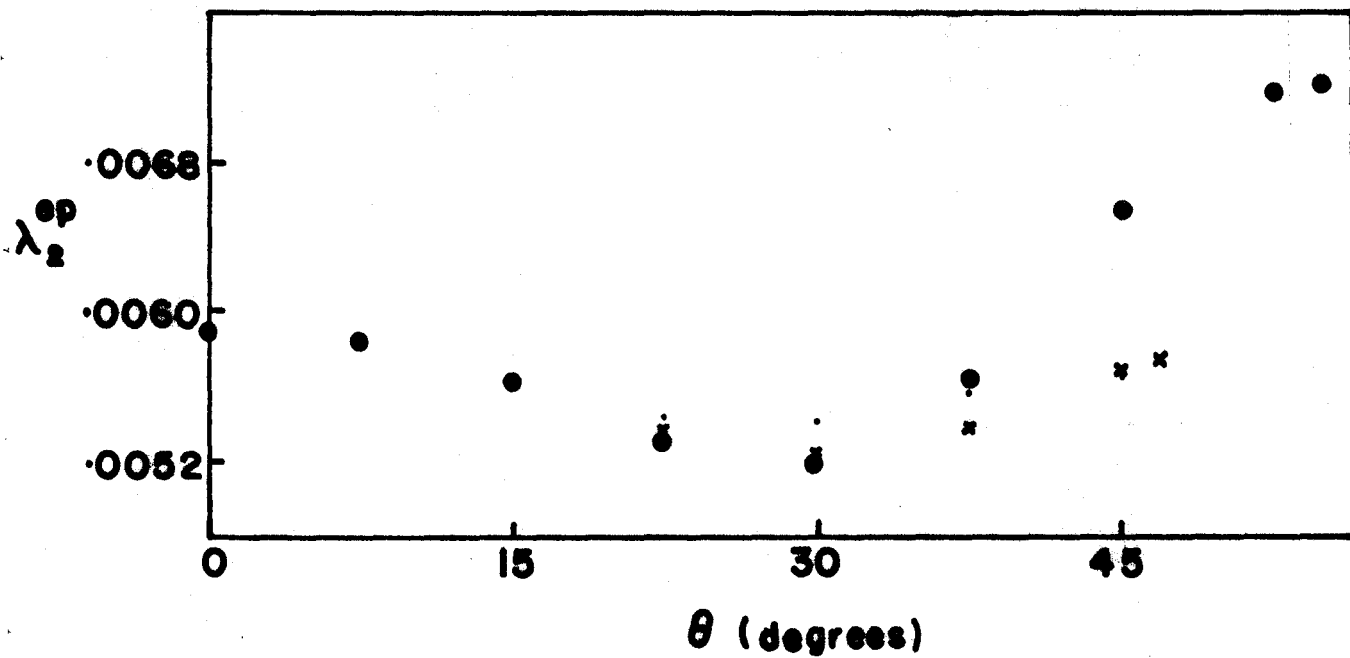
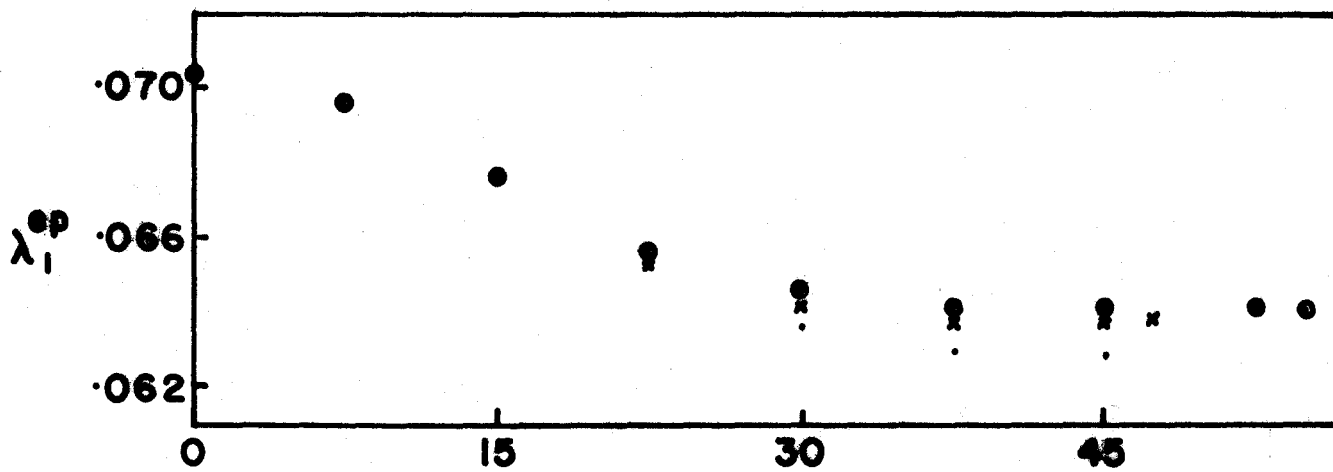
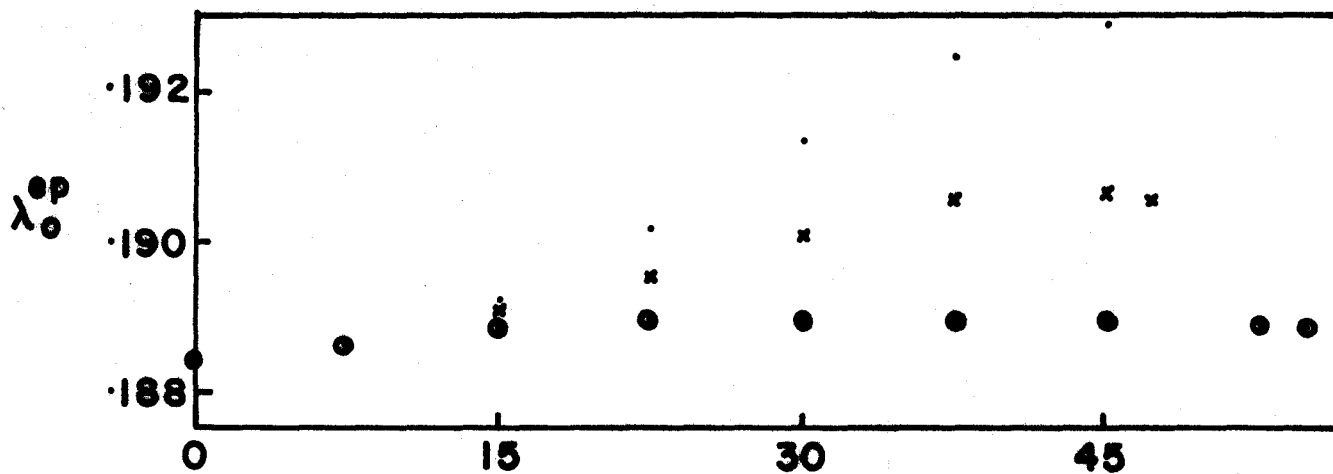


FIGURE A.4 The directional functions $\lambda_0^{\text{ep}}(\underline{k})$, $\lambda_1^{\text{ep}}(\underline{k})$
and $\lambda_2^{\text{ep}}(\underline{k})$ for K as calculated with Ashcroft's
pseudopotential. The legend for the points is
the same as in figure A.3.

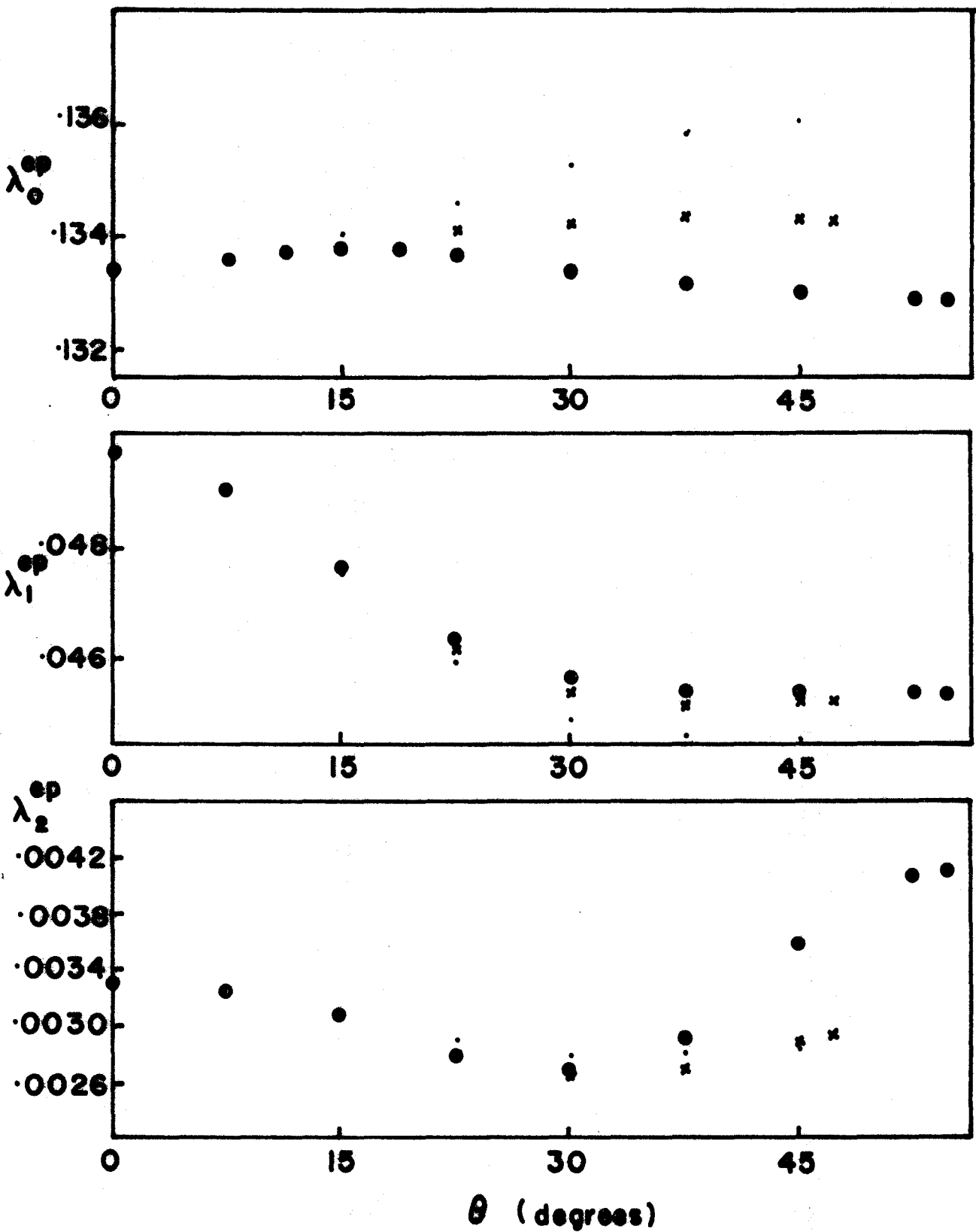


FIGURE A.5 The directional functions $\lambda_0^{\text{ep}}(\underline{k})$, $\lambda_1^{\text{ep}}(\underline{k})$
and $\lambda_2^{\text{ep}}(\underline{k})$ for Rb as calculated with Ashcroft's
pseudopotential. The legend for the points
is the same as in figure A.3.

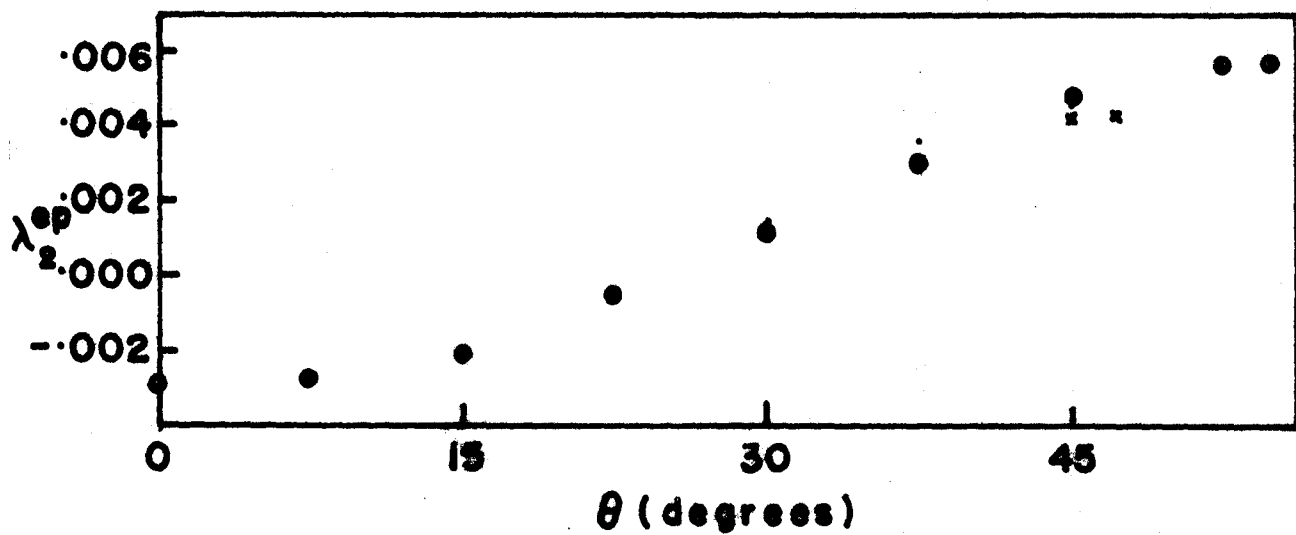
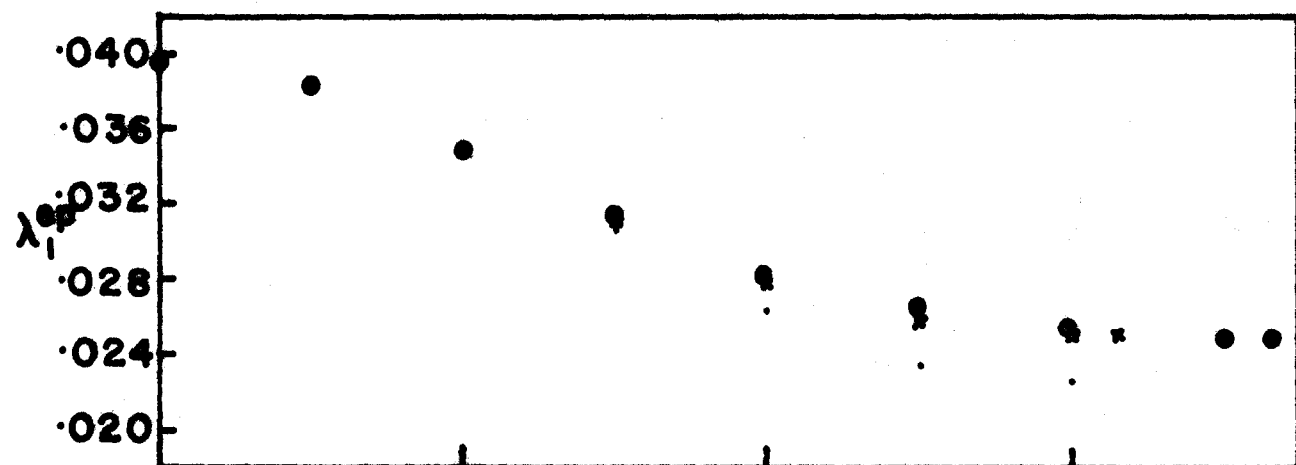
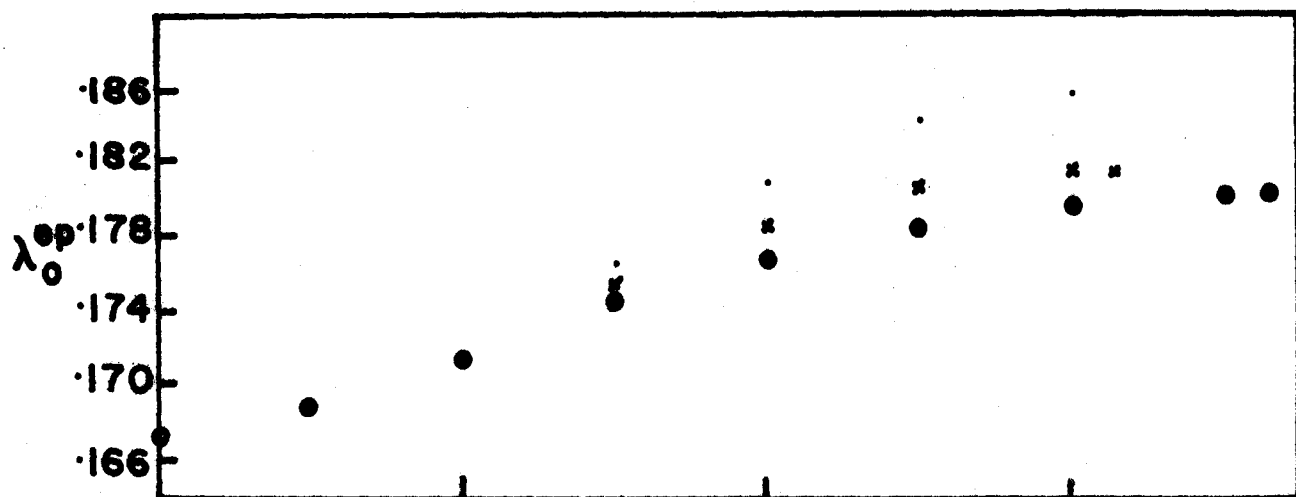


FIGURE A.6 The directional functions $\lambda_0^{\text{ep}}(\underline{k})$, $\lambda_1^{\text{ep}}(\underline{k})$
and $\lambda_2^{\text{ep}}(\underline{k})$ for Na as calculated with Shaw's
pseudopotential. The legend for the points
is the same as in figure A.3.

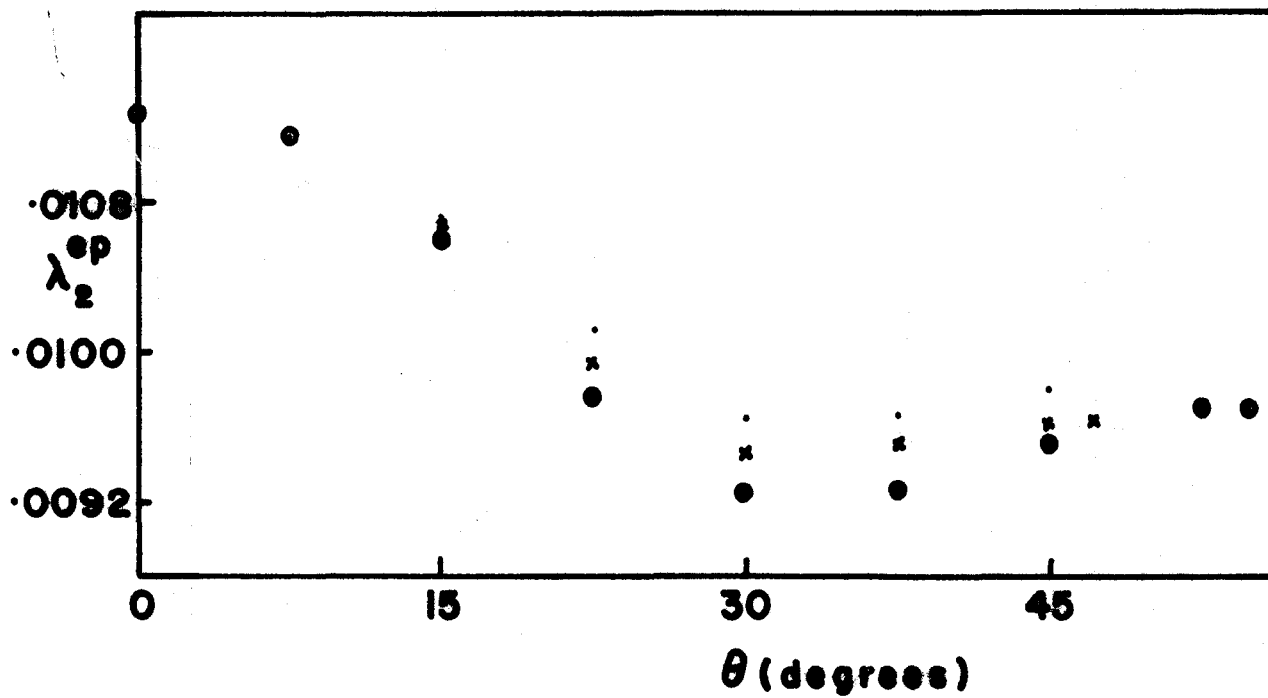
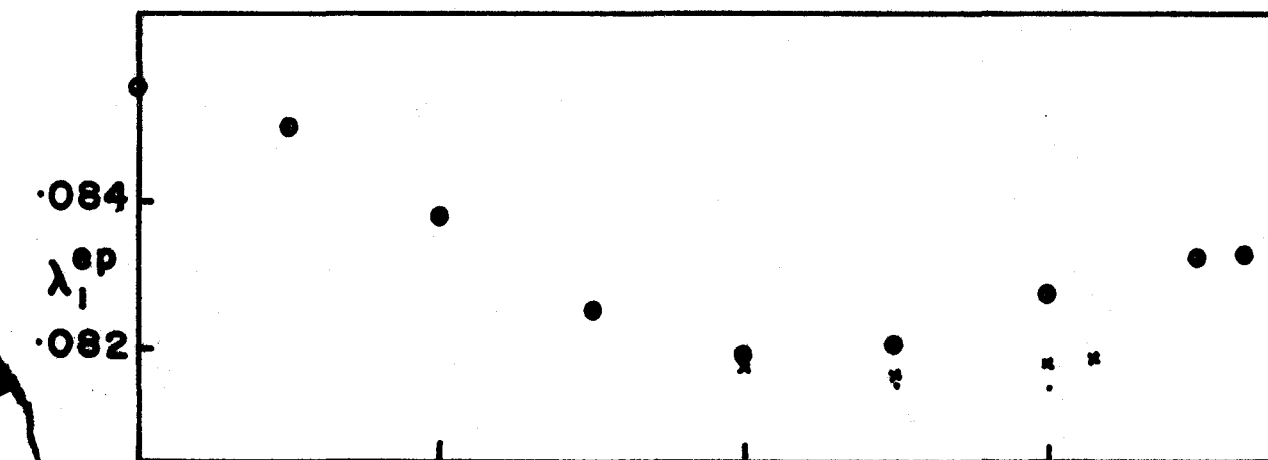
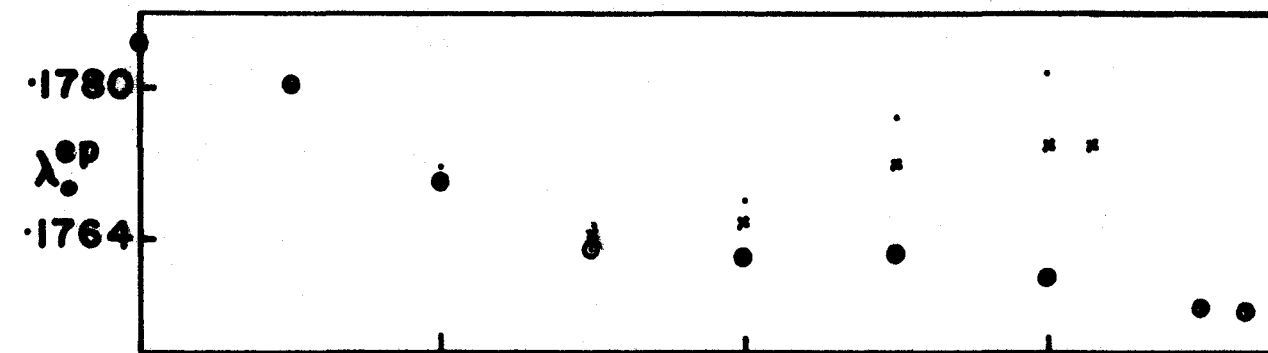


FIGURE A.7 The directional functions $\lambda_0^{\text{ep}}(\underline{k})$, $\lambda_1^{\text{ep}}(\underline{k})$
and $\lambda_2^{\text{ep}}(\underline{k})$ for K as calculated with Shaw's
pseudopotential. The legend for the points
is the same as in figure A.3.

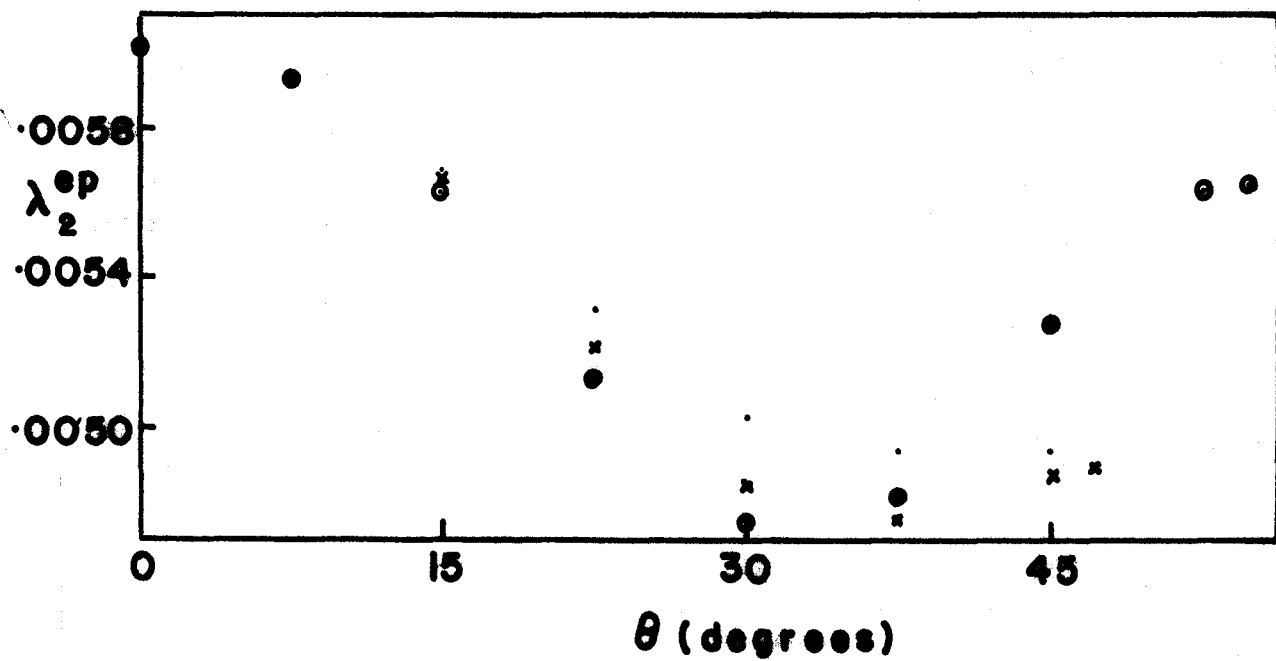
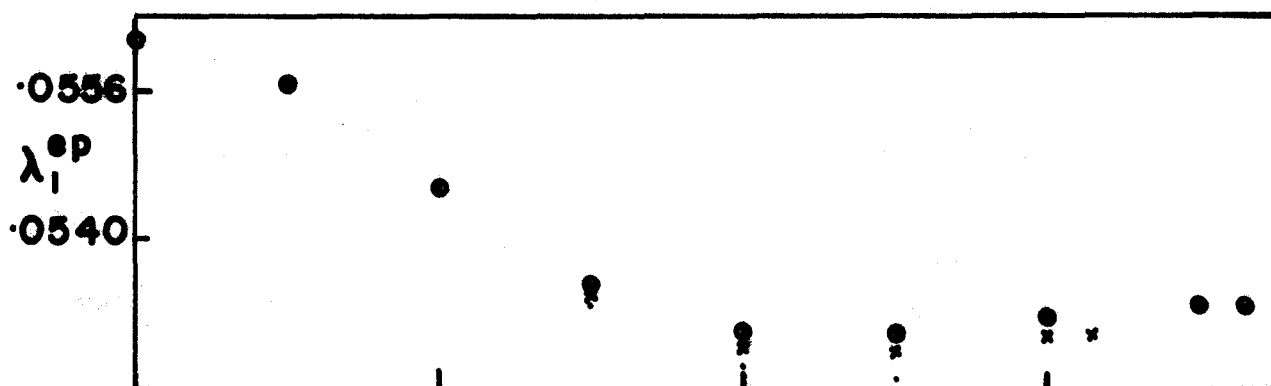
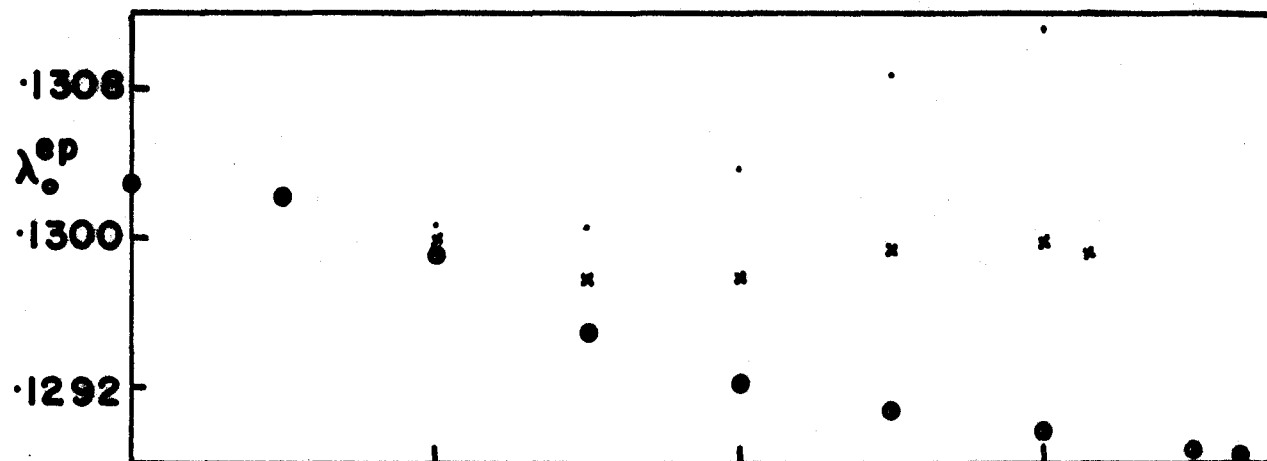


TABLE A.1

ANISOTROPY OF THE MOMENTS OF THE ELECTRON-PHONON
SCATTERING FUNCTION

SODIUM

ℓ	a_ℓ	
	(1)	(2)
0	.024	.016
1	.12	.05
2	.36	.20

POTASSIUM

ℓ	a_ℓ	
	(1)	(2)
0	.024	.018
1	.11	.07
2	.48	.24

RUBIDIUM

ℓ	a_ℓ	
	(1)	(2)
0	.10	-
1	.60	-
2	4.6	-

- (1) Ashcroft pseudopotential with r_c adjusted to fit the low temperature electrical resistivity.
 (2) Shaw pseudopotential.

table reveals that the amount of anisotropy in the $g_{\ell}^{\text{ep}}(\underline{k})$'s depends quite sensitively on the pseudopotential. This is particularly true for the higher moments. For both pseudopotentials the anisotropy is appreciable, especially for the higher moments. The anisotropy for rubidium is very considerable.

In tables A.2, A.3 and A.4 we report our results for the phonon renormalized electronic effective mass m_{ep}^* and for the average moments g_{ℓ}^{ep} for Na, K and Rb respectively. Also included are the results for these same quantities as calculated in reference (82). We note that, almost without exception, there is order of magnitude agreement between the results calculated with the different pseudopotentials but that the quantitative agreement is not good, particularly for the higher moments. However, not all of the difference between our results and those of Rice are attributable to the different pseudopotentials used. Some of it is due to the way in which Rice obtains information about the phonons propagating in non-symmetry directions. He uses the method of Darby and March⁽⁹⁰⁾. The phonon spectrum is expanded in Kubic harmonics and the expansion coefficients are obtained by fitting the inelastic neutron scattering data which is available for the symmetry directions. He also assumes that the polarization vectors are purely longitudinal or transverse so that the electrons are coupled to transverse phonons only for umklapp processes. Grimvall⁽⁹¹⁾

TABLE A.2

LEGENDRE POLYNOMIAL MOMENTS OF THE ELECTRON-PHONON SCATTERING FUNCTION FOR SODIUM

	$\frac{m^*}{m}$	g_0^{ep}	g_1^{ep}	g_2^{ep}	g_3^{ep}	g_4^{ep}	g_5^{ep}	g_6^{ep}
(1)	1.190	1.60×10^{-1}	5.46×10^{-2}	4.8×10^{-3}	1.4×10^{-3}	-9.7×10^{-4}	-4.4×10^{-4}	5.7×10^{-5}
(2)	1.177	1.51×10^{-1}	7.02×10^{-2}	8.4×10^{-3}	-6.0×10^{-3}	-8.0×10^{-4}	-1.2×10^{-3}	8.0×10^{-5}
(3)	1.15	1.3×10^{-1}	$5. \times 10^{-2}$	$-1. \times 10^{-3}$	$2. \times 10^{-3}$			

Calculated with:

- (1) Ashcroft pseudopotential with r_c adjusted to fit the low temperature electrical resistivity⁽⁸⁸⁾;
 (2) Shaw pseudopotential⁽⁸⁹⁾;
 (3) Ashcroft pseudopotential^(82,87).

TABLE A.3

LEGENDRE POLYNOMIAL MOMENTS OF THE ELECTRON-PHONON SCATTERING FUNCTION FOR POTASSIUM

	$\frac{m^*_{ep}}{m}$	g_0^{ep}	g_1^{ep}	g_2^{ep}	g_3^{ep}	g_4^{ep}	g_5^{ep}	g_6^{ep}
(1)	1.134	1.19×10^{-1}	4.05×10^{-2}	2.7×10^{-3}	1.9×10^{-3}	-1.0×10^{-5}	-1.9×10^{-4}	1.2×10^{-4}
(2)	1.130	1.15×10^{-1}	4.73×10^{-2}	4.6×10^{-3}	-1.4×10^{-3}	-8.1×10^{-4}	-2.8×10^{-4}	2.0×10^{-6}
(3)	1.12	1.1×10^{-1}	$5. \times 10^{-2}$	$-1. \times 10^{-3}$				
(4)	1.11	1.0×10^{-1}	$4. \times 10^{-2}$	$1. \times 10^{-3}$				

Calculated with:

- (1) Ashcroft pseudopotential with r_c adjusted to fit the low temperature electrical resistivity⁽⁸⁸⁾;
- (2) Shaw pseudopotential⁽⁸⁹⁾;
- (3) Ashcroft pseudopotential^(82,87);
- (4) Lee-Falicov pseudopotential^(82,81).

TABLE A.4

LEGENDRE POLYNOMIAL MOMENTS OF THE ELECTRON-PHONON SCATTERING FUNCTION FOR RUBIDIUM*

$\frac{m^*}{m}$	g_0^{ep}	g_1^{ep}	g_2^{ep}	g_3^{ep}	g_4^{ep}	g_5^{ep}	g_6^{ep}
1.179	1.51×10^{-1}	2.41×10^{-2}	1.6×10^{-3}	3.1×10^{-3}	-5.4×10^{-4}	4.2×10^{-4}	1.0×10^{-5}

* Calculated with the Ashcroft form of the pseudopotential with r_c adjusted to fit the low temperature electrical resistivity⁽⁸⁸⁾.

finds that this approximation tends to underestimate the phonon renormalized effective mass enhancement for sodium by about 10%. This accounts for a large measure of the discrepancy between our values of m_{ep}^* and those of reference (82). Nevertheless it is clear from our investigation that the choice of a reliable pseudopotential is very important in the calculation of the electron-phonon contribution to the Fermi liquid parameters.

Grimvall⁽⁹²⁾ has derived a relation between the high temperature ($T \gg \theta_D$) electrical resistivity and the first two moments of the electron-phonon scattering function. This relation enables one to obtain an experimental value for the difference $g_0^{ep} - g_1^{ep}$. In table A.5 we compare our results for this difference with the 'experimental' results determined by Grimvall. The agreement is quite satisfactory for both pseudopotentials.

TABLE A.5

EXPERIMENTAL TESTS OF THE DIFFERENCE BETWEEN THE FIRST TWO MOMENTS OF THE ELECTRON-PHONON SCATTERING FUNCTION

ELEMENT	EXPERIMENT	THEORY	
		(1)	(2)
Na	.10	.105	.080
K	.07	.078	.068
Rb	-	.127	-

TABLE A.5 - CONTINUED

Calculated with:

- (1) Ashcroft pseudopotential with r_c adjusted to fit the low temperature electrical resistivity⁽⁸⁸⁾;
- (2) Shaw pseudopotential⁽⁸⁹⁾.

On the basis of this comparison it seems that the fitted Ashcroft pseudopotential is preferable to that of Shaw for Na but that there is little to choose between them for K.

Brinkman, Platzman and Rice⁽⁹³⁾ have derived an exact sum rule for the Legendre polynomial moments of the electron-phonon scattering function. It is

$$\sum_{\ell=0}^{\infty} (2\ell+1) g_{\ell}^{\text{ep}} = C^{\text{ep}} \quad , (A.12)$$

where

$$C^{\text{ep}} \equiv \frac{k_F^2}{6m^* M} \sum_{\lambda} \langle \left(\frac{\underline{\epsilon}(\underline{q}, \lambda) \cdot \hat{\underline{q}}}{V_{\lambda}(\hat{\underline{q}})} \right)^2 \rangle_{AV}$$

and where $\hat{\underline{q}}$ is a unit vector in the direction of \underline{q} and $V_{\lambda}(\hat{\underline{q}})$ is the sound velocity in the direction $\hat{\underline{q}}$ for the λ th mode. The average is over all directions $\hat{\underline{q}}$. In table A.6 we compare our results for C^{ep} calculated using the force constant model for the phonons with those of reference (93) which were calculated from the experimental elastic constants. The agreement between the two calculations is good.

It is interesting to see how well our calculated

TABLE A.6

CALCULATED VALUES OF THE PHONON AVERAGE ENTERING THE SUM
 RULE FOR THE MOMENTS, g_{ℓ}^{ep} , OF THE ELECTRON-PHONON
 SCATTERING FUNCTION

ELEMENT	$\frac{m^*}{m}$	c^{ep}	
		(1)	(2)
Na	1.24 ± .02	.330	.325
K	1.21 ± .02	.248	.235
Rb	1.20 ± .05	.239	--

m^*/m is taken from reference (94)

- (1) Calculated from a force constant fit to the dispersion curves measured by means of inelastic neutron scattering.
- (2) Calculated from experimental elastic constants by Brinkman, Platzman and Rice⁽⁹³⁾.

moments, g_{ℓ}^{ep} , satisfy the sum rule (A.12). The comparison of the two sides of equation (A.12) is made in table A.7. We have truncated the sum at $\ell=6$ which is reasonable since $|13g_6^{\text{ep}}| \ll g_0^{\text{ep}}$. The agreement obtained with either pseudopotential is quite good although our results lie outside the experimental uncertainty in m^*/m . Since, in calculating the g_{ℓ}^{ep} 's, we have consistently set m_{ee}^* equal to m and m^* equal to m_{ep}^* it is perhaps a better test of the electron-phonon part of our calculation to set m^* equal to m_{ep}^* on the right hand side of the sum rule (A.12). To this end we have included the values of $(m^*/m_{\text{ep}}^*)C^{\text{ep}}$ in table A.7. With this modification the sum rule is satisfied very well for Na and K with the Ashcroft pseudopotential giving somewhat better agreement than the Shaw pseudopotential. Since some of the higher moments are quite different for the two pseudopotentials (both as regards magnitude and sign) it is rather disconcerting that the sum rule does not give a clear cut answer as to which pseudopotential is the better.

It should be clear from the above results that there is much work to be done in calculating the electron-phonon contribution to the Landau Fermi liquid parameters. Since the results for both the average moments and the anisotropy in the directional moments are very sensitive to the choice of pseudopotential it is evident that the greatest need is for an accurate pseudopotential, if indeed such a thing exists.

TABLE A.7

SUM RULE TEST OF THE CALCULATED MOMENTS OF THE
ELECTRON-PHONON SCATTERING FUNCTION

(1) Ashcroft pseudopotential with r_c adjusted to fit the low temperature electrical resistivity.

ELEMENT	C^{ep}	$\frac{m^*}{m_{ep}} C^{ep}$	$\sum_{\ell=0}^6 (2\ell+1) g_{\ell}^{ep}$
Na	.330	.344	.345
K	.248	.265	.266
Rb	.232	.237	.253

(2) Shaw pseudopotential.

ELEMENT	C^{ep}	$\frac{m^*}{m_{ep}} C^{ep}$	$\sum_{\ell=0}^6 (2\ell+1) g_{\ell}^{ep}$
Na	.330	.348	.341
K	.248	.266	.260